FoxO3a modulates the activation of innate and adaptive immune cells

Naveen Haribabu

Supervisor: Dr. Subash Sad, Ph.D.

A thesis submitted to the Faculty of Graduate and Postdoctoral Studies in partial fulfillment of requirements for the degree of Master of Science in Microbiology and Immunology

Department of Biochemistry Microbiology and Immunology

Faculty of Medicine

University of Ottawa

ABSTRACT

The innate immune response mediates immediate control of the pathogen and is followed by the acquired immune response which is slower but ensures comprehensive elimination of the pathogen. Dendritic cells are unique innate immune cells that can phagocytose the pathogen and generate pathogen-associated antigenic peptides for presentation to T cells in order to initiate the acquired immune response. Dendritic cells also express cytokines which facilitate pathogen control and development of acquired immune responses, thus acting as a bridge between innate and acquired immune responses. $CD8^+$ T cells are important cells of the adaptive immune system that play a key role in mediating clearance and protection against intracellular pathogens. Upon engagement by antigen-presenting cells, $CD8^+$ T cells undergo massive expansion followed by a swift, extensive contraction to restore homeostasis. The mechanisms behind the expansion and contraction of $CD8^+$ T cells are yet to be completely elucidated. FoxO3a is a transcription factor that is involved in the regulation of various vital cellular processes ranging from cell proliferation and cell metabolism to stress resistance and cell death. I have, therefore, investigated the role of FoxO3a signaling in the activation of dendritic cells and $CD8^+$ T cells. My initial experiments indicated that FoxO3a regulates the homeostasis of various immune cells including $CD8^+$ T cells and dendritic cells. $CD8^+$ T cells lacking FoxO3a displayed enhanced proliferation, as evaluated by cell imaging, CFSE dilution and Ki67 staining, upon polyclonal stimulation *in vitro*. The modulation of cell proliferation by FoxO3a seemed to be $p27^{kip}$-independent, as evaluated by western blotting. At later stages of stimulation, FoxO3a-deficient $CD8^+$ T cells underwent reduced cell death, as assessed by cell counting and 7-AAD staining, and this

seemed to be independent of Bim, Caspase 8 or Caspase 3 activation. In addition, FoxO3a regulated cytokine expression by $CD8^+$ T cells while displaying similar NFκB activation in comparison to WT $CD8^+$ T cells. Similar results were observed in dendritic cells upon LPS stimulation *in vitro*, wherein cytokine expression was higher in the FoxO3a-deficient dendritic cells and they also displayed enhanced antigen presentation to $CD8^+$ T cells, as evaluated by CFSE dilution. Taken together, these results indicate that FoxO3a acts as a negative regulator of $CD8^+$ T cell and dendritic cell activation.

ACKNOWLEDGEMENTS

First and foremost, I would like to thank my supervisor, Dr. Subash Sad, first for agreeing to let me assist him in his research and for supporting me, both academically and financially, making it possible for me to learn a lot in a short span of two years; both in science and in life. He has been a great teacher and an excellent mentor to me. I would also like to thank Dr. Julie Joseph for without a lot of her training, I would not be as well-equipped in various laboratory techniques as I am today. I would like to thank my TAC members, Dr. Lionel Filion and Dr. Seung-Hwan Lee for their valuable inputs and advice on my project and presentation skills. I would like to thank all past and current Sad Lab members during my time in the lab; Dr. Scott McComb, Dr. Bojan Shutinoski, Rajen Patel, Erin Cessford, Gerard Agbayani and Tina Nyugen who all have helped me in many ways, both inside and outside the lab, to make this graduate program an enjoyable experience amidst all the stress. I would like to thank our technician/lab manager, Kwangsin Kim, and our previous lab technicians, Renu Dudani, Komal Gurnani, Ahmed Zafer and Susanne MacLean for their generous and extensive technical assistance. I would like to thank Dr. Lionel Filion and Dr. Vera Tang for their training and assistance in flow cytometry. I would also like to thank my friends and family for their constant moral support and motivation. Last but not least, I would like to thank the almighty for his constant blessings and for helping me take yet another step towards the development of my education and career.

TABLE OF CONTENTS

LIST OF ABBREVIATIONS

μg – microgram
μl – microlitre
μM - micromolar
7-AAD – 7-aminoactinomycin D
ANOVA – Analysis of Variance
AP-1 – Activator Protein – 1
APC – antigen-presenting cell
BSA – Bovine Serum Albumin
CCR – C-C chemokine Receptor
CD – Cluster of Differentiation
cDC – conventional Dendritic Cell
CDK – Cyclin Dependent Kinase
CFSE – carboxyflourescein isothiocyanate
CTL – Cytotoxic T Lymphocyte
DAMP – Danger Associated Molecular Pattern
DC – Dendritic Cell
DMSO – Dimethyl Sulfoxide
DNA – Deoxy ribonucleic acid
EDTA - Ethylenediaminetetraacetic acid
ERK – Extracellular signal Regulated Kinase
FBS – Fetal Bovine Serum
GADD45 – Growth Arrest and DNA Damage
iDC – inflammatory Dendritic Cell
IFN - Interferon
IKK – Inhibitor of kappa B Kinase
IL - Interleukin
IκB – Inhibitor of kappa B
JNK – c-Jun N-terminal Kinase
LBP – Lipopolysaccharide-Binding Protein
LC – Langerhans Cell
LCMV – Lymphocytic choriomeningitis Virus
LPS - Lipopolysaccharide
MAPK – Mitogen-Activated Protein Kinase
MCP – Monocyte Chemotactic Protein
MHC – Major Histocompatibility Complex
MIP – Macrophage Inflammatory Protein
MnSOD – Manganese Superoxide Dismutase

moDC – monocyte-derived Dendritic Cell
MPEC – Memory Precursor Effector Cells
mRNA – messenger Ribonucleic acid
Mst1 – Mammalian Sterile 20-like 1 Kinase
MTT - 3-(4,5-dimethylthiazol-2-yl)-2,5-diphenyltetrazolium bromide
MyD88 – Myeloid Differentiation primary response 88
NFAT – Nuclear Factor of Activated T cells
NFκB – Nuclear Factor kappa-light chain enhancer of activated B cells
NLR – Nod-Like Receptor
PAMP – Pathogen Associated Molecular Pattern
PBS – Phosphate Buffered Saline
pDC – plasmacytoid Dendritic Cell
PI3K – Phosphatidyl Inositol 3 Kinase
PKC – Protein Kinase C
PTM – Post Translational Modification
R8 – RPMI-1640 + 8% FBS
RANTES – Regulated on Activated, Normal T cell Expressed and Secreted
RLR – Rig1-Like Receptor
ROS – Reactive Oxygen Species
RT – Room Temperature
SDS-PAGE – Sodium Dodecyl Sulphate–Polyacrylamide Gel Electrophoresis
SGK – Serum/Glucocorticoid regulated Kinase
Sirt3 – Sirtuin 3
SLEC – Short Lived Effector Cells
STAT – Signal Transducer and Activator of Transcription
TBS – Tris Buffered Saline
TCR – T Cell Receptor
TIRAP – Toll-Interleukin-1 Receptor (TIR) Associated Protein
TLR – Toll-Like Receptor
TMRE – Tetramethyl Rodamine Ethyl ester
TNF – Tumour Necrosis Factor
TRIF – TIR domain containing adaptor-inducing interferon-β
WT – Wild-type

LIST OF FIGURES

1. INTRODUCTION

1.1. Immune system

The immune system is arguably one of the most vital systems present in a multicellular host. It helps the host overcome infection by pathogens (Janeway, 2001), thereby, proper functioning of this system is crucial for host survival. The immune system is segregated into the innate immune system and the adaptive immune system, both of which work together to recognize the pathogen and perform various functions in order to mediate comprehensive elimination and protection against pathogens (Janeway, 2001).

1.2. Innate immunity

The innate immune system is the first line of defense against the pathogen. Various cells and molecules of this system act in a non-specific manner to facilitate early control of infection (Akira *et al*., 2006). This is accomplished by recognition of pathogen derived molecules that display varying degree of structural similarity among pathogens, called pathogen associated molecular patterns (PAMPs) (Medzhitov and Janeway, 1997). At the molecular level, complement proteins can either recognize and directly bind to components of pathogens or bind to other molecules that can detect PAMPs on the surface of pathogens. This leads to elimination of the pathogen by membrane rupture or clearance by innate immune cells that engulf and kill them through phagocytosis (Carroll, 2004). There are also other enzymes like lysozymes (Beutler, 2004), that cleave the peptidoglycans on the bacterial cell walls, and defensins (Ganz and Lehrer, 1998), that induce membrane permeability, thereby destroying the bacterial membranes and killing them in the process.

At the cellular level, various cells of the innate immune system such as neutrophils, macrophages and dendritic cells are able to detect PAMPs by virtue of specialized germline-encoded receptors called pattern recognition receptors (PRRs) (Medzhitov and Janeway, 1997). There are various classes of PRRs such as Toll-like receptors (TLRs), Nod-like receptors (NLRs), RIG-1 like receptors (RLRs) etc. (Takeda and Akira, 2005; Yoneyama and Fujita, 2009). Various subtypes of each of these receptor-classes can identify specific PAMPs and activate signaling cascades that culminate in the activation of these cells (Medzhitov, 2001).

1.2.1. Dendritic cells

Dendritic cells (DCs) are a unique class of innate immune cells, which in addition to performing their innate effector functions like phagocytosis and secretion of cytokines and anti-microbial peptides (Steinman and Hemmi, 2006), also act as a bridge between the innate and adaptive immune systems (Banchereau *et al*., 2000). They accomplish this by virtue of their capacity for antigen presentation to cells of the adaptive immune system (Guermonprez *et al*., 2002). The importance of DCs in mediating a protective T cell response was demonstrated in a study where depletion of DCs during an intracellular bacterial infection failed to mount an effective cytotoxic T lymphocyte (CTL) response (Jung *et al*., 2002).

1.2.1.1. Dendritic cell subsets

DC subsets are broadly classified into classical (cDC) and non-classical DCs. cDCs include $CD8\alpha^+$ DCs, which are important for cross-presentation, IL-12 secretion and induction of

$CD8^+$ T cell-mediated immune responses, and $CD11b^+$ DCs, which are superior in the induction of $CD4^+$ T cell-mediated immune responses (den Haan *et al*., 2000). Non-classical DCs include plasmacytoid DCs (pDCs), monocyte-derived DCs (moDCs) and Langerhans cells (LCs) (Mildner and Jung, 2014). pDCs are characterized by their ability to secrete high levels of type 1 interferons during a viral infection (Shortman and Liu, 2002). moDCs arise from differentiation of circulating monocytes upon infiltrating the site of infection or inflammation. Hence, these DCs are also termed inflammatory DCs (iDCs) (Hespel and Moser, 2012). LCs are a unique population of DCs that reside in the skin epidermal layers and sample their microenvironment for antigens. Upon encountering antigen, they migrate to skin draining lymph nodes and activate naïve T cells (Mildner and Jung, 2014).

1.2.1.2. Dendritic cell maturation

These cells arise from the bone marrow as myeloid progenitor cells and migrate to non-lymphoid tissues as immature DCs. These immature DCs survey the tissues for foreign invaders and non-self molecules, are highly phagocytic, and are not highly efficient at activating T cells (Cella *et al*., 1997). Once they encounter a pathogen or other inflammatory stimuli, they undergo the process of maturation. Various factors that can induce maturation and activation of DCs are PAMPs, cytokines and even the co-stimulatory molecule such as CD40L on T cells (Banchereau *et al*., 2000). During maturation, they lose their phagocytic activity but gain the ability to present antigen to T cells efficiently (Cella *et al*., 1997; Guermonprez *et al*., 2002). Their surface expression of major histocompatibility complex class-II (MHC-II) and co-stimulatory molecules increases along with the induction of

inflammatory cytokine and chemokine expression. These changes help the mature DCs to migrate to lymphoid tissues from the circulation and from non-lymphoid tissues in order to present antigen to and activate naïve T cells (Guermonprez *et al*., 2002).

1.2.1.3. Lipopolysaccharide (LPS) and Toll-like receptor 4 (TLR4) signaling

Bacterial lipopolysaccharide (LPS) is a component of cell membranes of gram negative bacteria (Osborn *et al*., 1974) and is a potent activator of innate immune cells through TLR4 engagement (Beutler, 2000). TLRs are transmembrane receptors with leucine-rich repeats in their extracellular domains that aid in PAMP recognition, leading to the activation of various signaling cascades and culminating in the activation of immune cells (Medzhitov, 2001). The importance of TLR4 recognition for induction of inflammatory responses against LPS was shown in a study where TLR4-deficiency resulted in hyporesponsiveness to LPS (Hoshino *et al*., 1999). Macrophages from TLR4-deficient mice produced poor levels of TNF-α and nitrite ions upon LPS stimulation. In addition, B cells from TLR4-deficient mice proliferated poorly in response to LPS (Hoshino *et al*., 1999). It was later reported that LPS first binds a soluble plasma protein, called LPS-binding protein (LBP) (Triantafilou and Triantafilou, 2002). This complex of LPS-LBP is transported by CD14 to the receptor complex of TLR4 and MD2 (Nagai *et al*., 2002). This leads to the recruitment of adaptor proteins, TIRAP and MyD88, to mediate early transcription of inflammatory cytokines (Kawai and Akira, 2006). This receptor-ligand complex dimer is then internalized into an endosome where it recruits another adaptor protein, TRIF, to mediate late transcription of inflammatory cytokines (Kawai and Akira, 2006). Both the MyD88 and TRIF-dependent

pathways have to be engaged downstream of TLR4 signaling to induce the expression of inflammatory cytokines (Kawai and Akira, 2006, 2010).

1.2.1.4. Cytokine expression and functions

Cytokines are proteins that are expressed by cells in order to influence their function or the function of neighboring cells (Arai *et al*., 1990). They are broadly classified into two types based on whether they promote or inhibit inflammation; henceforth referred to as pro-inflammatory or anti-inflammatory cytokines respectively (Dinarello, 2000). Activated DCs secrete a wide variety of pro-inflammatory cytokines such as interleukin-1 (IL-1), IL-6, tumor necrosis factor-α (TNF-α), IL-12 and interferon-α (IFN-α) (Morelli *et al*., 2001). IL-1 and TNF-α are classic pro-inflammatory cytokines that enhance endothelial cell adhesion molecule expression in order to facilitate extravasation of immune cells to the site of inflammation (Dinarello, 2000). IL-12 is an important inflammatory cytokine that promotes cell-mediated immune responses as it induces IFN-γ expression by various cells and directs helper T cells towards a pro-inflammatory phenotype (Joffre *et al*., 2009). IFN-α plays a critical role during a viral infection as it interferes with viral replication and also promotes the expansion of T cell responses (Kolumam *et al*., 2005). In addition to secreting pro-inflammatory cytokines, activated DCs can also express anti-inflammatory cytokines such as IL-10 and TGF-β, which downregulate immune responses by inhibiting the activation of other immune cells, inhibiting pro-inflammatory cytokine expression and promoting tissue repair and wound healing (Opal and DePalo, 2000).

In addition to cytokine expression, activated DCs also express chemokine receptors like CCR1, CCR5 and CCR7 among others (Cyster, 1999). CCR7 is particularly important as it is involved in the homing of activated DCs to lymph nodes where they can activate T cells (Yanagihara *et al.*, 1998).

1.2.1.5. Antigen processing and presentation to T cells

DCs, after internalization of antigen or pathogen through phagocytosis, initiate the process of degrading pathogen-derived proteins into peptides and loading them onto major histocompatibility complex (MHC) proteins, followed by presenting the MHC-peptide complex on their surface to stimulate antigen-specific T cells (Cella *et al.*, 1997).

There are two pathways of antigen processing and presentation, the cytosolic and endocytic pathways. The endocytic pathway is engaged when pathogens, infected cells or dead cells are internalized by phagocytosis or macropinocytosis and the internalized contents are localized to the phagosomes. Fusion of phagosomes with lysosomes results in degradation of proteins into peptides and loading of peptides onto MHC-II molecules (Guermonprez *et al.*, 2002). This pathway is responsible for the activation of $CD4^+$ T cells as their TCRs are MHC-II restricted. On the other hand, the cytosolic pathway is engaged when proteins in the cytosol are processed into peptides, through proteasomal degradation, and loaded onto MHC-I molecules to stimulate $CD8^+$ T cells (Thery and Amigorena, 2001). This phenomenon occurs when the antigen-presenting cell itself has been invaded by intracellular pathogens, such as viruses, that reside within the cytoplasm of the cell. However, there are circumstances wherein endocytic pathogens/antigens can induce a

$CD8^+$ T cell response through a mechanism known as cross-presentation (den Haan *et al*., 2000).

During antigen presentation, additional co-stimulatory molecules on the surface of dendritic cells engage their corresponding receptors on T cells. The interaction between CD80/86 on DCs with CD28 on T cells engages co-stimulatory signaling that leads to increased activation of DCs and T cells (Orabona *et al*., 2004). Similarly, CD40-CD40 ligand (CD40L) interaction also results in activation of DCs and amplification of T cell proliferation (Banchereau *et al*., 1994). The importance of CD40-CD40L interaction in DCs was shown in a study where absence of that interaction resulted in a lack of IL-12 production by DCs and thereby diminished protective $CD4^+$ and $CD8^+$ T cell responses to soluble antigen (Fujii *et al*., 2004). These co-stimulatory interactions lead to amplification of various signaling cascades that lead to increased activation, enhanced cytokine expression and more efficient antigen presentation and T cell activation.

1.3. Adaptive immunity

An adaptive (or acquired) immune response is the second line of defense against the pathogen, which ensures that the pathogen is comprehensively eliminated. The adaptive immune system consists of various types of lymphocytes that act synergistically to control pathogens. Lymphocytes contain re-arranged receptors on the cell surface that recognize specific pathogen-derived peptides in association with MHC molecules (Bonilla and Oettgen, 2010). In addition to specificity, another defining feature of adaptive immune responses is immunological memory. Activated lymphocytes differentiate into effector and

memory cells; effector cells mediate immediate protection and are cleared by the system whereas the memory cells are long-lived and provide a more rapid and robust response upon secondary exposure to the same pathogen (Bonilla and Oettgen, 2010). There are two main types of lymphocytes; B-lymphocytes or B cells and T-lymphocytes or T cells.

B cells harbor membrane-bound immunoglobulins that can directly detect antigenic determinants. Upon activation, B cells differentiate into plasma cells and memory cells (Bonilla and Oettgen, 2010). Plasma cells are specialized B cells that secrete high levels of antigen-specific antibodies which help neutralize the pathogen or mediate its killing through complement-mediated lysis (Rus *et al*., 2005) or Fc receptor-mediated phagocytosis (Swanson and Hoppe, 2004).

On the other hand, T cells can only recognize peptides when presented in the context of MHC. There are two main types of T cells which are identified based on whether their TCRs are MHC-I restricted or MHC-II restricted and are called $CD8^+$ and $CD4^+$ T cells respectively (Huseby *et al*., 2005). $CD4^+$ T cells, also called helper T (T_H) cells, ‘‘help’’ direct an adaptive response towards a cellular, humoral or a suppressive phenotype (Zhu and Paul, 2008). Once activated, these $CD4^+$ T cells differentiate into a wide variety of effector cells that are functionally distinguished based on their cytokine expression profiles and resulting effector responses (Mosmann and Sad, 1996; Zhu and Paul, 2008).

1.3.1. $CD8^+$ T cells

$CD8^+$ T cells are critical components of an adaptive immune response. Their TCRs are MHC-I restricted and since all nucleated cells in the host are capable of expressing MHC-I, these

$CD8^+$ T cells can mediate surveillance against any cell (Wong and Pamer, 2003). As they can directly, and specifically, mediate cytotoxicity to infected host cells, $CD8^+$ T cells are also called cytotoxic T lymphocytes (CTL) (Bonilla and Oettgen, 2010).

1.3.2. $CD8^+$ T cell maturation

$CD8^+$ T cells arise from the bone marrow as lymphoid progenitor cells which migrate to the thymus to undergo the process of maturation. During T cell maturation, each precursor cell undergoes positive and negative selection. During positive selection, T cells bearing TCRs that are capable of binding self-peptide-MHC ligand are selected and during negative selection, T cells bearing high-affinity TCRs for self-peptide-MHC ligand are deleted. Hence, at the end of the process, the mature T cell is both self-MHC restricted and self-tolerant. Mature T cells egress the thymus and home to secondary lymphoid organs (Germain, 2002).

1.3.3. $CD8^+$ T cell activation

Complete activation of a naïve $CD8^+$ T cell requires three signals; 1) antigen receptor or T cell receptor induced signals, 2) co-stimulatory signals mediated by cell surface interactions between ligands and receptors on antigen-presenting cells and T cells, and 3) cytokine-derived signals from DCs (eg. IL-12 and IFN-I) which amplify $CD8^+$ T cell responses (Curtsinger *et al*., 2003).

1.3.3.1. TCR signaling and CD28 co-stimulation

Upon recognition of the peptide-MHC complex by the TCR, the T cell undergoes activation through engagement of various signaling cascades. First, the CD8 co-receptor associates

with the MHC molecule followed by activation of the co-receptor associated tyrosine kinase, Lck (Veillette *et al*., 1988). Lck phosphorylates the Immunoreceptor Tyrosine Activation Motif (iTAM) residues in the intracellular domains of the CD3 receptor complex (Smith-Garvin *et al*., 2009). This leads to the recruitment and activation of other kinases and the consequent activation of three important pathways. First, induction of calcium signaling leads to the activation of the transcription factor, nuclear factor of activated T cells (NF-AT). Second, the activation of protein kinase C (PKC) leads to the activation of the transcription factor, nuclear factor kappa B (NFκB). Third, the activation of Ras pathway leads to the activation of mitogen-activated protein kinase (MAPK) which in turn leads to phosphorylation of *Fos* and its association with phosphorylated *Jun* to form the transcription factor, activated protein 1 (AP-1) (Smith-Garvin *et al*., 2009). All these three transcription factors, namely NFAT, NFκB and AP-1, act synergistically to upregulate the transcription of genes involved in T cell activation, survival and function (Gerondakis and Siebenlist, 2010; Macian, 2005).

Co-stimulatory signaling, such as CD28 engagement, activates the PI3K-Akt pathway. Akt (or protein kinase B {PKB}) has been shown to enhance the activation and nuclear translocation of NFκB, NFAT and AP-1, thereby potentiating the effects of TCR signaling (Smith-Garvin *et al*., 2009). Akt signaling has also been shown to enhance IL-2 mRNA stability and thereby lead to increased IL-2 expression (Acuto and Michel, 2003). In addition, Akt also inactivates transcription factors that cause cell cycle arrest and death, thereby leading to enhanced cell cycle progression and cell survival (Boise *et al*., 1995; Brunet *et al*., 1999). Studies have shown that, T cells that receive TCR stimulation in the absence of CD28 co-stimulation enter

a state of unresponsiveness, called anergy and are refractory to further stimulation (Schwartz, 2003). To summarize, CD28 signaling must be engaged in addition to TCR signaling to promote complete activation of the T cell. The importance of CD28 signaling in promoting an efficient T cell response was emphasized in a study where CD28-deficient mice exhibited significantly lower number of antigen-specific T cells during an intracellular bacterial infection (Mittrucker *et al*., 2001). Indeed, there are other molecules on T cells that have been identified with co-stimulatory potential like 4-1BB and OX40, but CD28 mediated co-stimulation is said to induce a more robust response as it is directly associated with downstream protein kinases (Smith-Garvin *et al*., 2009).

1.3.4. $CD8^+$ T cell differentiation

Antigen-specific $CD8^+$ T cells, when activated, undergo differentiation into two main types of cells, namely effector (T_E) and memory (T_M) cells. Effector cells mediate rapid function and reside mainly in the non-lymphoid organs to provide immediate protection against pathogen encounters at those sites. These effector cells are classified into two types, short lived effector cells (SLEC) and memory precursor effector cells (MPEC). SLECs provide bulk of the immediate effector functions but do not exhibit long term survival whereas MPECs contribute mainly towards generation of memory cells (Stemberger *et al*., 2007; Zhang and Bevan, 2011). These two effector cell types can be discriminated based on the cell surface expression of receptors involved in effector functions, Killer cell Lectin like Receptor G1 (KLRG1) and α-chain of IL-7 receptor, IL-7Rα (CD127). SLECs are $CD127^{lo}$ $KLRG1^{hi}$ whereas MPECs are $CD127^{hi}$ $KLRG1^{lo}$. Memory cells, on the other hand, persist for extended periods

to provide long term protection against re-infection by the same pathogen (Cho *et al*., 1999). They are classified into two subtypes, effector memory (T_{EM}) and central memory (T_{CM}) cells. Central memory cells exhibit high proliferative potential, circulate through the lymphoid compartment for extended periods and differentiate into effectors/effector memory cells upon pathogen encounter (Huster *et al*., 2006). These two subtypes are distinguished based on the cell surface expression of CD127 and a lymph node homing receptor (CD62L). T_{EM} cells are $CD127^{hi}$ $CD62L^{lo}$ whereas T_{CM} cells are $CD127^{hi}$ $CD62L^{hi}$ (Stemberger *et al*., 2007).

1.3.5. Effector functions

1.3.5.1. Cytokine expression

Activated $CD8^+$ T cells express a variety of cytokines including IL-2, IFN-γ and TNF-α. IL-2, a T cell growth factor, up-regulates metabolism and stimulates proliferation of the cell by inducing cell cycle progression (Smith-Garvin *et al*., 2009) although in a paradoxical manner, it also increases the cell's susceptibility to activation-induced cell death (Masopust and Ahmed, 2004). Expression of TNF-α and IFN-γ by $CD8^+$ T cells leads to activation of other immune cells like macrophages and NK cells (Mosmann *et al*., 1997).

Activated $CD8^+$ T cells also produce chemokines such as macrophage inflammatory protein (MIP-1α), monocyte chemoattractant protein (MCP-1) and ''Regulated upon Activation Normal T cell Expressed and Secreted protein'' (RANTES) in order to recruit other immune cells to the site of infection or inflammation (Kim *et al*., 1998).

1.3.5.2. Cytotoxic molecules

In addition to the expression of cytokines mentioned before, the effector function of $CD8^+$ T cells is also facilitated by two cytotoxic molecules, namely perforins and granzymes. Perforins form pores in the target cell's plasma membrane thereby disrupting its membrane integrity (Lowin *et al.*, 1994; Trapani and Smyth, 2002). Granzymes use the pores created by perforin to penetrate the cell and induce DNA fragmentation, thereby causing death of the target cell by apoptosis (Heusel *et al.*, 1994; Trapani and Smyth, 2002). In addition to mediating cytotoxic activities, perforin has also been reported to regulate $CD8^+$ T cell expansion during an infection (Harty and Badovinac, 2002). Another important mediator of $CD8^+$ T cell effector function is Fas ligand (FasL). Binding of FasL to the Fas receptor (Fas or CD95) on the target cell activates the extrinsic apoptotic cell death pathway which also leads to target cell death through caspase activation (Lowin *et al.*, 1994).

1.3.6. $CD8^+$ T cell response to infection

A $CD8^+$ T cell response is divided into four phases; activation, expansion, contraction and memory. As a naïve cell receives priming signals 1, 2 and 3 mentioned before (see $CD8^+$ T cell activation), it undergoes activation. Primed antigen-specific cells undergo clonal expansion, which can reach up to ten thousand fold under ideal conditions, during which the cells differentiate into effector cells. This enormous burst of antigen-specific effector cell expansion helps eliminate the pathogen comprehensively, which is typically at day 7-9 post infection (Bevan, 2004). Following expansion, around 90-95% of the primed cells

undergo contraction during which they die by apoptosis (Williams and Bevan, 2007). The remaining 5-10% of the primed population survives to differentiate into memory cells in order to provide long term protection during a secondary exposure (Harty and Badovinac, 2008). The mechanisms governing the expansion and contraction of primed antigen-specific $CD8^+$ T cells are so intricate and tightly regulated, that a complete picture is yet to be clear.

1.4. FoxO3a

FoxO3a is a transcription factor that belongs to a subclass of the Forkhead family of proteins. It was originally discovered in the fly, *Drosophila melanogaster* and was named dFOXO. The name, Forkhead, was derived with respect to the fly's ectopic head structures, resembling a fork, when this gene was mutated. Forkhead proteins are also referred to as 'winged-helix' proteins with reference to the structure of their DNA-binding domains, which are also termed 'Forkhead' domains (Huang and Tindall, 2007).

In total, there are four FoxO proteins identified in mice and humans; FoxO1, FoxO3a, FoxO4 and FoxO6. The name, FoxO3a, was established to differentiate it from a pseudogene identified in humans called FoxO3b (Anderson *et al*., 1998; Donlon *et al*., 2012). Currently, FoxO3a and FoxO3 are used interchangeably. FoxO1, FoxO3 and FoxO4 are widely expressed in various tissues such as lungs, liver and spleen, albeit with a heterogeneous expression pattern, whereas FoxO6 expression is limited to the brain (Dejean *et al*., 2011). The activity of these transcription factors is controlled by several post-translational modifications and is mediated by both transcriptional activation and transcriptional repression (Calnan and Brunet, 2008).

1.4.1. Post-translational modifications (PTM)

Various PTMs play important roles in controlling the transcriptional activities of FoxO3a and they include phosphorylation, ubiquitination, acetylation and methylation. These processes affect the sub-cellular localization, stability, target-specificity and DNA-binding activity (Calnan and Brunet, 2008).

Phosphorylations of serine and threonine residues play a critical role in modifying the transcriptional activity of FoxO3a by altering its sub-cellular localization. Ubiquitination regulates the total protein levels of FoxO3a in the cell. Acetylation controls the DNA-binding ability of FoxO3a and thereby its transcriptional activity. Methylation at the Akt-consensus sites prevents Akt-mediated phosphorylation of FoxO3a and its nuclear export whereas methylation within the DNA-binding domain inhibits its transcriptional activity (Calnan and Brunet, 2008; Eijkelenboom and Burgering, 2013).

1.4.2. Roles of FoxO3a in cell signaling

One of the first studies to characterize the physiological role of FoxO3a *in vivo* showed that it was responsible for the suppression of ovarian follicle activation and that lack of FoxO3a led to premature ovarian failure and infertility (Castrillon *et al*., 2003). Various studies thereafter have shown that FoxO3a also plays an important role in regulating vital cellular processes ranging from cell metabolism and cell proliferation to stress resistance and cell death (Eijkelenboom and Burgering, 2013).

1.4.2.1. Cell metabolism

Early studies in the nematode, *Caenorhabditis elegans* showed the role of a factor, DAF-16 which was regulated by insulin signaling, in regulating metabolism and longevity of the organism (Ogg *et al*., 1997). The mouse and human homologs of DAF-16, called FoxO3a, are regulated by the same growth factor mediated PI3K-Akt signaling pathway indicating a conserved role of FoxO3a across species. The importance of this pathway in regulating insulin signaling was highlighted when its dysregulation was found to result in cancer and diabetes (Eijkelenboom and Burgering, 2013). This cemented FoxO3a as a tumor suppressor and a pro-longevity factor. FoxO3a has been shown to inhibit mTOR signaling through upregulation of glutamine synthetase leading to glutamine accumulation and induction of autophagy (van der Vos *et al*., 2012). Another study in atrophying muscles showed that FoxO3a regulates autophagy through activation of both proteasomal and lysosomal proteolytic pathways (Zhao *et al*., 2007).

1.4.2.2. Cell death

Growth factor mediated signaling pathway activates Akt, a cell survival kinase, which can translocate to the nucleus to phosphorylate FoxO3a at three conserved Akt-consensus sites leading to its association with 14-3-3 protein and nuclear export. Upon growth factor withdrawal, FoxO3a translocates to the nucleus where it activates gene transcription and induces apoptosis through a FasL-dependent mechanism (Brunet *et al*., 1999) or through upregulation of Bim (Marie *et al*., 2002) and Puma (You *et al*., 2006). Bim and Puma are known to mediate mitochondrial membrane damage and thereby initiate the intrinsic

apoptotic pathway whereas the binding of FasL to Fas promotes activation of Caspase 8 and initiates the extrinsic apoptotic pathway (Hedrick *et al*., 2010). FoxO3a also mediates cell death through downregulation of anti-apoptotic proteins. FoxO3a was reported to modulate endothelial cell survival by downregulation of FLIP (Skurk *et al*., 2004) and also through activation of JNK and suppression of NFκB (Lee *et al*., 2008). Apoptotic death of HIV-1-infected macrophages was also reported to be mediated by FoxO3a signaling (Min *et al*., 2008).

1.4.2.3. Cell cycling

FoxO3a up-regulates the expression of a cell cycle arrest protein, $p27^{kip}$ and a cell death protein, Bim upon IL-2 withdrawal (Marie *et al*., 2002). This study underlined the role of FoxO3a signaling in regulating T cell proliferation and survival in response to IL-2. Under growth inhibitory conditions, FoxO3a regulates the expression of Gadd45 in order to mediate DNA repair at the G_2-M checkpoint of cell cycle (Tran *et al*., 2002). Activation of FoxO3a resulted in a decrease in mRNA and protein levels of cyclin D1 and cyclin D2 and inhibition of cyclin-dependent kinase 4 (CDK-4) activity, which resulted in cell cycle inhibition, independently of $p27^{kip}$ expression (Schmidt *et al*., 2002). This effect did not involve direct binding of FoxO3a to cyclin D1 and D2 promoters, suggesting a role of FoxO3a as a transcriptional co-factor.

1.4.2.4. Oxidative stress resistance

ROS induced oxidative stress leads to the activation of FoxO3a through JNK mediated phosphorylation and nuclear import. This nuclear FoxO3a up-regulates the expression of

anti-oxidant enzymes such as catalase and manganese superoxide dismutase (MnSOD) to counteract the stress (Kops *et al*., 2002). Mst1 phosphorylates and activates FoxO3 to induce upregulation of anti-oxidant defenses and protect cells from oxidative stress. This Mst1-FoxO3 signaling pathway resulted in a reduction in ROS levels and protection from apoptosis, thereby maintaining homeostasis of naïve T cells (Choi *et al*., 2009). Sirt3 has been shown to deacetylate FoxO3a during oxidative stress in order to protect mitochondria from oxidative damage (Tseng *et al*., 2013). This effect is mediated through upregulation of genes essential for mitophagy which aids in clearing defective mitochondria and maintaining mitochondrial homeostasis.

1.4.3. Role of FoxO3a in a T cell response

In humans, $CD4^+$ central memory T cells (T_{CM}) were reported to display enhanced survival *ex vivo* compared to effector memory $CD4^+$ T cells. This effect was attributed to enhanced FoxO3a phosphorylation and a concomitant reduction in the levels of pro-apoptotic protein, Bim (Riou *et al*., 2007). They showed that phosphorylation of FoxO3a required both TCR and cytokine signaling and suggested that FoxO3a was involved in the persistence of $CD4^+$ T_{CM} cells.

In FoxO3a-deficient mice, $CD4^+$ T cells were reported to display signs of hyperactivation which were attributed to enhanced NFκB signaling (Lin *et al*., 2004). The study showed decreases in the levels of IκB proteins in the FoxO3a-deficient $CD4^+$ T cells and suggested that FoxO3a modulates NFκB signaling through reciprocal regulation of inhibitory IκB proteins.

There appears to be a discrepancy between various studies as to whether there is an intrinsic or extrinsic effect of FoxO3a signaling in T cells during LCMV infection in mice. One study reported that FoxO3a signaling in dendritic cells limited IL-6 expression which in turn decreased the survival of primed $CD8^+$ T cells (Dejean *et al*., 2009). Another study reported a $CD8^+$ T cell intrinsic effect of FoxO3a in regulating $CD8^+$ T cell death during the expansion phase of the response to LCMV infection leading to enhanced accumulation of antigen-specific $CD8^+$ T cells during the peak of the response (Sullivan et al., 2012a). During a bacterial (*Listeria monocytogenes*) infection in mice, FoxO3a signaling decreased the maintenance of antigen-specific memory $CD8^+$ T cells in a cell-intrinsic manner (Tzelepis *et al*., 2013).

1.5. Rationale

Cell cycling, cell death, cell metabolism and stress resistance are all vital cellular processes and are proposed to be involved during various phases of a $CD8^+$ T cell response to infection. Based on various scientific findings, FoxO3a signaling has been reported to be involved in all of the aforementioned cellular processes (see previous sections) although this has not been evaluated thoroughly in immune cells. Therefore, understanding how FoxO3a signaling influences the activation of $CD8^+$ T cells is crucial as how the cell is activated eventually dictates its course during a response. In addition, determining the role of FoxO3a signaling in a $CD8^+$ T cell response to infection will be useful in targeting its signaling components for novel therapeutic strategies in vaccine development. Also, it has been shown that DCs are primarily responsible for priming antigen-specific $CD8^+$ cells *in vivo*

(Jung *et al*., 2002) and the way DCs are activated will eventually influence the $CD8^+$ T cell response that ensues (Joffre *et al*., 2009). Therefore, deciphering the role of FoxO3a signaling in DC activation also becomes an essential piece of the puzzle.

1.6. Hypothesis

The various functions of FoxO3a in cell signaling seem to be cell type and context dependent. I hypothesized that FoxO3a modulates the activation of innate and adaptive immune cells by regulating the transcription of cell death genes.

1.7. Objectives

1. To determine the role of FoxO3a signaling in $CD8^+$ T cell activation
2. To determine the role of FoxO3a signaling in DC activation

2. MATERIALS AND METHODS

2.1. Mice

All mice were maintained in animal care facilities at the University of Ottawa (Ottawa, Ontario, Canada) under the guidelines of the Canadian Council on Animal Care (CCAC). Wild type (WT) C57BL/6J mice, OT-1 TCR transgenic mice and B6.SJL mice were obtained from The Jackson Laboratory (Bar Harbor, Maine, USA). FoxO3a-deficient mice and FoxO3a-deficient OT-1 mice were generated as previously described (Tzelepis et al., 2013). FoxO3a-deficient mice were derived by disabling the FoxO3a allele using a gene-trap targeting strategy (Lin et al., 2004). The FoxO3a-deficient mice were maintained as a heterozygous colony and screened by polymerase chain reactions (PCR) to determine +/+ and -/- genotypes. FoxO3a-deficient OT-1 ($CD45.2^+$) mice were generated by mating OT-1 ($CD45.2^+$) mice with FoxO3a-deficient mice. WT OT-1 ($CD45.1^+$ $CD45.2^+$) mice were generated by mating B6.SJL ($CD45.1^+$) mice with OT-1 ($CD45.2^+$) mice. All mice were used when they were between the ages of 6-8 weeks.

2.2. Media, Buffers and Reagents

R8 medium (RPMI-1640 {Gibco, catalog #31800-089} + 8% fetal bovine serum {Wisent, catalog #115667}) was used for all cell culture experiments. Phosphate Buffered Saline (PBS) was prepared in the lab at a stock concentration of 25X which was diluted to 1X with distilled water and used as required. Flow cytometry staining buffer used was a 1% solution of BSA (Sigma, catalog #A7906) in PBS (PBS-BSA). The recommended buffer used for

magnetic isolation of cells was a solution of PBS containing 2% FBS and 1mM EDTA {Fisher Scientific, catalog #123814}. Flow fixative buffer used for flow cytometry was a solution of PBS containing 1% paraformaldehyde {Sigma, catalog #F8775} and 0.02% sodium azide {Sigma, catalog #S2002}. Permeabilizing buffer (PFT) used for flow cytometry was a solution of PBS containing 1% FBS and 0.25% Triton X-100 {Sigma, catalog #X100}. Coating buffer used for ELISA was a solution of 1X PBS unless otherwise stated. Blocking buffer used for ELISA was a solution of PBS containing 1% FBS unless otherwise stated. Wash buffer (PBS-T) for ELISA was a solution of PBS containing 0.05% Tween-20 (Sigma, catalog #P1379).

2.3. Bacterial strain

Stocks of a recombinant strain of Ovalbumin-expressing *Salmonella typhimurium* that translocates Ova to the cytosol (ST-YopE-Ova) were prepared as previously described (Tzelepis et al., 2012). The bacteria were grown in LB broth containing Streptomycin and Ampicillin at 37°C. They were then frozen in culture medium containing 20% glycerol and stored at -80°C in small aliquots.

2.4. $CD8^+$ T cell purification

Spleens were homogenized using frosted glass slides (Fisherbrand, catalog #12-556-343) in R8 medium. The homogenate was passed through a 70 μm cell strainer (Fisherbrand, catalog #22363548) to obtain a single cell suspension devoid of clumps and aggregates. Cells were counted using a hemocytometer (Hausser, catalog #1483) and $CD8^+$ T cells were purified as per manufacturer's instructions using a $CD8^+$ T cell enrichment kit (STEMCELL, catalog #19853A). Briefly, whole spleen cells were resuspended in the recommended

buffer, transferred to the 14 ml tubes (BD, catalog #352057) and normal rat serum (STEMCELL, catalog #13551) was added to prevent non-specific binding of antibodies. An antibody cocktail containing a combination of biotinylated monoclonal antibodies directed against cell surface antigens on mouse cells of hematopoietic origin (CD4, CD11b, CD11c, CD19, CD24, CD45R, CD49b, TCR$\gamma\delta$ and Ter119) was added followed by addition of streptavidin-coated magnetic particles. The tube was placed in a magnet (STEMCELL, catalog #18001) and inverted so that the buffer containing only $CD8^+$ T cells would flow out. The purified $CD8^+$ T cells were resuspended in R8, counted and used as required. A purity check was ascertained by flow cytometry and an average purity of 95% was achieved.

2.5. $CD8^+$ T cell stimulation

Cell lines secreting antibodies against CD3 (145-2C11) and CD28 (37.51) were grown in DMEM medium. Antibodies were purified from cell culture supernatants by affinity chromatography using protein G columns. The anti-CD3 and anti-CD28 antibodies were coated on 96 or 24 well flat-bottom plates (Falcon, catalog #353072 or 353047) in Phosphate Buffered Saline (PBS), at 1 μg/ml each, overnight at 4°C. The wells were washed twice with PBS to remove unbound antibodies and the purified $CD8^+$ T cells were seeded at 10^5 cells per well (96 well plate) in 200 μl R8 medium or 10^6 cells per well (24 well plate) in 1 ml R8 medium and placed in a CO_2 incubator (Thermo, Heracell 150i) for the indicated time points. For the apoptosis-inhibition experiments, z-VAD (Apexbio, catalog #A1902), a pan-caspase inhibitor, was added to the purified $CD8^+$ T cells at 10 μM in DMSO (Sigma, catalog # D2650) and stimulated with anti-CD3 and anti-CD28 antibodies. For the IL-6 neutralization

experiments, anti-IL-6 neutralizing antibody (eBioscience, catalog #16-7061-81) was added to the purified $CD8^+$ T cells at 1 μg/ml in PBS and stimulated with anti-CD3 and anti-CD28 antibodies.

2.6. CFSE labeling

Whole spleen cells were labeled with 0.125 μM CFSE (eBioscience, catalog #65-0850), as per manufacturer's instructions, before performing $CD8^+$ T cell purification. Cells were washed with PBS to remove the serum proteins and CFSE was added to the cells at the desired concentration and incubated in a 37°C shaker for 10 min in the dark. The labeling was stopped by adding an equal volume of serum and incubating on ice for 5 min. The labeled cells were washed, resuspended in R8 medium and cultured as required.

2.7. MTT assay

10 μl of 5 mg/ml solution of MTT {3-(4,5-dimethylthiazol-2-yl)-2,5-diphenyltetrazolium bromide} (Sigma, catalog #M5655) was added to cells in 100 μl of R8 medium and incubated for 2 h at 37°C. Following incubation, crystals formed in healthy/proliferating cells were solubilized by lysing cells with 100 μl acid propanol (0.04N hydrochloric acid {Fisher, catalog #351278-212} in isopropanol {Fisher, catalog #BP26184}). The absorbance was read at 570nm with a reference wavelength of 650nm using a spectrophotometer (Molecular Devices, Filtermax F5).

2.8. Flow Cytometry

Briefly, $1x10^6$ cells were transferred to 5 ml tubes (Fisher, catalog # 14-961-10) and washed with PBS twice. To prevent non-specific binding of antibodies, Fc block (anti-CD16/32; BD, catalog #553142) was added to the cells in PBS-BSA, followed by incubation for 10 min at 4°C. Fluorochrome-tagged antibodies against various cell surface receptors (anti-CD8-APC-Cy7, anti-CD11c-PE, anti-CD19-FITC, anti-CD45R{B220}-PE-Cy7, anti-CD4-APC, anti-TCRβ-PE, anti-CD11b-APC, anti-Ly6G-FITC, anti-Ly6C-e450, anti-CD44-PE, anti-CD62L-e450, anti-CD127-APC, anti-CD69-PE-Cy7, anti-CD80-APC, anti-CD86-FITC and anti-MHC-II-e506) were added in PBS-BSA followed by incubation for 20 min at 4°C. The cells were washed with PBS to remove excess unbound antibodies and fixed in flow fixative buffer before acquisition on the flow cytometer (Beckman Coulter, CyAn ADP analyzer). For live-dead cell discrimination, 7-AAD (BD, catalog #559925) was added to the cells post surface staining and incubated at RT for 10 min prior to acquisition. For intracellular Ki67 staining, cells were fixed in 70% ice cold ethanol for 1 h at 4°C followed by washing in permeabilizing PFT buffer. FITC-conjugated anti-Ki67 antibody (BD, catalog #556026) was added to the cells in PFT buffer and incubated for 30 min at RT, protected from light. The cells were then washed with PFT buffer and re-suspended in PBS before acquisition. All cell surface receptor antibodies were purchased from eBioscience. Data were analyzed with Kaluza software (Beckman Coulter, version 1.3).

2.9. TMRE staining

Cells were harvested from the wells at various time points post stimulation and washed with RPMI-1640 without phenol red (Gibco, catalog #11835-030) followed by staining with TMRE (Gibco, catalog #T-669) in the same media and incubated for 30 min at 37°C in the CO_2 incubator. Following incubation, the stained cells were immediately assessed on the flow cytometer.

2.10. SDS-PAGE and Western Blotting

Briefly, 10^6 cells were washed with PBS to remove all the media components. The cell pellet was then lysed in RIPA buffer (150mM sodium chloride, 1% NP-40, 0.5% sodium deoxycholate, 0.1% SDS, 50mM Tris-HCl (pH 8.0) followed by incubation on ice for 5 min. The lysate was centrifuged at 8000g for 10 min at 4°C to pellet the cell debris (Thermo, legend micro 21). Proteins present in the supernatant were estimated using a BCA protein assay kit as per manufacturer's instructions, (Thermo, catalog #23235). In this assay, the protein lysate was incubated with bicinchonic acid and copper sulphate solution in a carbonate buffer. The peptides reduced the copper ions and the bicinchonic acid binds to the reduced copper ions and absorbs light which is measured as a function of protein concentration. Normalized protein amounts were then denatured by addition of Laemmli buffer (60mM Tris-Cl{pH 6.8}, 10% glycerol, 5% β-mercaptoethanol, 2% SDS, 0.01% bromophenol blue) and heated at 95°C in a heating block (Fisher, isotemp) for 10 min. The samples were resolved on 8% or 15% SDS-polyacrylamide gels and transferred onto polyvinylidene difluoride membranes (Biorad, catalog #162-0177) by electroblotting for 80

min at a constant amperage of 0.4 A. The membranes were blocked with 5% milk in Tris Buffered Saline solution containing 0.1% Tween-20 (TBS-T) for 1 h at RT followed by probing with the primary antibody of interest and overnight incubation at 4°C on a rocker (VWR). The primary antibody was removed and the membrane was washed with TBS-T followed by addition of the appropriate secondary antibody and incubation for 1 h at RT. The membrane was washed with TBS-T followed by addition of substrate (Biorad, catalog #170-5061) and the images were developed using a luminescent image analyzer (GE, Imagequant LAS4000). The protein band intensities were quantified by densitometry using ImageJ software (NIH, version 1.48). β-actin was used as a loading control. Primary antibodies that were purchased from Cell Signaling Technology (Danvers, MA, USA) were against $p27^{kip1}$ (3698), cleaved Caspase-9 (9509), Bim (2933), phosphorylated and total NFκB (3033, 8242) and phosphorylated and total IκBα (2859, 4814). Primary antibodies purchased from Santa Cruz Biotechnology (Dallas, Texas, USA) were against Caspase-3 (sc-7148) and β-actin (sc-81178). Anti-mouse Caspase-8 (ALX-804-447) was purchased from Enzo Life Sciences (Farmingdale, NY, USA). Secondary antibodies purchased from Cell Signaling Technology were anti-rabbit IgG (7074) and anti-mouse IgG (7076). For the Caspase-8 primary antibody, an anti-rat IgG (112970) secondary antibody was used which was purchased from Jackson Immuno Research (West Grove, PA, USA). Primary antibodies were used at 1:1000 dilution.

2.11. Dendritic cell (DC) purification

For DC purification, spleens were placed on a petri dish (Fisherbrand, catalog #FB0875713) minced using sterile blades (Fisher Scientific, catalog #08-918-5D) into a homogeneous

paste followed by addition of spleen dissociation medium (STEMCELL, catalog #07915) containing collagenase, DNase and FBS to maximize the recovery and viability of mouse splenic DCs. The homogenate, with the medium, was transferred to a tube and incubated horizontally for 30 min on a rocker at RT followed by dissociating the fragments into a smooth suspension by passing it through an 18-gauge needle (BD, catalog #305196) and a 5cc syringe (BD, catalog #309646). EDTA was added at a final concentration of 10 mM and the tube was incubated horizontally for 5 min at RT. The entire suspension was passed through a primed 70 μm cell strainer to remove any remaining aggregates or clumps. The single cell suspension was counted using a hemocytometer and resuspended in the recommended medium, described above, and DCs were purified as per manufacturer's instructions using a $CD11c^+$ positive selection kit (STEMCELL, catalog #18758). Initially, mouse FcR blocker was added to prevent non-specific binding of antibodies followed by addition of CD11c-PE labeling reagent to label all $CD11c^+$ cells. Then, a PE selection cocktail containing tetrameric antibody complexes specific against PE and dextran was added followed by addition of magnetic dextran iron particles. The tube was then placed inside the magnet, described above, and the buffer containing all un-labeled cells were decanted into the waste. The $CD11c^+$ cells bound to the magnet were washed and resuspended in R8, counted using a hemocytometer and stimulated as required. Purity check was ascertained by flow cytometry and an average purity of 85% was achieved.

2.12. Dendritic cell stimulation

Purified DCs were seeded in 96 well plates at 10^5 cells in 200µl R8 medium and lipopolysaccharide (LPS; Sigma, catalog #L2630) was added to the cells at 100 ng/ml followed by incubation in the CO_2 incubator for the indicated time points.

2.13. Antigen presentation assay

DCs were purified from spleens of WT and FoxO3a-deficient mice and seeded onto 96 well plates at $5x10^4$ cells per well. A frozen stock of ST-YopE-OVA (Tzelepis et al., 2012) was thawed and washed to remove the DMSO. The bacteria were then re-suspended in R8 medium and added on top of the cells at different multiplicities of infection (MOI) and incubated for 30 min at 37°C to allow for infection to occur. The wells were then washed with R8 medium to remove remaining extracellular bacteria and fresh R8 medium containing 50 µg/ml gentamycin (Gibco, catalog #15750-060) was added and incubated for 2 h at 37°C. Following the 2 h incubation, the wells were washed with R8 medium again and fresh R8 medium containing 10 µg/ml gentamycin was added. $CD8^+$ T cells were purified from the spleens of WT OT-1 and FoxO3a-deficient OT-1 mice, labeled with CFSE as described above, and seeded on top of the infected DCs at $5x10^4$ cells per well. The reduction in CFSE intensity in the proliferating OT-1 $CD8^+$ T cells was measured by flow cytometry at 72 h post-stimulation.

2.14. Cytokine expression profiling

All cytokines were measured in the cell culture supernatants by sandwich ELISA.

2.14.1. IL-1β, TNF-α, IL-10 and IL-12

All cytokine standards, anti-cytokine capture antibodies, biotinylated anti-cytokine detection antibodies and streptavidin-conjugated horse radish peroxidase (HRP) were purchased as kits (BD OptEIA sets) from BD Biosciences (San Diego, CA, USA). Cytokines were assayed as per manufacturer's instructions. Special ultra-high binding polystyrene 96 well flat-bottom plates (Thermo, catalog #3855) were coated with 50 µl anti-cytokine capture antibody in coating buffer overnight at 4°C. The wells were washed with PBS-T followed by addition of 100 µl blocking buffer (PBS containing 1% FBS) and incubated for 1 h at RT. The wells were washed with PBS-T followed by addition of 50 µl cell culture supernatants and 50 µl cytokine standards. After 2 h incubation at RT, wells were washed with PBS-T followed by addition of 50 µl biotinylated anti-cytokine detection antibody and incubation for 1 h at RT. The wells were washed with PBS-T followed by addition of 50 µl streptavidin conjugated HRP and incubation for 30 min at RT. The wells were washed with PBS-T followed by addition of 50 µl tetramethylbenzidine (TMB) substrate (R&D, catalog #DY999). The reaction was stopped by addition of 25 µl of 2N sulphuric acid {H_2SO_4} (Sigma, catalog #302501).

2.14.2. IL-1α and IL-6

Anti-IL-1α capture antibody (catalog #16-7011-85), biotinylated anti-IL-1α detection antibody (catalog #13-7111-85), anti-IL-6 capture antibody (catalog #14-7061-85) and biotinylated anti-IL-6 detection antibody (catalog #13-7062-85) were purchased from eBioscience. Streptavidin-conjugated HRP (catalog #1029223B) was purchased from

Invitrogen. The coating buffer and blocking buffer used for these cytokines was PBS and PBS-BSA respectively. The procedure for the sandwich ELISA was similar to the one described for the cytokines in the previous section.

2.14.3. IFN-γ

Anti-IFN-γ capture antibody (catalog #16-7312-81) was purchased from eBioscience and biotinylated anti-IFN-γ detection antibody (XMG1.2) was prepared in the lab. A cell line secreting antibody against IFN-γ (R4-6A2) was grown in R8 medium. The antibodies were purified from cell culture supernatants by affinity chromatography using protein G columns. The purified anti-IFN-γ antibody was then conjugated to biotin to obtain biotinylated anti-IFN-γ detection antibody. The procedure for the sandwich ELISA was similar to the one described in section 2.14.1.

The absorbance (OD) was read at 450nm using the spectrophotometer. Estimation of cytokine levels was achieved using Softmax Pro software (Molecular Devices, version 6.2.2).

2.15. Statistical analysis

All experiments were performed in triplicates. All values were compared using two-way ANOVA or unpaired t test depending on the number of variables involved and factors to be compared. The individual figure legends indicate the statistical test used for the analyses and the p values. Statistical analyses were done using the Prism software (GraphPad, version 5.01). The differences were considered significant when the p value was <0.05.

3. RESULTS

3.1. FoxO3a signaling promotes immune cell homeostasis in the spleen

FoxO3a has been shown to be expressed in immune cells and modulate certain functions (Lin et al., 2004). However, how FoxO3a influences immune functions is not clear. Hence, the numbers of various immune cell subsets in the spleens of WT and FoxO3a-deficient mice were evaluated by flow cytometry. Spleens were harvested from 6-8 week old mice, placed in R8 media and homogenized using frosted glass slides to prepare single cell suspensions. The cells were counted and resuspended at 10^6 cells per 100 µl and cell surface receptor antibodies against various immune cell subsets were added to quantify their relative proportions in the spleen. The FoxO3a-deficient spleens were approximately 1.5 to 2 times the size of their WT counterparts (Figure 1C) and their total splenic cellularity was significantly higher compared to WT (Figure 1B). There were increased numbers of $CD4^+$ T cells ($TCR\beta^+$ $CD4^+$), $CD8^+$ T cells ($TCR\beta^+$ $CD8^+$), dendritic cells ($CD11c^+$), neutrophils ($CD11b^+$ $Ly6G^+$), monocytes ($CD11b^+$ $Ly6G^-$ $Ly6C^{hi}$) and macrophages ($CD11b^+$ $Ly6G^-$ $Ly6C^{lo}$) in the spleens of FoxO3a-deficient mice. Interestingly, there was no impact of FoxO3a signaling on the numbers of B cells ($CD19^+$) (Figure 1D).

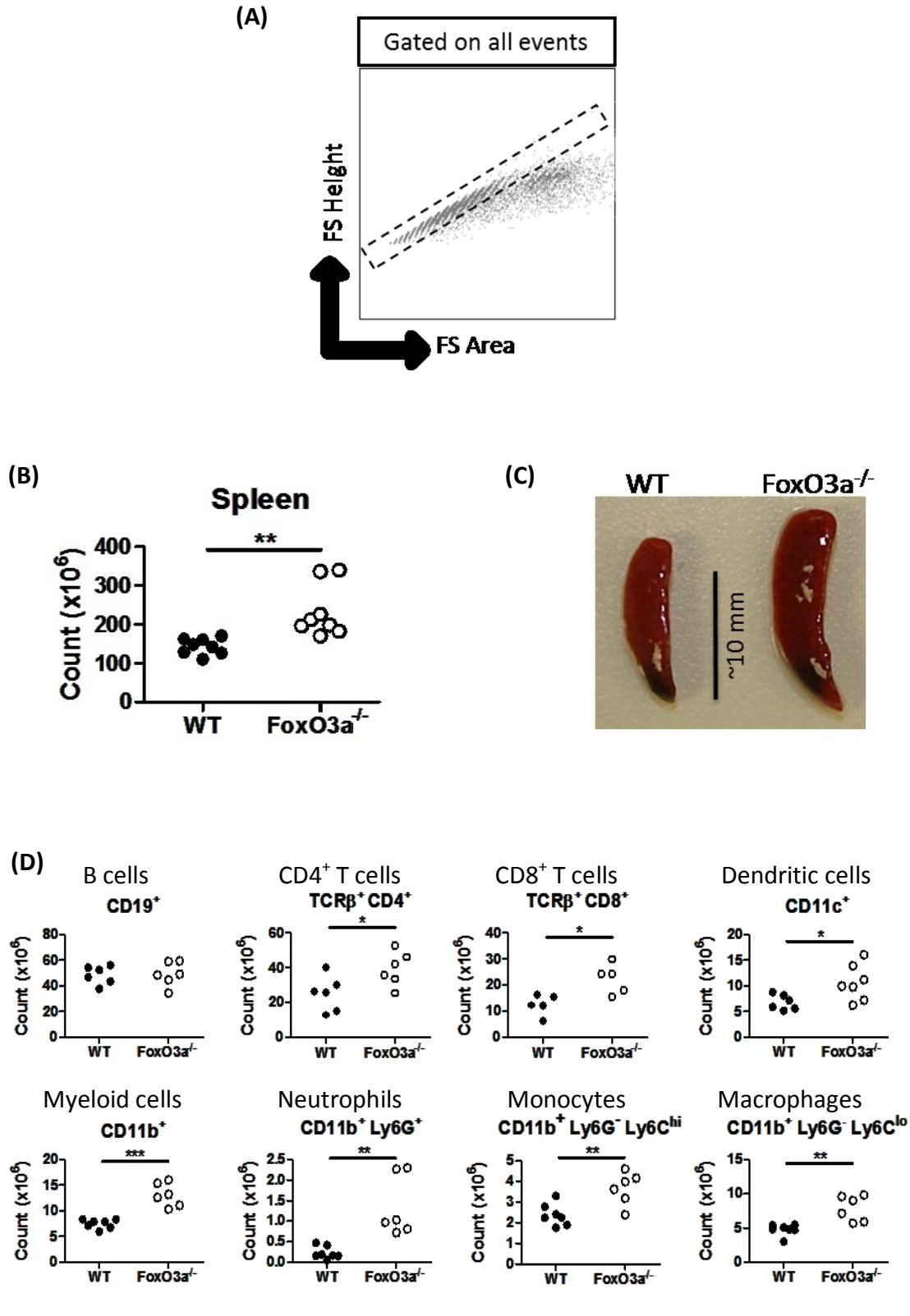
(A)
Gated on all events
FS Helght
FS Area
(B)
Spleen
**
Count (x10^6)
400
300
200
100
0
WT
FoxO3a-/-
(C)
WT
FoxO3a-/-
~10 mm
(D)
B cells
CD19+
CD4+ T cells
TCRβ+ CD4+
CD8+ T cells
TCRβ+ CD8+
Dendritic cells
CD11c+
Myeloid cells
CD11b+
Neutrophils
CD11b+ Ly6G+
Monocytes
CD11b+ Ly6G- Ly6Chi
Macrophages
CD11b+ Ly6G- Ly6Clo
Count (x10^6)
WT
FoxO3a-/-

Figure 1 – FoxO3a signaling promotes immune cell homeostasis in the spleen.

Spleens of 6-8 week old WT and FoxO3a-deficient mice were harvested in R8 medium and single cell suspensions were prepared by homogenization using frosted glass slides. Whole spleen cells were stained with Trypan blue and live cells were counted and using a hemocytometer. 10^6 cells were washed with PBS before staining with fluorophore-conjugated antibodies against various cell surface receptors to perform immune-phenotyping analysis by flow cytometry. After performing doublet-exclusion, various immune cell populations (indicated in the graph titles) were gated on and enumerated.

(A) The gating strategy used to perform doublet-exclusion is displayed. Cells that had an equal distribution of height and area on the forward light scatter were gated as single cells.

(B) A graph displaying the total spleen cell numbers of WT and FoxO3a-deficient mice is displayed.

(C) Representative images of spleens from WT and FoxO3a-deficient mice are displayed.

(D) Graphs displaying the numbers of various immune cell subsets in the spleens of WT and FoxO3a-deficient mice are displayed as indicated in the individual graph titles.

Each circle represents a mouse; a black circle represents a WT C57BL/6J mouse and a white circle represents a FoxO3a-deficient mouse. Data were collected over 6-8 independent experiments (n=6-8). Statistical significance was calculated by unpaired t test. *$p<0.05$, **$p<0.01$, ***$p<0.001$

3.2. Role of FoxO3a in $CD8^+$ T cell activation

3.2.1. Absence of FoxO3a signaling does not influence the activation status of $CD8^+$ T cells in naïve mice

A key question that needed to be addressed was whether the increased numbers of $CD8^+$ T cells in FoxO3a-deficient mice displayed any evidence of activation. Naïve $CD8^+$ T cells express high levels of L-selection (CD62L), α-chain of IL-7 receptor (CD127) and display minimal expression of CD69 whereas activated cells display reduced levels of CD62L, CD127 and higher levels of CD69 (Wherry and Ahmed, 2004). Therefore, the expression of various activation markers on WT and FoxO3a-deficient $CD8^+$ T cells were evaluated by flow cytometry. As indicated in Figure 2, the majority of $CD8^+$ T cells in both WT and FoxO3a-deficient mice were phenotypically naïve. These results indicate that although FoxO3a-deficient mice have significantly higher numbers of $CD8^+$ T cells in their spleens, they still maintain a naïve phenotype.

3.2.2. Lack of FoxO3a signaling enhances $CD8^+$ T cell activation upon polyclonal TCR stimulation and co-stimulation

T cells can be stimulated polyclonally by incubation on anti-CD3 and anti-CD28 antibody coated plates which results in stimulation of both the TCR and the co-stimulatory receptor. This model eliminates the differences in activation thresholds that may occur due to variations in peptide affinities for their respective TCRs and therefore all T cells are activated similarly. Also, this model eliminates the need for high antigen amounts and effective antigen presenting cells (Riddell and Greenberg, 1990).

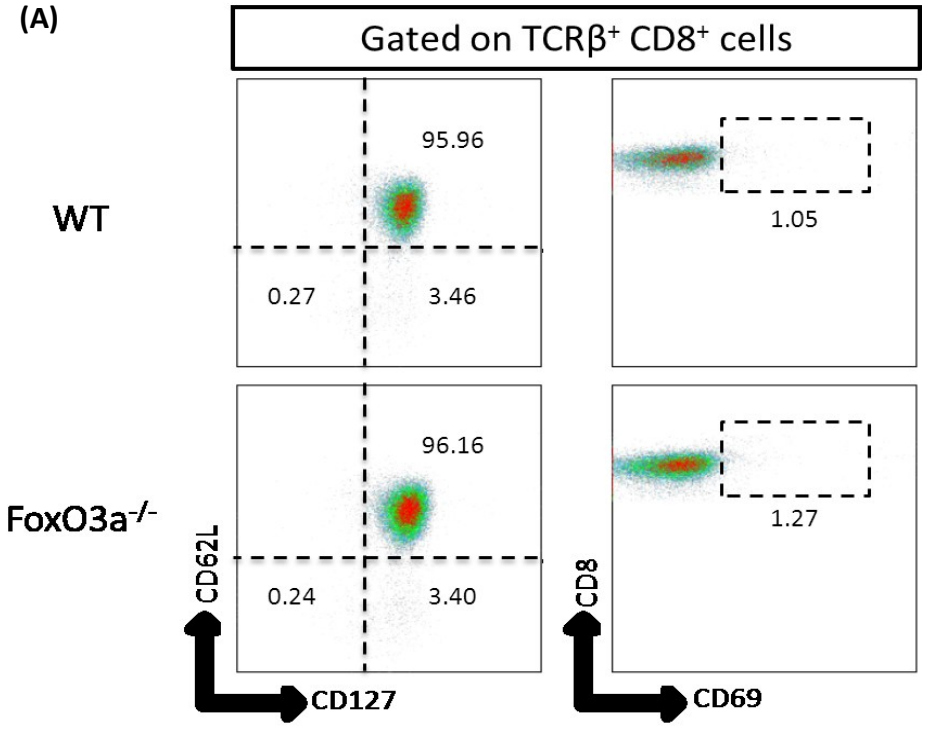
(A)
Gated on TCRβ+ CD8+ cells
WT
FoxO3a-/-
95.96
0.27
3.46
1.05
96.16
0.24
3.40
1.27
CD62L
CD127
CD8
CD69

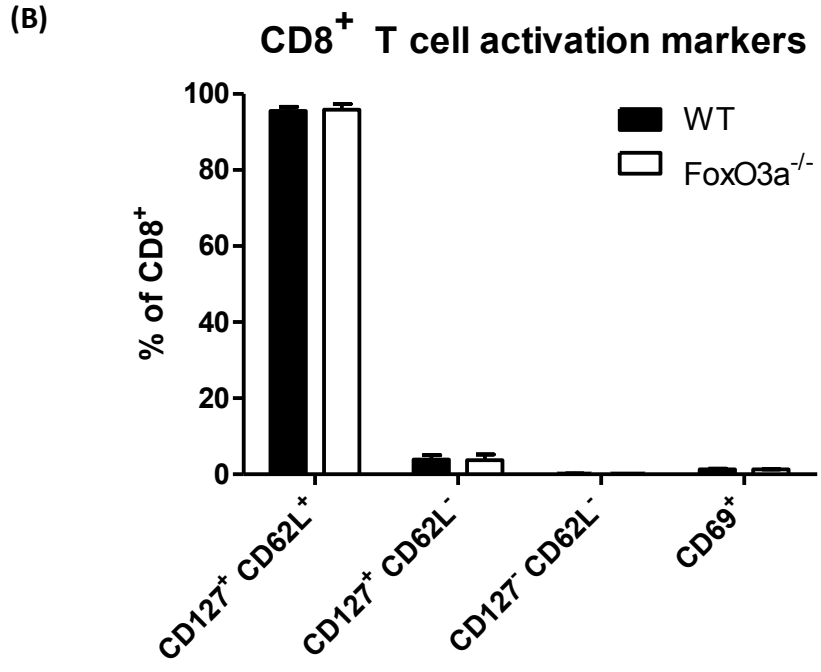
(B)
CD8+ T cell activation markers
WT
FoxO3a-/-
% of CD8+
100
80
60
40
20
0
CD127+ CD62L+
CD127+ CD62L-
CD127- CD62L-
CD69+

Figure 2 – FoxO3a signaling does not affect the activation status of $CD8^+$ T cells in naïve mice.

Single cell suspensions were prepared from whole spleens of 6-8 week old WT and FoxO3a-deficient mice as described before. 10^6 cells were stained with fluorophore-tagged antibodies against TCRβ and CD8 and against various activation markers (CD69, CD62L and CD127). After doublet-exclusion, $CD8^+$ T cells were gated as $TCR\beta^+$ $CD8^+$ and they were then gated on dot plots of CD62L vs. CD127 and CD8 vs. CD69. Naïve cells were gated as $CD127^+$ $CD62L^+$ and effector cells were gated as $CD127^-$ $CD62L^-$.

(A) Representative dot plots displaying the expression of CD62L, CD127 and CD69 by $CD8^+$ T cells are displayed. Percentages of the populations in the respective gates are indicated.

(B) A graph showing the percentages of the various subsets of $CD8^+$ T cells based on their expression of activation markers is displayed. Data are represented as mean ± SEM pooled from three independent experiments (n=3).

Upon polyclonal stimulation using plate-bound anti-CD3 and anti-CD28 antibodies, FoxO3a-deficient $CD8^+$ T cells exhibited increased MTT reduction, compared to WT $CD8^+$ T cells at various time points post-stimulation (Figure 3A). In addition, even non-stimulated FoxO3a-deficient $CD8^+$ T cells displayed a subtle increase in MTT reduction compared to WT $CD8^+$ T cells (Figure 3B).

Upon visual examination of the cells under a microscope, the clusters of proliferating cells were larger in FoxO3a-deficient $CD8^+$ T cells compared to those with WT $CD8^+$ T cells at 48 h post-stimulation with no visible differences at 24 h post-stimulation (Figure 4).

Also, an examination of cellular size and granularity through forward and side light scatter analysis respectively, revealed increased number of lymphoblasts in FoxO3a-deficient $CD8^+$ T cells compared to those of WT $CD8^+$ T cells at various time points post-stimulation (Figure 5A-B).

3.2.3. $CD8^+$ T cell proliferation is limited by FoxO3a signaling

As MTT reduction can be indicative of both cell proliferation and metabolism, a different assay was used to specifically measure cell proliferation post-stimulation. CFSE is a fluorescent dye that binds to intracellular proteins and is distributed equally among daughter cells as the parent cell divides.

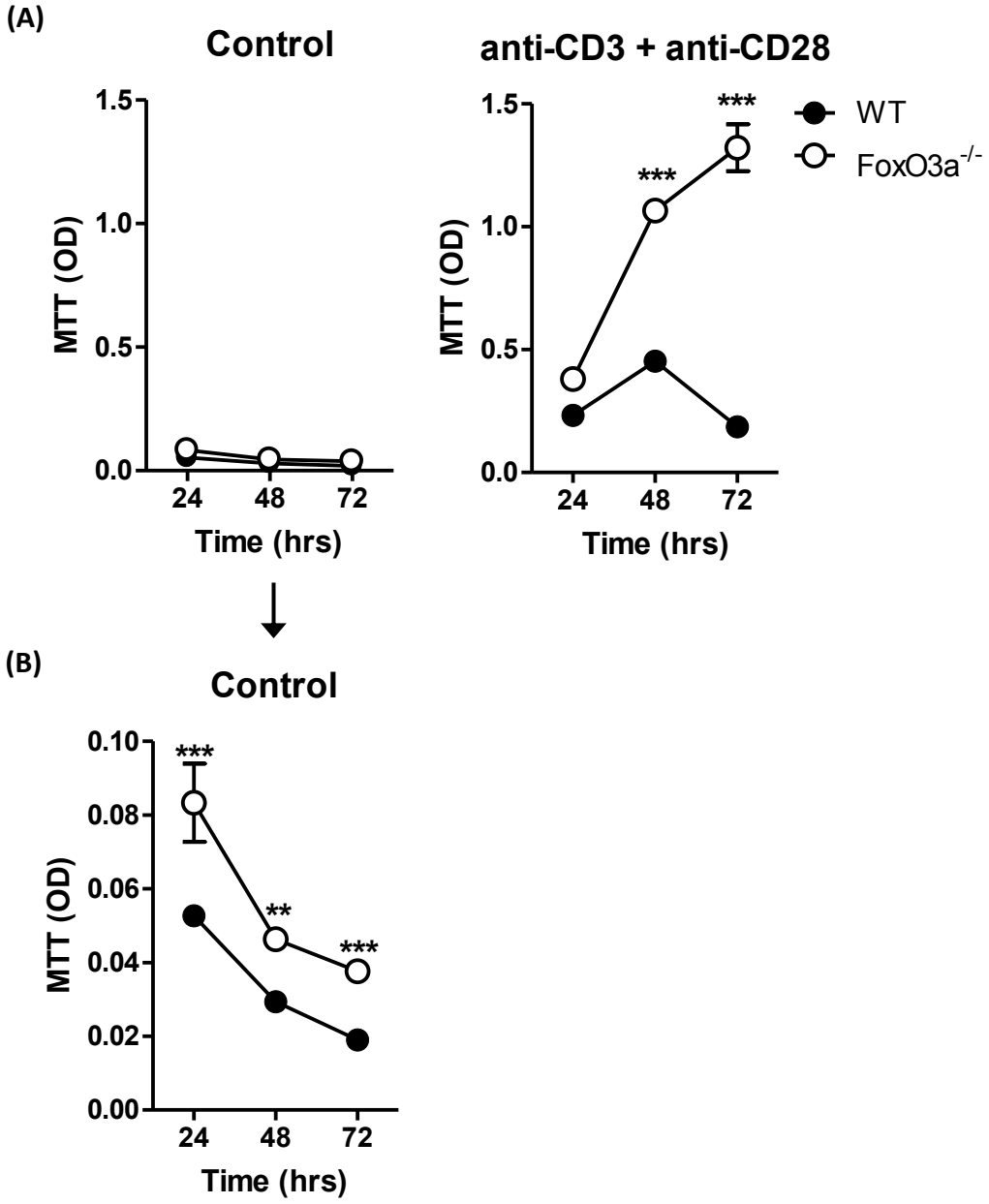
(A)
Control
anti-CD3 + anti-CD28
MTT (OD)
1.5
1.0
0.5
0.0
24
48
72
Time (hrs)
***
***
WT
FoxO3a-/-
(B)
Control
0.10
0.08
0.06
0.04
0.02
0.00
***
**
***

Figure 3 – Enhanced activation of FoxO3a-deficient $CD8^+$ T cells stimulated with anti-CD3 and anti-CD28 antibodies.

$CD8^+$ T cells were isolated from the spleens of WT and FoxO3a-deficient mice and stimulated (10^5 cells) in 96 well flat-bottom plates coated with plate-bound anti-CD3 and anti-CD28 antibodies at 1 μg/ml each. PBS was used as an unstimulated control. MTT assay was performed at the indicated time points post-stimulation and the absorbance of the reduced product was measured.

(A) Graphs showing the absorbance (OD) values of the reduced product from MTT assays on WT and FoxO3a-deficient $CD8^+$ T cells at various time points post-stimulation are displayed. Data are presented as mean ± SEM and are a representative of three independent experiments (n=3). Statistical significance was calculated by two-way ANOVA using GraphPad Prism software and asterisks indicate significant differences. ***p<0.001

(B) A magnified view of the OD values of unstimulated WT and FoxO3a-deficient $CD8^+$ T cells with a reduced scale on y-axis is displayed. **p<0.01, ***p<0.001

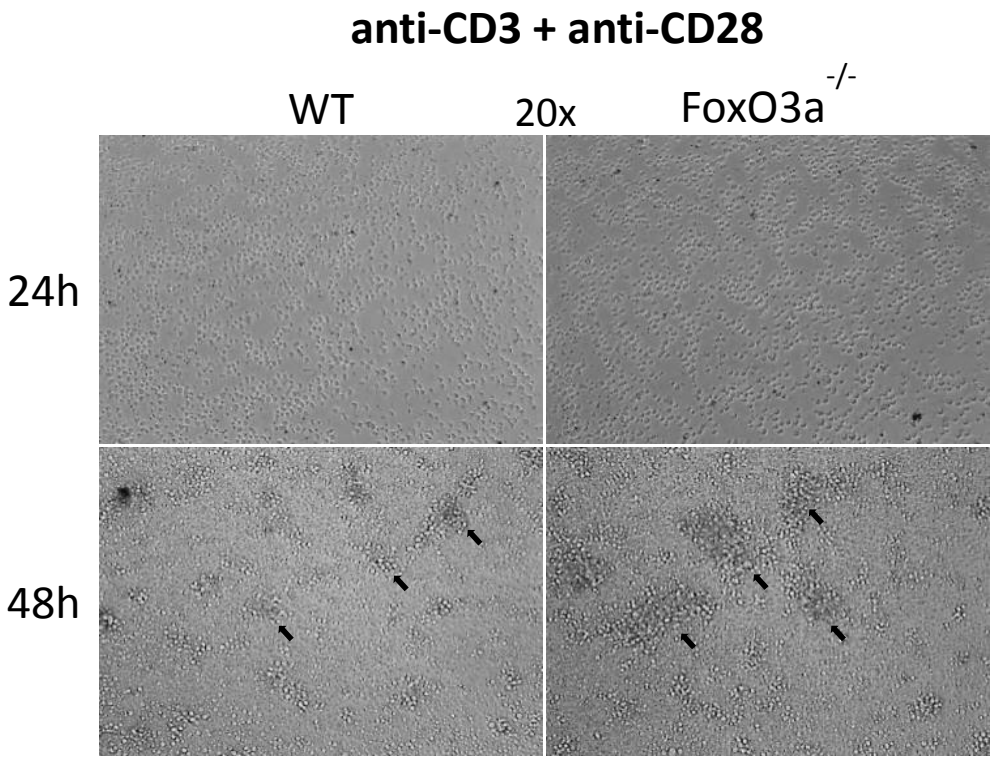
anti-CD3 + anti-CD28
WT
20x
FoxO3a-/-
24h
48h

Figure 4 – Increase in size of proliferating clusters of activated FoxO3a-deficient $CD8^+$ T cells stimulated with anti-CD3 and anti-CD28 antibodies.

$CD8^+$ T cells were purified from spleens of WT and FoxO3a-deficient mice and stimulated with plate-bound anti-CD3 and anti-CD28 antibodies as described before.

Microscopic images were taken at various time points post-stimulation and representative images from three independent experiments (n=3) are shown. The arrows point towards clusters of proliferating $CD8^+$ T cells at 48 h post-stimulation.

(A)

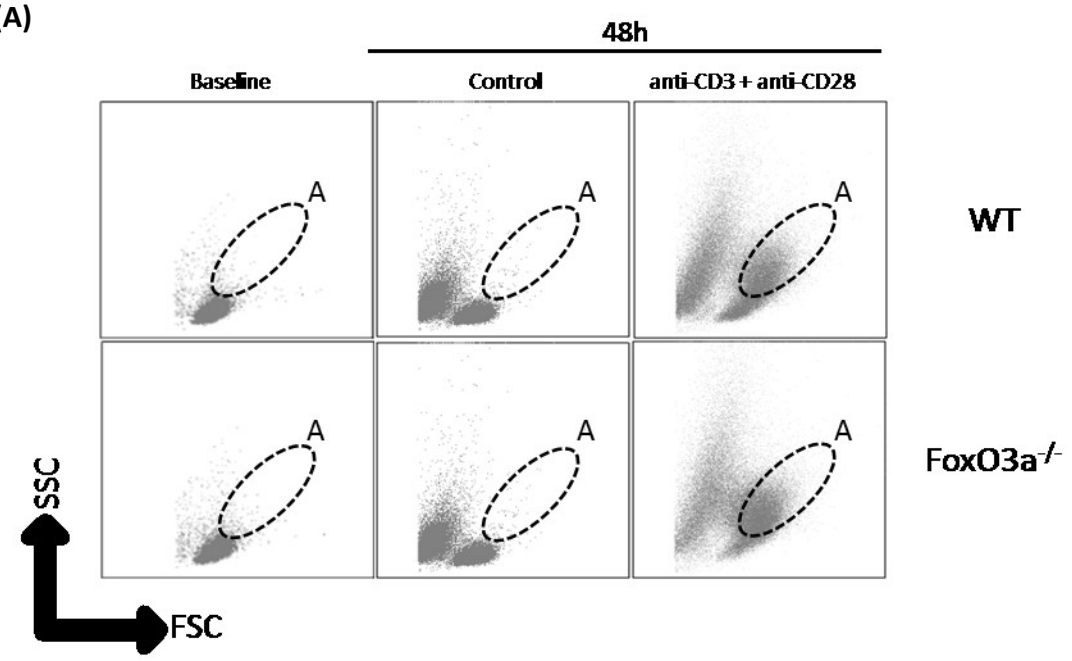
48h
Baseline
Control
anti-CD3 + anti-CD28
A
WT
FoxO3a-/-
SSC
FSC

(B)

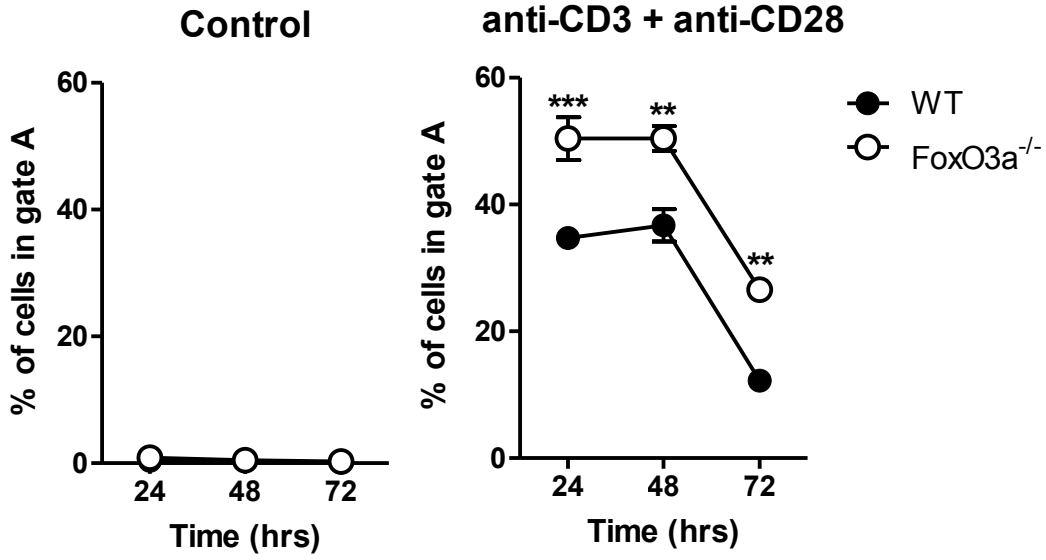
Control
anti-CD3 + anti-CD28
% of cells in gate A
60
40
20
0
24
48
72
Time (hrs)
***
**
**
WT
FoxO3a-/-

Figure 5 –FoxO3a-deficient $CD8^+$ T cells display increased activation following stimulation.

$CD8^+$ T cells from WT and FoxO3a-deficient mice were stimulated with anti-CD3 and anti-CD28 antibodies as described above. At various time points post-stimulation, WT and FoxO3a-deficient $CD8^+$ T cells were analyzed and compared on the basis of size and granularity by flow cytometry after doublet-exclusion.

(A) Representative dot plots of forward scatter (FSC) versus side scatter (SSC) are shown. The population of cells in the gate indicated (gate A) are lymphoblasts.

(B) The percentages of lymphoblasts were quantified at various time points post-stimulation and are represented in the graphs shown. Data are presented as mean ± SEM and are representative of three independent experiments (n=3). Statistical significance was calculated by two-way ANOVA. **p<0.01, ***p<0.001

Therefore, a reduction in the intensity of CFSE fluorescence (evaluated by flow cytometry), is used as a measure of cell proliferation or cell division. CFSE-labeled WT and FoxO3a-deficient $CD8^+$ T cells were stimulated with anti-CD3 and anti-CD28 antibodies. At the indicated time points, cells were harvested and labeled with 7-AAD, a viability dye, in order to measure the proliferation of live ($7AAD^-$) cells (Figure 6A). As indicated in Figure 6, FoxO3a-deficient $CD8^+$ T cells underwent significantly enhanced proliferation in comparison to WT $CD8^+$ T cells at 48 and 72 h post-stimulation (Figure 6B). There was no discernible dilution in CFSE fluorescence at 24 h post-stimulation in either WT or FoxO3a-deficient $CD8^+$ T cells.

As indicated in the Figure 6A, successive peaks starting from the one on the far right (undivided cells) indicate successive cell divisions. I observed that a higher proportion of FoxO3a-deficient $CD8^+$ T cells had undergone more than 2 and 3 divisions compared to the WT $CD8^+$ T cells (Figure 6C). In addition, the proportion of $CD8^+$ T cells that had not undergone any cell division was higher in WT than in FoxO3a-deficient $CD8^+$ T cells. Thus, by examination of MTT reduction, cell imaging, as well as by CFSE dilution analysis, FoxO3a-deficient $CD8^+$ T cells appear to display increased proliferation following TCR stimulation.

3.2.4. Cycling of activated $CD8^+$ T cells is limited by FoxO3a signaling

To further reveal whether FoxO3a impacts the cycling of $CD8^+$ T cells, I evaluated the intracellular expression of Ki67 in proliferating $CD8^+$ T cells by flow cytometry.

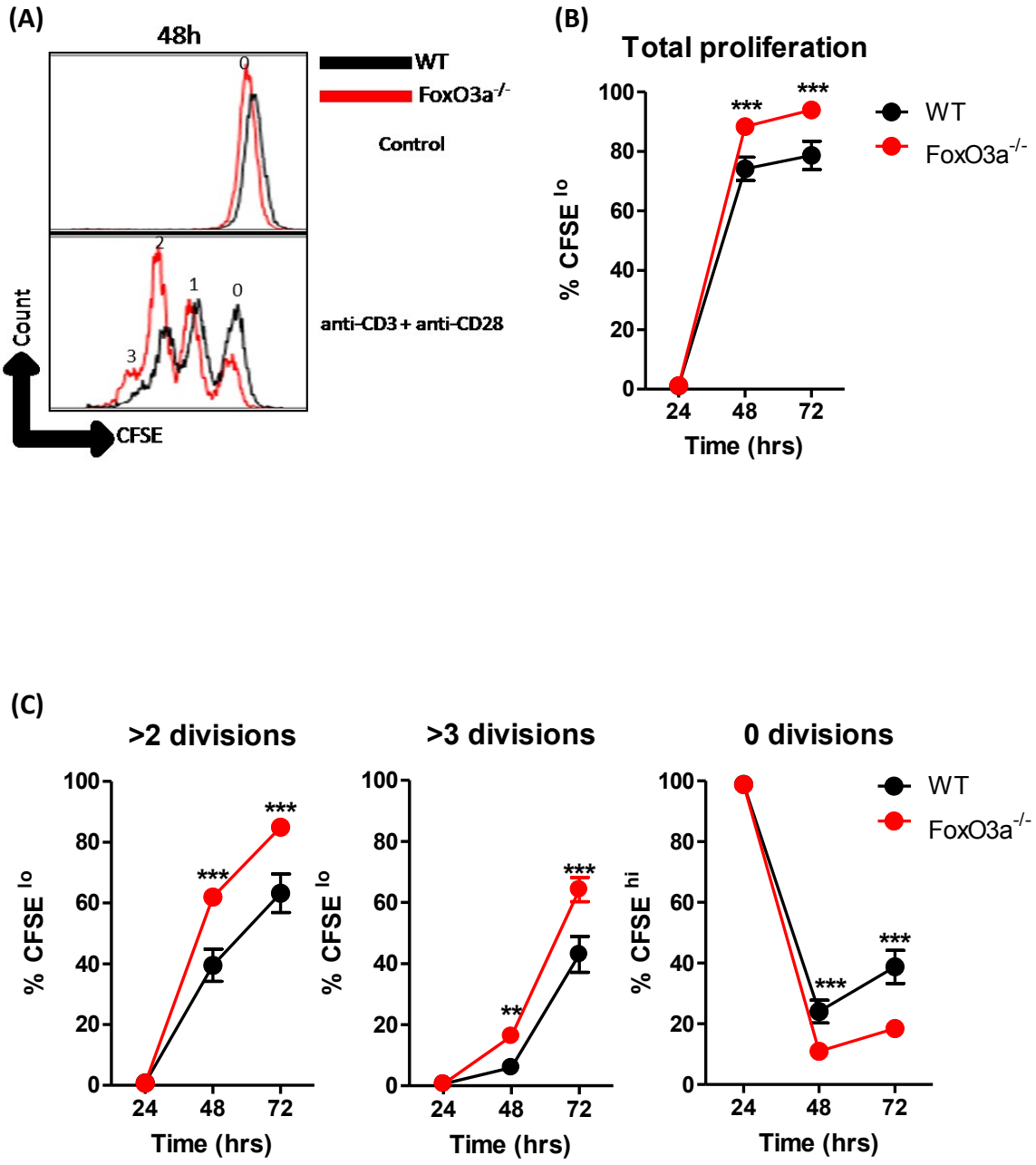
(A)
48h
WT
FoxO3a-/-
Control
anti-CD3 + anti-CD28
Count
CFSE
0
1
2
3
(B)
Total proliferation
% CFSE lo
Time (hrs)
WT
FoxO3a-/-
***
(C)
>2 divisions
>3 divisions
0 divisions
% CFSE lo
% CFSE hi
Time (hrs)
**

Figure 6 – FoxO3a signaling limits the proliferation of activated $CD8^+$ T cells.

CFSE-labeled $CD8^+$ T cells were stimulated with anti-CD3 and anti-CD28 antibodies as described before. At the indicated time points post-stimulation, the reduction in CFSE intensity was measured by flow cytometry to assess proliferation. Total $7AAD^-$ (live) cells were gated for evaluation of CFSE dilution (proliferation).

(A) Representative CFSE histograms of live WT and FoxO3a-deficient $CD8^+$ T cells at 48 h post-stimulation are displayed. The number at the top of each peak indicates the division number.

(B) A graph showing the total CFSE dilution of WT and FoxO3a-deficient $CD8^+$ T cells at the indicated time points post-stimulation is shown. Data are presented as mean ± SD of three independent experiments (n=3). Statistical significance was calculated by two-way ANOVA. ***p<0.001

(C) Graphs indicating the CFSE dilutions of activated $CD8^+$ T cells from the second or third division onwards indicated by >2 divisions and >3 divisions respectively are shown. Also, a graph quantifying the percentage of unstimulated cells (0 divisions) is indicated. All data are presented as mean ± SD and are representative of three independent experiment (n=3). Statistical significance was calculated by two-way ANOVA. **p<0.01, ***p<0.001

Ki67 is a nuclear protein that is upregulated once the cell enters the G1 phase from the resting G0 phase. An increased level of Ki67 expression is associated with increased cell cycling. At various time points post-stimulation, WT and FoxO3a-deficient $CD8^+$ T cells were stained with FITC-conjugated Ki67 by intracellular staining and the percentage of $Ki67^+$ cells was evaluated by flow cytometry (Figure 7A). An increased proportion of $Ki67^+$ FoxO3a-deficient $CD8^+$ T cells was observed compared to $Ki67^+$ WT $CD8^+$ T cells at various time points post-stimulation (Figure 7B).

3.2.5. Lack of FoxO3a signaling does not influence $p27^{kip}$ expression in activated $CD8^+$ T cells

$p27^{kip}$ is a cell cycle arrest protein which 'arrests' the cell in the G0 phase thereby preventing cell cycle progression. Previous studies have shown that FoxO3a regulates the expression of $p27^{kip}$ in T cells (Marie et al., 2002) and so I wanted to find out if a decreased level of $p27^{kip}$ expression was the mechanism underlying the enhanced cell cycling of FoxO3a-deficient $CD8^+$ T cells. At various time points post-stimulation, cell lysates were collected from WT and FoxO3a-deficient $CD8^+$ T cells and the expression of $p27^{kip}$ was assessed by Western blotting and quantified by densitometry (Figure 8A). As the cells progressed through the cell cycle following TCR stimulation, the levels of $p27^{kip}$ decreased, which was followed by gradual restoration of $p27^{kip}$ levels. However, there were no statistical differences in the protein expression levels of $p27^{kip}$ between WT and FoxO3a-deficient $CD8^+$ T cells at various time points post-stimulation (Figure 8B).

(A)

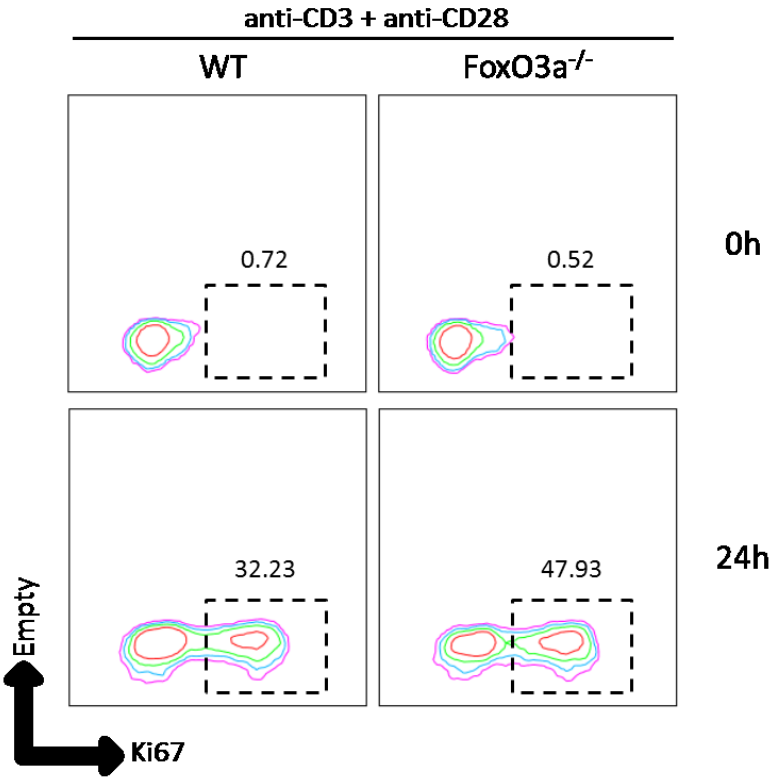
anti-CD3 + anti-CD28
WT
FoxO3a-/-
0.72
0.52
0h
32.23
47.93
24h
Empty
Ki67

(B)

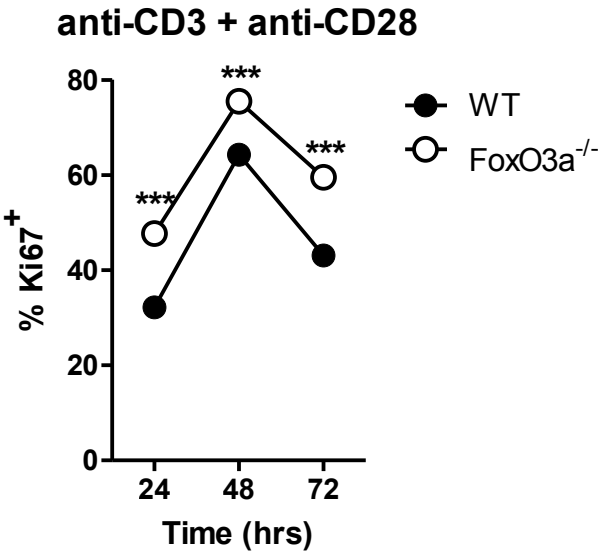
anti-CD3 + anti-CD28
80
60
40
20
0
% Ki67+
***
***
***
24
48
72
Time (hrs)
WT
FoxO3a-/-

Figure 7 – Increased expression of Ki67 in activated FoxO3a-deficient $CD8^+$ T cells.

WT and FoxO3a-deficient $CD8^+$ T cells were stimulated with anti-CD3 and anti-CD28 antibodies as described before. At the indicated time points post-stimulation, cells were fixed and permeabilized. The permeabilized cells were then stained with anti-Ki67 antibody by intracellular staining and the percentage of $Ki67^+$ cells were assessed and compared between activated WT and FoxO3a-deficient $CD8^+$ T cells.

(A) Representative dot plots showing Ki67 expression in WT and FoxO3a-deficient $CD8^+$ T cells at the time points indicated are shown. The percentages of $Ki67^+$ cells are indicated above the gates.

(B) A graph representing the percentages of $Ki67^+$ WT and FoxO3a-deficient $CD8^+$ cells is displayed. Data are presented as mean ± SD and are representative of three independent experiments (n=3). Statistical significance was calculated by two-way ANOVA. ***$p<0.001$

(A)

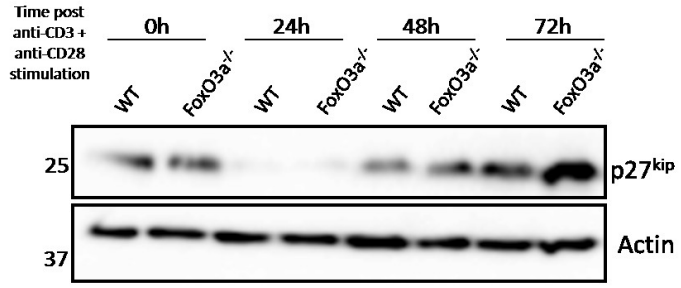
Time post anti-CD3 + anti-CD28 stimulation
0h
24h
48h
72h
WT
FoxO3a-/-
WT
FoxO3a-/-
WT
FoxO3a-/-
WT
FoxO3a-/-
25
p27kip
37
Actin

(B)

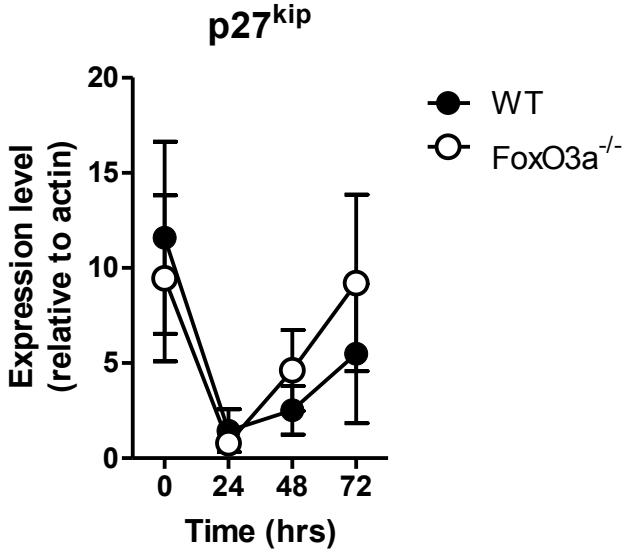
p27kip
Expression level (relative to actin)
20
15
10
5
0
0
24
48
72
Time (hrs)
WT
FoxO3a-/-

Figure 8 – FoxO3a does not impact $p27^{kip}$ expression in activated $CD8^+$ T cells.

WT and FoxO3a-deficient $CD8^+$ T cells (10^6) were stimulated in 24 well plates with anti-CD3 and anti-CD28 antibodies as described before. At the time points indicated, the cells were lysed and the total protein was resolved by SDS-PAGE and transferred onto PVDF membranes by electroblotting. The expression of a cell cycle arrest protein, $p27^{kip}$, was determined by western blotting. The band intensities were quantified by densitometry and were compared to β-actin (loading control).

(A) Representative image of a western blot showing $p27^{kip}$ expression in WT and FoxO3a-deficient $CD8^+$ T cells at various time points post-stimulation are shown.

(B) A graph showing the relative expression level of $p27^{kip}$ in WT and FoxO3a-deficient $CD8^+$ T cells at the indicated time points post-stimulation is displayed. Data are presented as mean ± SEM and are pooled from three independent experiments (n=3).

3.2.6. FoxO3a regulates the threshold of $CD8^+$ T cell activation

Since the FoxO3a-deficient $CD8^+$ T cells underwent enhanced proliferation in comparison to WT $CD8^+$ T cells upon polyclonal stimulation, I wanted to determine if FoxO3a signaling regulates the threshold of $CD8^+$ T cell activation. WT and FoxO3a-deficient $CD8^+$ T cells were stimulated with varying concentrations of anti-CD3 antibody (and 1 μg/ml anti-CD28 antibody) and the magnitude of proliferation was measured by CFSE dilution.

Indeed, at a low concentration (0.2 μg/ml) of anti-CD3 antibody, FoxO3a-deficient $CD8^+$ T cells displayed significantly enhanced proliferation compared to WT $CD8^+$ T cells which exhibited little to no dilution in CFSE intensity (Figure 9A-B). It is known that CD28 co-stimulation potentiates the effects of TCR stimulation-induced T cell activation (Acuto and Michel, 2003). So I wanted to determine if TCR stimulation alone was enough to induce (co-stimulation independent) activation of FoxO3a-deficient $CD8^+$ T cells compared to WT $CD8^+$ T cells. While CD28 engagement resulted in an enhancement in $CD8^+$ T cell activation, FoxO3a-deficient $CD8^+$ T cells displayed enhanced MTT reduction even in the absence of CD28 engagement compared to WT $CD8^+$ T cells (Figure 10). Taken together, these results indicate that FoxO3a signaling influences the direct TCR driven mechanism of $CD8^+$ T cell proliferation.

(A)

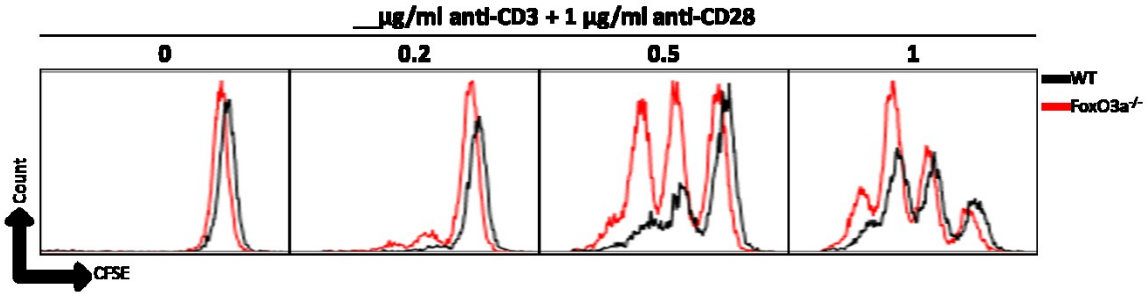
__µg/ml anti-CD3 + 1 µg/ml anti-CD28
0
0.2
0.5
1
WT
FoxO3a-/-
Count
CFSE

(B)

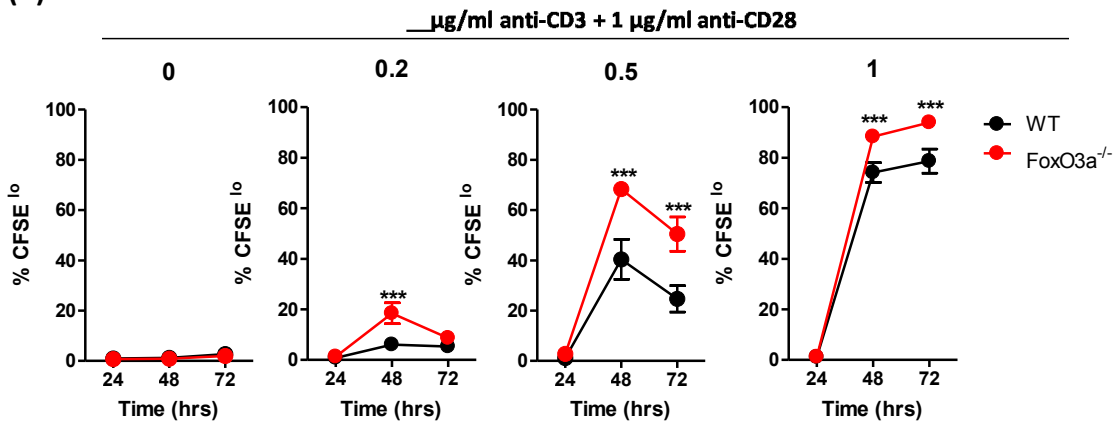
__µg/ml anti-CD3 + 1 µg/ml anti-CD28
0
0.2
0.5
1
% CFSE lo
Time (hrs)
24
48
72
***
WT
FoxO3a-/-

Figure 9 – FoxO3a modulates the threshold of activation of $CD8^+$ T cells.

CFSE-labeled WT and FoxO3a-deficient $CD8^+$ T cells were stimulated with varying concentrations of anti-CD3 antibody with a constant concentration anti-CD28 antibody. CFSE dilution was quantified at the indicated time points by flow cytometry to evaluate their proliferation.

(A) Representative histograms showing CFSE dilution of WT and FoxO3a-deficient $CD8^+$ T cells stimulated with varying concentrations of anti-CD3 antibody (histogram titles) and a constant concentration of anti-CD28 antibody as indicated at 48 h post-stimulation are displayed.

(B) Graphs indicating the CFSE dilutions of WT and FoxO3a-deficient $CD8^+$ T cells at varying anti-CD3 concentrations (graph titles) and constant anti-CD28 are shown. Data are presented as mean ± SD and are representative of two independent experiments (n=2). Statistical significance was calculated by two-way ANOVA. ***$p<0.001$

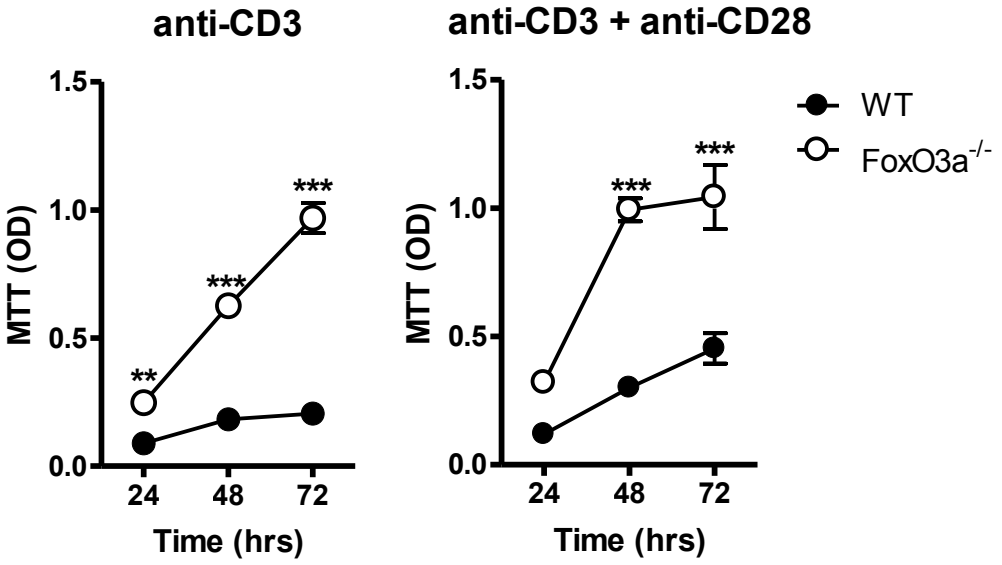
anti-CD3
anti-CD3 + anti-CD28
MTT (OD)
1.5
1.0
0.5
0.0
24
48
72
Time (hrs)
**
***
***
***
***
WT
FoxO3a-/-

Figure 10 – Enhanced co-stimulation independent activation of FoxO3a-deficient $CD8^+$ T cells.

WT and FoxO3a-deficient $CD8^+$ T cells were stimulated with either 1 μg/ml anti-CD3 or 1 μg/ml each of anti-CD3 and anti-CD28. MTT assay was performed at the indicated time points post-stimulation.

Graphs showing the absorbance (OD) values of WT and FoxO3a-deficient $CD8^+$ T cells at the indicated time points post-stimulation are displayed. Data are presented as mean ± SEM and are representative of three independent experiments (n=3). Statistical significance was calculated by two-way ANOVA. **p<0.01, ***p<0.001

3.2.7. FoxO3a signaling influences activated $CD8^+$ T cell death during the late stages of cell division

Since the MTT signals were higher in the FoxO3a-deficient $CD8^+$ T cells compared to WT $CD8^+$ T cells (Figure 3A), it was also possible that FoxO3a-deficient CD8+ T cells underwent reduced cell death following activation. To address this, the numbers of viable cells and dead cells following stimulation were determined.

There were significantly higher numbers of viable FoxO3a-deficient $CD8^+$ T cells as compared to WT $CD8^+$ T cells at 48 and 72 h post-stimulation as measured by Trypan blue staining (Figure 11). There also seemed to be a slightly higher number of viable FoxO3a-deficient $CD8^+$ T cells compared to WT $CD8^+$ T cells at 24 h post-stimulation as well although the differences were not significant.

I used a combination of a fluorescent viability dye and flow cytometry to enumerate the number of dead cells. 7-Aminoactinomycin D (7-AAD) is a fluorescent dye that can enter cells with compromised membrane integrities (dead cells) and intercalate in double-stranded DNA. Therefore, dead cells will appear $7AAD^+$ whereas live cells will be $7AAD^-$. At various time points post-stimulation, WT and FoxO3a-deficient CD8+ T cells were stained with 7AAD and the percentages of dead cells ($7AAD^+$) were quantified by flow cytometry (Figure 12A). A significantly lower number of dead FoxO3a-deficient $CD8^+$ T cells was observed as compared to WT $CD8^+$ T cells at 48 and 72 h post-stimulation (late stages of activation) whereas there was no difference at 24 h post-stimulation (Figure 12B).

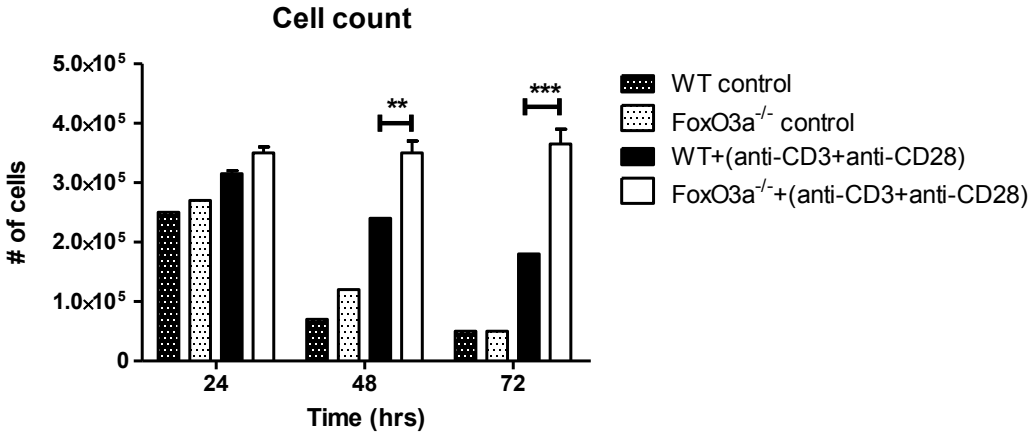
Cell count
5.0x10^5
4.0x10^5
3.0x10^5
2.0x10^5
1.0x10^5
0
# of cells
**
***
24
48
72
Time (hrs)
WT control
FoxO3a-/- control
WT+(anti-CD3+anti-CD28)
FoxO3a-/-+(anti-CD3+anti-CD28)

Figure 11 –Increased number of viable FoxO3a-deficient $CD8^+$ T cells post-stimulation with anti-CD3 and anti-CD28 antibodies.

WT and FoxO3a-deficient $CD8^+$ T cells ($5x10^5$) were stimulated in 24 well plates with anti-CD3 and anti-CD28 antibodies as described before. At the indicated time points post-stimulation, the numbers of viable cells were enumerated by Tryphan blue staining and counting using a hemocytometer.

A graph showing the numbers of viable WT and FoxO3a-deficient $CD8^+$ T cells is displayed. Data are presented as mean ± SEM of three independent experiments (n=3). Statistical significance was calculated using two-way ANOVA. **p<0.01, ***p<0.001

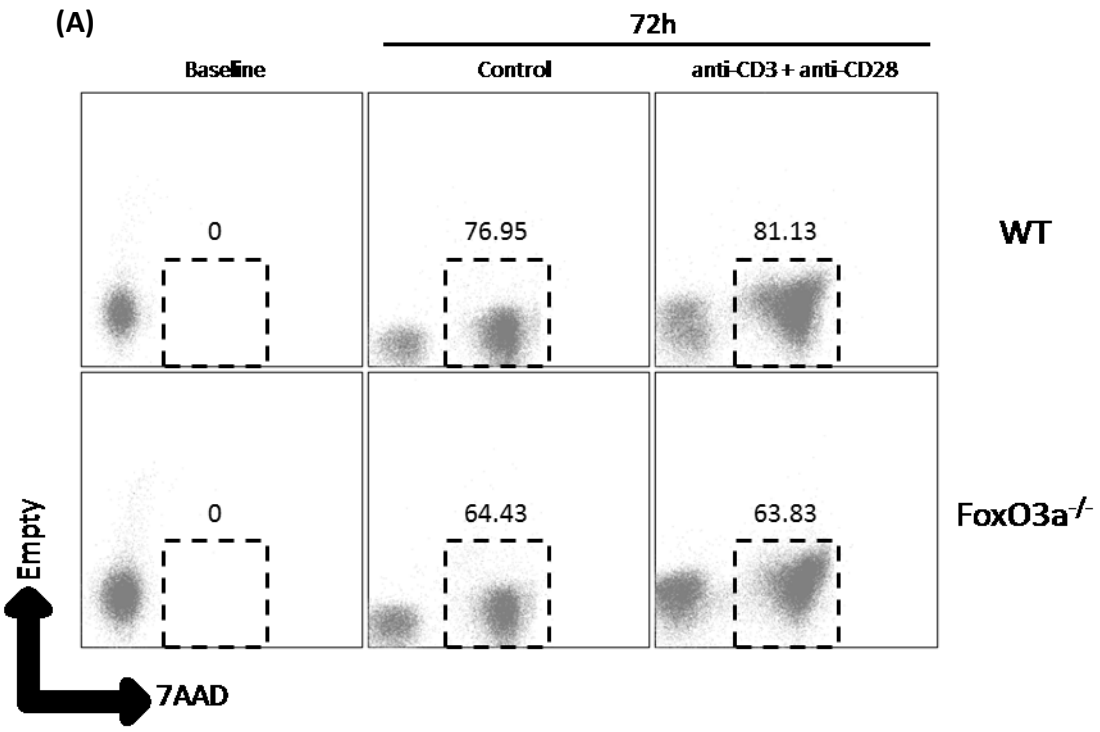
(A)
72h
Baseline
Control
anti-CD3 + anti-CD28
0
76.95
81.13
WT
0
64.43
63.83
FoxO3a-/-
Empty
7AAD

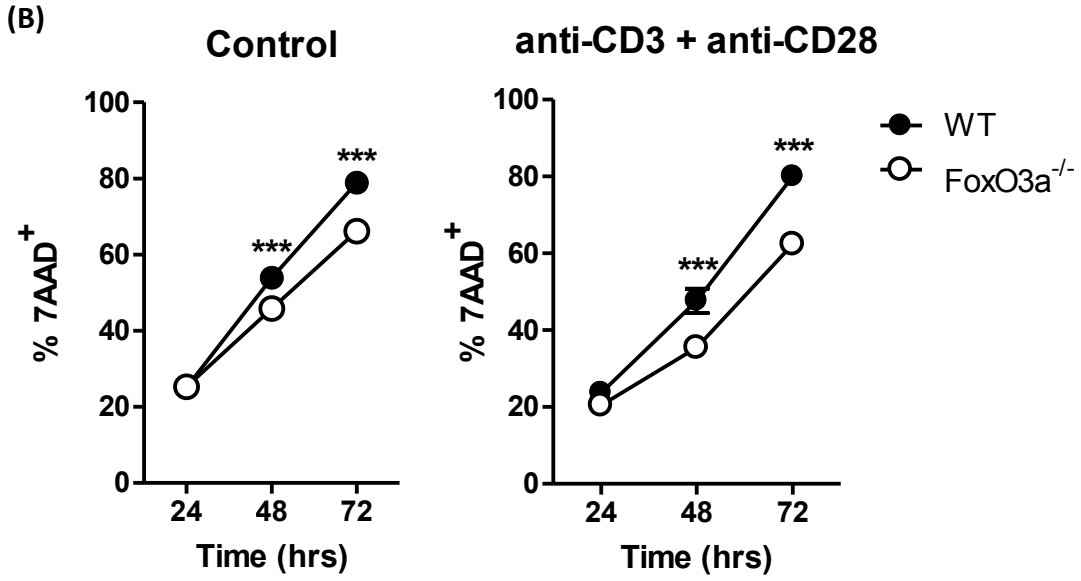
(B)
Control
anti-CD3 + anti-CD28
% 7AAD+
100
80
60
40
20
0
***
***
***
***
24
48
72
Time (hrs)
WT
FoxO3a-/-

Figure 12 – FoxO3a signaling modulates $CD8^+$ T cell death.

WT and FoxO3a-deficient $CD8^+$ T cells were stimulated with anti-CD3 and anti-CD28 antibodies as described before. At various time points post-stimulation, their viability was assessed by 7-AAD staining. Cells were washed with PBS and stained with 7-AAD followed by incubation at RT for 10 min. The stained cells were acquired on the flow cytometer immediately and the percentage of $7AAD^+$ cells was quantified.

(A) Representative dot plots showing 7AAD expression in WT and FoxO3a-deficient $CD8^+$ T cells at 72 h post-stimulation are displayed. The numbers indicate the percentages of cells in the gates.

(B) Graphs displaying the percentages of $7AAD^+$ WT and FoxO3a-deficient $CD8^+$ T cells at the indicated time points are shown. Data are presented as mean ± SEM and are representative of three independent experiments (n=3). Statistical significance was calculated by two-way ANOVA. ***$p<0.001$

In addition, there was significantly reduced cell death in unstimulated FoxO3a-deficient $CD8^+$ T cells compared to WT $CD8^+$ T cells at 48 and 72 h post-culture.

To get a better understanding of when FoxO3a signaling promotes the commitment of cells to death following activation, I evaluated 7AAD staining in cells as they went into various rounds of division (based on CFSE gating) (Figure 13A). By this analysis, several differences were noted. Firstly, at 72h post-stimulation, there were hardly any FoxO3a-deficient cells that had not committed to cell division in contrast to WT cells where a significant proportion of cells had still not undergone any division (Figure 13A). Secondly, the major commitment to cell death occurred early at 24h when cells were mainly in their initial cycles of proliferation, and there was no difference between WT and FoxO3a-deficient cells. Finally, during the later stages of cycling, FoxO3a-deficient cells displayed reduced cell death commitment compared to WT $CD8^+$ T cells (Figure 13B-C).

3.2.8. FoxO3a signaling promotes apoptosis in activated $CD8^+$ T cells

It has been shown that FoxO3a mediates apoptotic cell death in CTLL-2 T cell lines through upregulation of a pro-apoptotic protein, Bim upon IL-2 withdrawal (Marie et al., 2002). First, I wanted to determine if decreased apoptosis was the reason behind the reduced cell death that was observed in activated FoxO3a-deficient $CD8^+$ T cells. In order to determine whether reduced apoptosis was occurring in activated FoxO3a-deficient $CD8^+$ T cells, purified $CD8^+$ cells from both WT and FoxO3a-deficient mice were treated with a pan-caspase inhibitor (z-VAD) prior to and during stimulation with anti-CD3 and anti-CD28 antibodies.

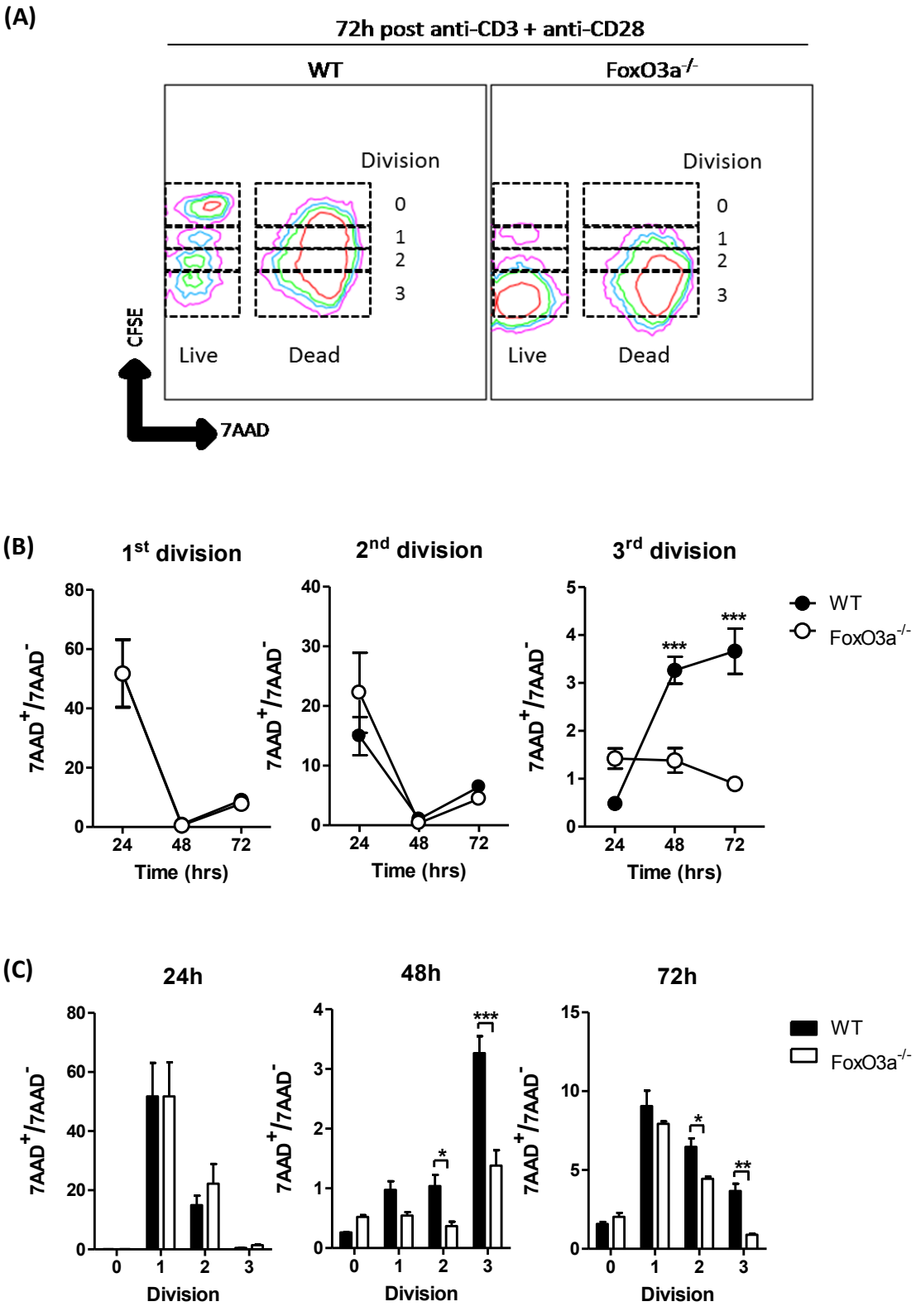
(A)
72h post anti-CD3 + anti-CD28
WT
FoxO3a-/-
Division
0
1
2
3
Live
Dead
CFSE
7AAD
(B)
1st division
2nd division
3rd division
7AAD+/7AAD-
Time (hrs)
WT
FoxO3a-/-
(C)
24h
48h
72h
Division

Figure 13 – FoxO3a signaling modulates $CD8^+$ T cell death at the late stages of cell division.

CFSE-labeled WT and FoxO3a-deficient $CD8^+$ T cells were stimulated with anti-CD3 and anti-CD28 antibodies as described before. At the indicated time points post-stimulation, cells were washed with PBS, stained with 7-AAD and acquired on the flow cytometer. A plot of CFSE vs. 7AAD was used to analyze the percentage of dead ($7AAD^+$) cells compared to live cells ($7AAD^-$) at every cell division.

(A) Representative dot plots of CFSE vs. 7AAD showing the gating strategy used for the analysis to compare the extent of cell death (ratio of the percentages of dead cells to live cells) at every cell division between activated WT and FoxO3a-deficient $CD8^+$ T cells are shown.

(B) Graphs showing the extent of cell death compared to live cells at a particular cell division over time are shown. Data are represented as mean ± SEM and are representative of two independent experiments (n=2). Statistical significance was calculated by two-way ANOVA. ***p<0.001

(C) Graphs showing the extent of cell death compared to live cells at every division during a particular time point is displayed. Data are represented as mean ± SEM and are representative of two independent experiments (n=2). Statistical significance was calculated by two-way ANOVA. *p<0.05, **p<0.01, ***p<0.001

At 72 h post-stimulation, I observed a significant increase in MTT reduction in WT $CD8^+$ T cells treated with z-VAD relative to vehicle control (DMSO) whereas there were no differences in the case of FoxO3a-deficient $CD8^+$ T cells (Figure 14). These results indicate that FoxO3a signaling promotes apoptotic commitment of activated $CD8^+$ T cells. The number of WT $CD8^+$ T cells that went through various rounds of cell division increased with z-VAD treatment, whereas there was no impact in FoxO3a-deficient cells (Figure 15); further suggesting that apoptosis of primed cells by FoxO3a signaling regulates their survival.

In order to gain a mechanistic insight into the modulation of apoptotic death in FoxO3a-deficient $CD8^+$ T cells, I compared the expression of various classical pro-apoptotic markers of cell death including Caspase-3, Caspase-8, Caspase-9 and Bim between WT and FoxO3a-deficient $CD8^+$ T cells. The basal expression of pro-Caspase 3 was very low and was upregulated post-activation whereas there were high basal levels of pro-Caspase 8 and there appeared to be no major changes post-activation. The cleaved (active) form of caspases 3 and 8 were clearly visible only at 48 and 72 h post-stimulation. The cleaved form of Caspase-9 was undetectable in activated $CD8^+$ T cells. The expression of Bim was only slightly upregulated upon activation compared to basal levels (Figure 16A). However, there were no differences in the expressions of cleaved caspases 3 and 8 and Bim between activated WT and FoxO3a-deficient $CD8^+$ T cells (Figure 16B). These results indicate that FoxO3a modulates apoptotic death of $CD8^+$ T cells in a Caspase-independent as well as Bim-independent manner.

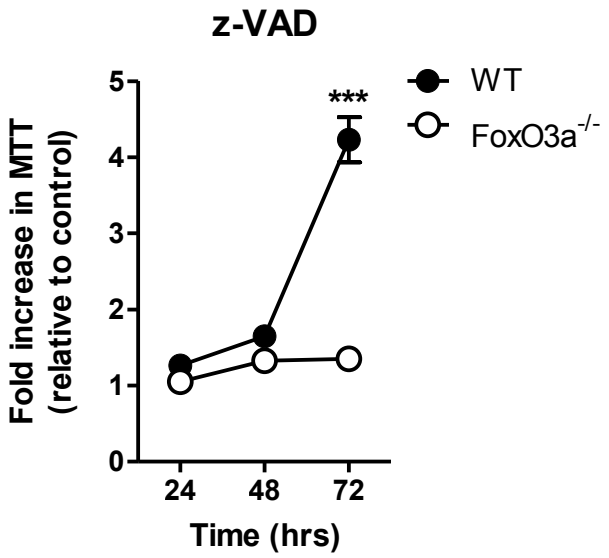
z-VAD
Fold increase in MTT
(relative to control)
5
4
3
2
1
0
24
48
72
Time (hrs)
***
WT
FoxO3a-/-

Figure 14 – FoxO3a promotes apoptotic death in activated $CD8^+$ T cells.

WT and FoxO3a-deficient $CD8^+$ T cells were stimulated with anti-CD3 and anti-CD28 antibodies in the presence of absence of a pan-caspase inhibitor, z-VAD. At various time points post-stimulation, MTT assay was performed and the absorbance values were compared relative to vehicle (DMSO) control.

A graph displaying the OD values of WT and FoxO3a-deficient $CD8^+$ T cells treated with z-VAD compared to DMSO control is shown. Data are presented as mean ± SEM and are representative of two independent experiments (n=2). Statistical significance was calculated by two-way ANOVA. ***$p<0.001$

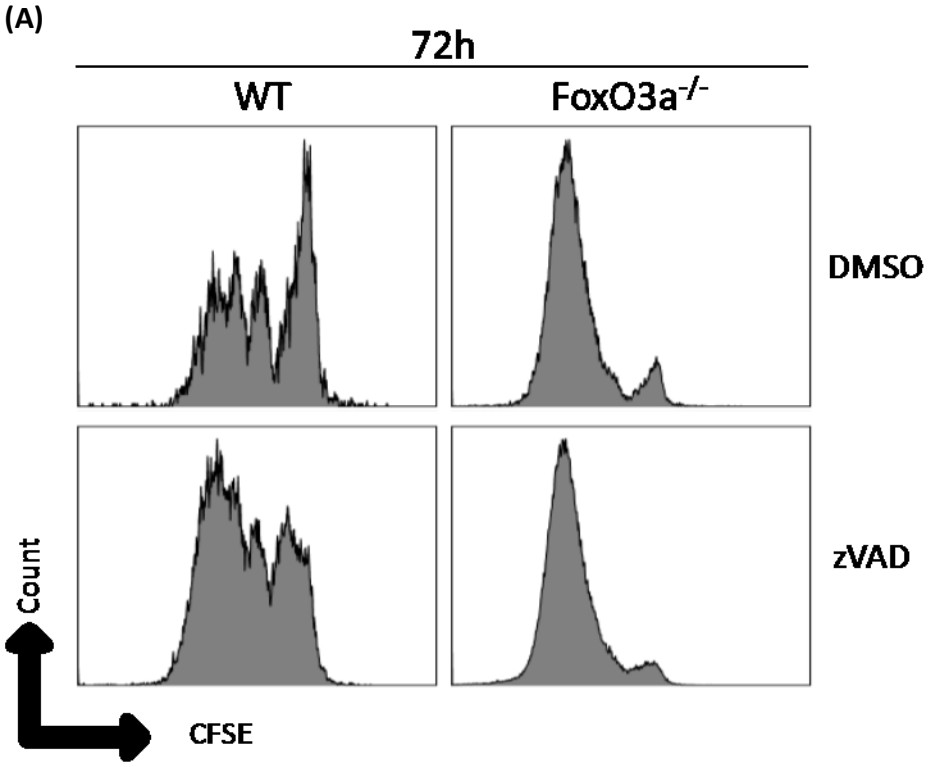
(A)
72h
WT
FoxO3a-/-
DMSO
zVAD
Count
CFSE

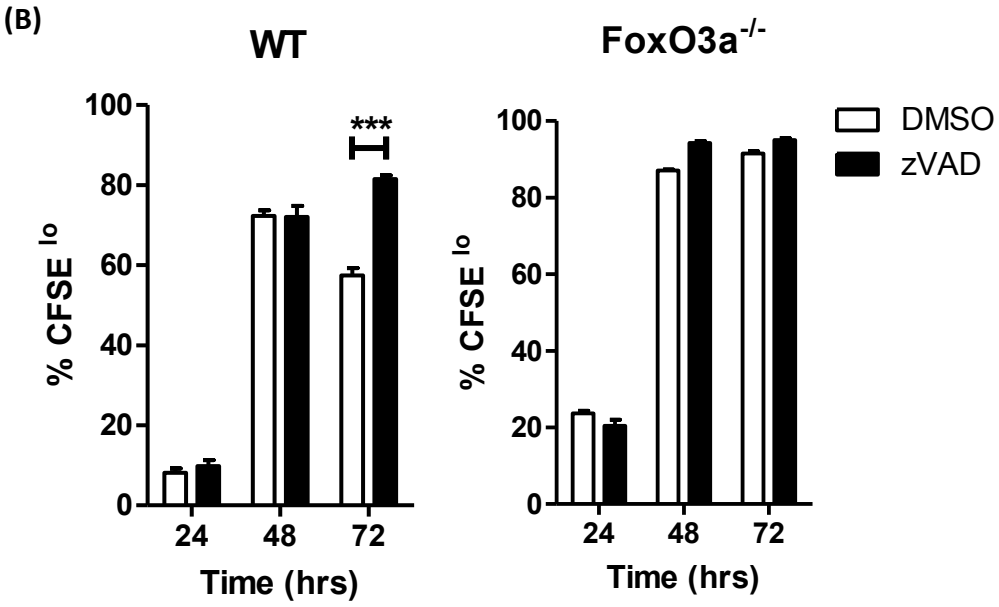
(B)
WT
FoxO3a-/-
***
% CFSE lo
100
80
60
40
20
0
24
48
72
Time (hrs)
DMSO
zVAD

Figure 15 – FoxO3a impacts apoptotic death of activated CD8$^+$ T cells at the late stages of activation.

CFSE-labeled WT and FoxO3a-deficient CD8$^+$ T cells were stimulated with anti-CD3 and anti-CD28 antibodies in the presence or absence of z-VAD. At various time points post-stimulation, cells were washed with PBS before labeling them with 7-AAD and acquired on the flow cytometer to assess their CFSE dilution. Total 7AAD$^-$ (live) cells were gated on CFSE histograms and CFSE dilution was quantified.

(A) Representative CFSE histograms of live WT and FoxO3a-deficient CD8$^+$ T cells at 72 h post-stimulation are shown.

(B) Graphs displaying the magnitudes of proliferation of control and z-VAD treated WT and FoxO3a-deficient CD8$^+$ T cells at various time points post-stimulation are shown. Data are presented as mean ± SEM and are representative of two independent experiments (n=2). Statistical significance was calculated by two-way ANOVA. ***p<0.001

(A)

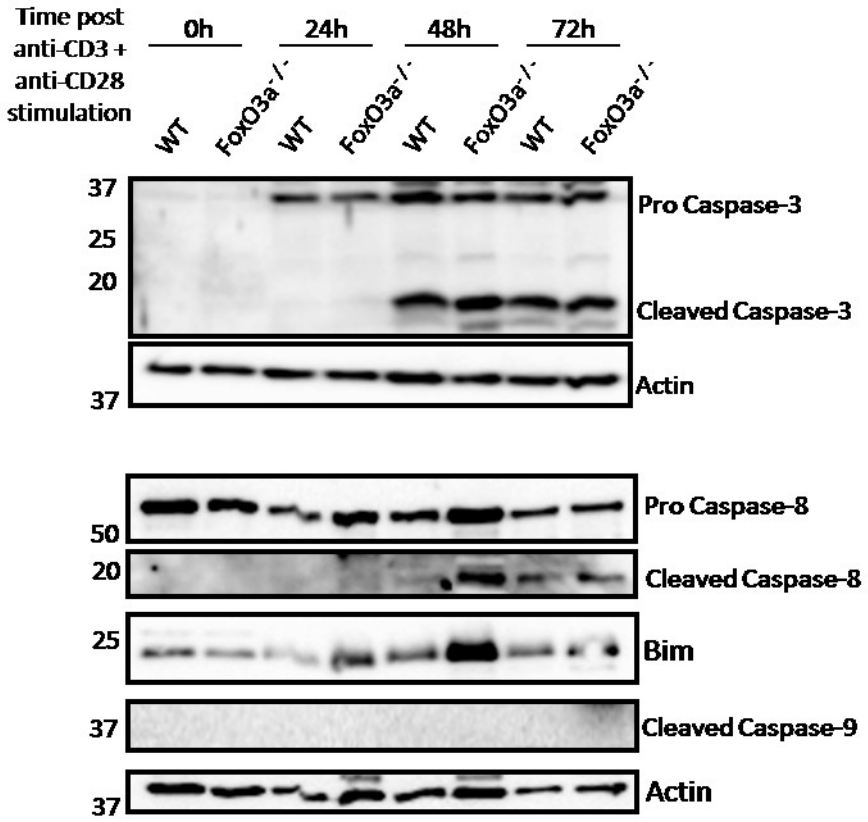
Time post anti-CD3 + anti-CD28 stimulation
0h
24h
48h
72h
WT
FoxO3a-/-
37
25
20
Pro Caspase-3
Cleaved Caspase-3
Actin
50
Pro Caspase-8
Cleaved Caspase-8
Bim
Cleaved Caspase-9

(B)

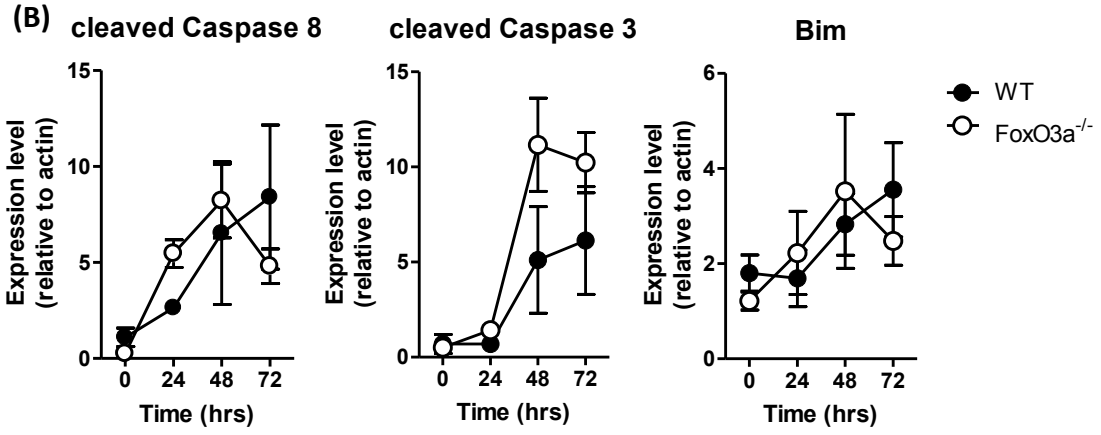
cleaved Caspase 8
cleaved Caspase 3
Bim
Expression level (relative to actin)
Time (hrs)
0
24
48
72
WT
FoxO3a-/-

Figure 16 – FoxO3a does not modulate the expression of classical pro-apoptotic cell death markers in activated $CD8^+$ T cells.

WT and FoxO3a-deficieit $CD8^+$ T cells (10^6) were stimulated in 24 well plates with anti-CD3 and anti-CD28 antibodies as described above. Cell lysates were collected at various time points post-stimulation and the expression of various pro-apoptotic cell death markers were assessed by western blotting. β-actin was used as a loading control.

(A) Representative images of western blots showing expression of Caspase-3, Capsase-8, cleaved caspase-9 and Bim in WT and FoxO3a-deficient $CD8^+$ T cells at various time points post-stimulation are shown.

(B) Graphs showing the relative expression levels of cleaved Caspase-3, cleaved Caspase-8 and Bim in WT and FoxO3a-deficient $CD8^+$ T cells at various time points post-stimulation are displayed. Data are presented as mean ± SEM pooled from three independent experiments (n=3).

3.2.9. FoxO3a signaling modulates mitochondrial activity in activated $CD8^+$ T cells

FoxO3a has been shown to regulate the intrinsic apoptotic pathway in neuronal cells through Bim regulation (Hagenbuchner et al., 2012) and it is known that Bim mediates intrinsic apoptosis through mitochondrial membrane damage (Kroemer et al., 2007). I wanted to evaluate mitochondrial activities in activated WT and FoxO3a-deficient $CD8^+$ T cells post-stimulation. Tetra Methyl Rhodamine Ethyl ester (TMRE) is a fluorescent cationic dye that sequesters to the membranes of active mitochondria due to their relative negatively charged membranes. Inactive or damaged mitochondria will be unable to sequester the dye. So cells with more active mitochondria will have a higher expression of TMRE as compared to cells with more damaged mitochondria.

A significantly higher intensity of TMRE fluorescence was observed in the FoxO3a-deficient $CD8^+$ T cells compared to WT $CD8^+$ T cells at 72 h post-stimulation (Figure 17A-B). There was a slight, although statistically insignificant, increase in TMRE intensity in FoxO3a-deficient $CD8^+$ T cells compared to WT $CD8^+$ T cells at 48 h but no difference at 24 h post-stimulation. There were no differences in the mitochondrial activities of unstimulated WT and FoxO3a-deficient $CD8^+$ T cells (Figure 17B).

3.2.10. FoxO3a signaling regulates cytokine expression by activated $CD8^+$ T cells

$CD8^+$ T cells express various cytokines to promote their functions. Some of these cytokines, such as TNF-α and IFN-γ, promote the activation of other immune cells eg. macrophages (Mosmann et al., 1997).

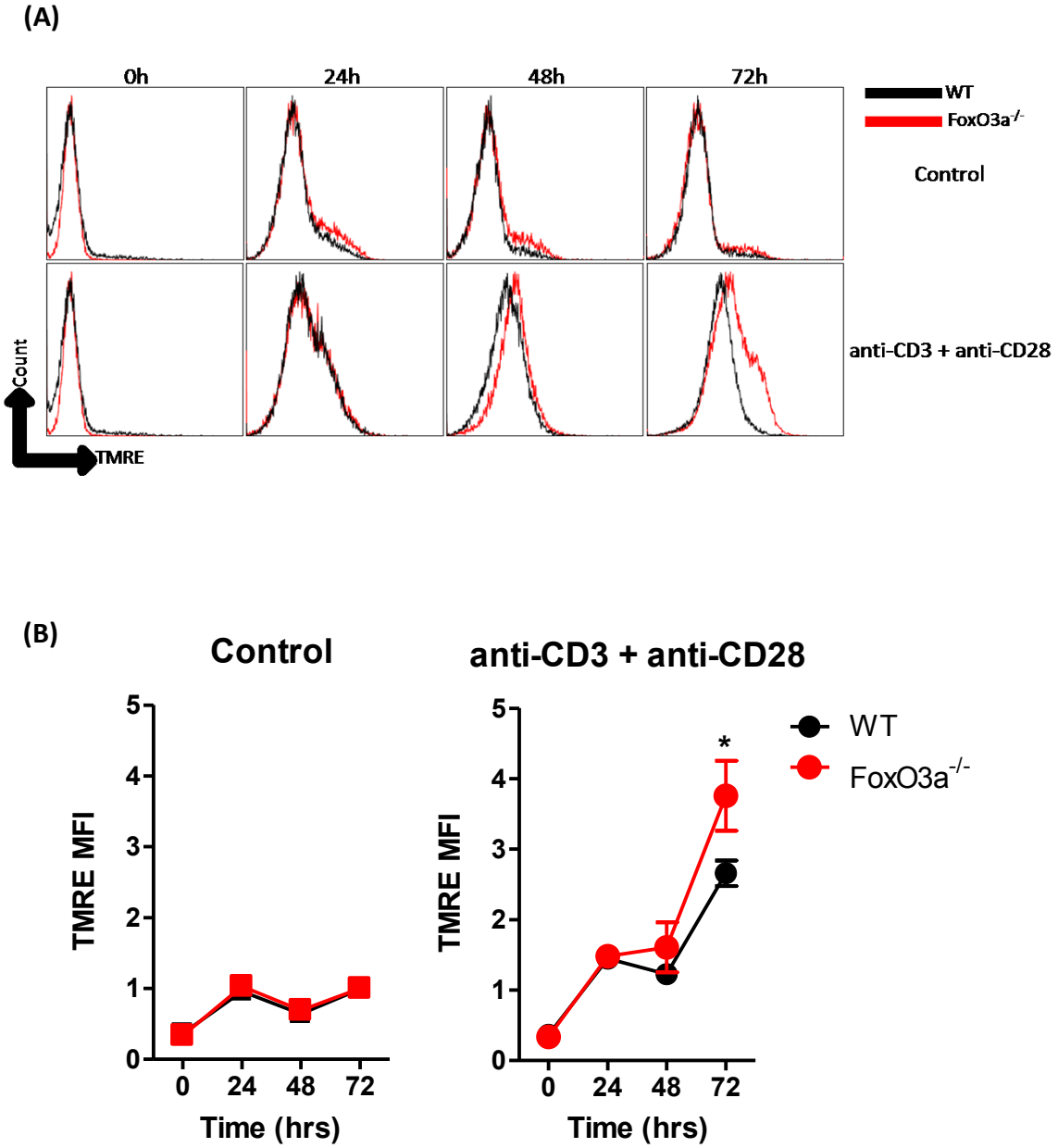
(A)
0h
24h
48h
72h
WT
FoxO3a-/-
Control
anti-CD3 + anti-CD28
Count
TMRE
(B)
Control
anti-CD3 + anti-CD28
TMRE MFI
Time (hrs)
0
24
48
72
1
2
3
4
5
*
WT
FoxO3a-/-

Figure 17 – FoxO3a signaling impacts mitochondrial activity in activated $CD8^+$ T cells.

WT and FoxO3a-deficient $CD8^+$ T cells were stimulated with anti-CD3 and anti-CD28 antibodies as described before. At various time points post-stimulation, cells were stained with TMRE in RPMI without phenol red. Following 30 min incubation at 37 °C, the cells were acquired in the flow cytometer to assess mitochondrial activity by measuring the intensity of TMRE fluorescence.

(A) Representative TMRE histograms of WT and FoxO3a-deficient $CD8^+$ T cells at various time points post-stimulation are shown.

(B) Graphs comparing the intensities of TMRE fluorescence in WT and FoxO3a-deficient $CD8^+$ T cells over time are shown. Data are presented as mean ± SEM and are representative of two independent experiments (n=2). Statistical significance was calculated by two-way ANOVA. *$p<0.05$

The cytokine expression profile was evaluated in activated WT and FoxO3a-deficient $CD8^+$ T cells. Cell culture supernatants were collected at various time points post-stimulation and cytokine measurements were performed by sandwich-ELISA. There were significantly increased levels of IFN-γ and IL-6 expressed by FoxO3a-deficient $CD8^+$ T cells compared to WT $CD8^+$ T cells at 24 h post-stimulation and a trend towards increased levels of TNF-α, although the differences were not statistically significant (Figure 18).

3.2.11. IL-6 signaling contributes to the enhanced survival of activated FoxO3a-deficient $CD8^+$ T cells

IL-6 is known to be a T cell survival factor as it prevents the downregulation of anti-apoptotic protein Bcl-2 (Teague et al., 1997). I wanted to determine if increased IL-6 signaling was responsible for the enhanced survival of the activated FoxO3a-deficient $CD8^+$ T cells compared to WT $CD8^+$ T cells. So IL-6 signaling was blocked, using an anti-IL-6 neutralizing antibody (MP5-20F3), in activated WT and FoxO3a-deficient $CD8^+$ T cells and their proliferation was assessed by CFSE dilution and their survival was assessed by 7-AAD binding (Figure 19A). When IL-6 signaling was blocked, there was significantly reduced proliferation (% $CFSE^{lo}$) (Figure 19B) and reduced survival (% $7AAD^-$) (Figure 19C) of activated FoxO3a-deficient $CD8^+$ T cells whereas there were no differences observed in WT $CD8^+$ T cells (Figure 19C).

3.2.12. FoxO3a signaling does not influence NFκB activation in $CD8^+$ T cells

Previous studies have shown that FoxO3a signaling regulates NFκB activation in $CD4^+$ T cells, however, the mechanism has remained elusive (Lin et al., 2004).

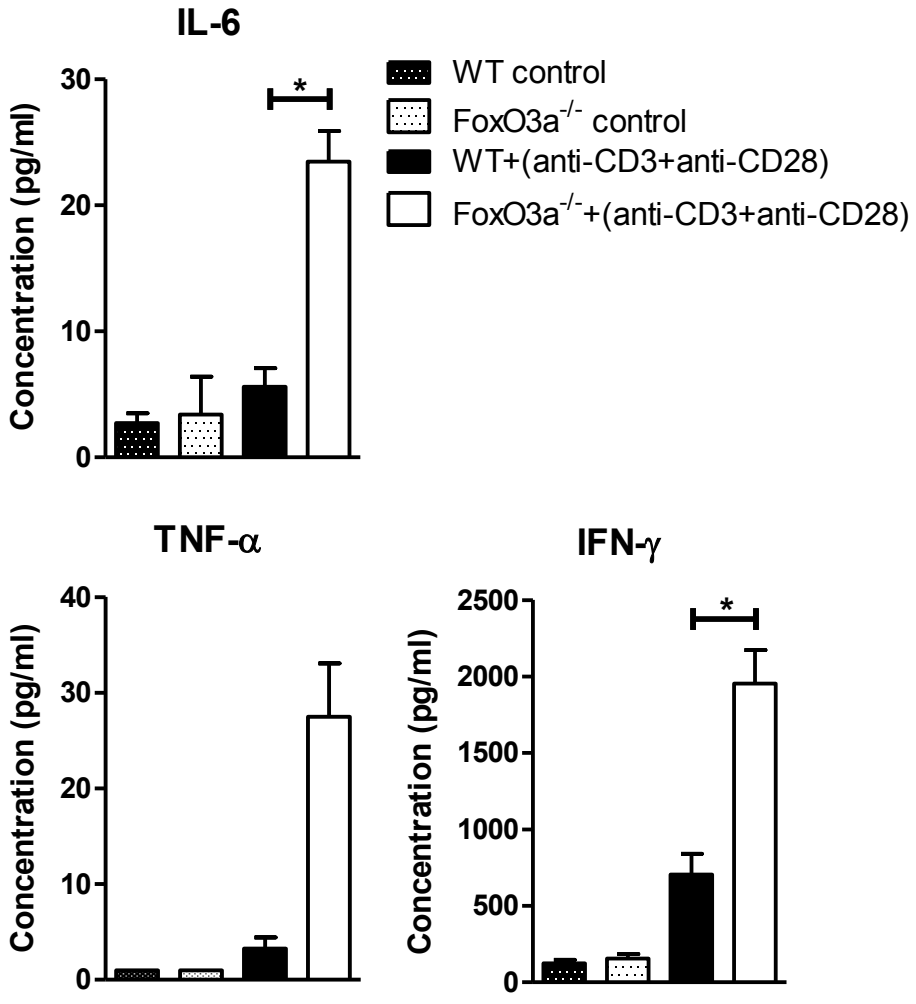
IL-6
Concentration (pg/ml)
30
20
10
0
*
WT control
FoxO3a-/- control
WT+(anti-CD3+anti-CD28)
FoxO3a-/-+(anti-CD3+anti-CD28)
TNF-α
Concentration (pg/ml)
40
30
20
10
0
IFN-γ
Concentration (pg/ml)
2500
2000
1500
1000
500
0
*

Figure 18 – FoxO3a signaling limits cytokine expression in activated $CD8^+$ T cells.

WT and FoxO3a-deficient $CD8^+$ T cells were stimulated with anti-CD3 and anti-CD28 antibodies in 24 well plates as described before. At 24 h post-stimulation, cell culture supernatants were collected and the amounts of various cytokines (IL-6, TNF-α and IFN-γ) were quantified by sandwich-ELISA as described in the methods section.

Graphs showing the cytokine expression profile of WT and FoxO3a-deficient $CD8^+$ T cells at 24 h post-stimulation are displayed. Data are presented as mean $\pm$ SEM and are representative of three independent experiments (n=3). Statistical significance was calculated by student's t test. *$p<0.05$

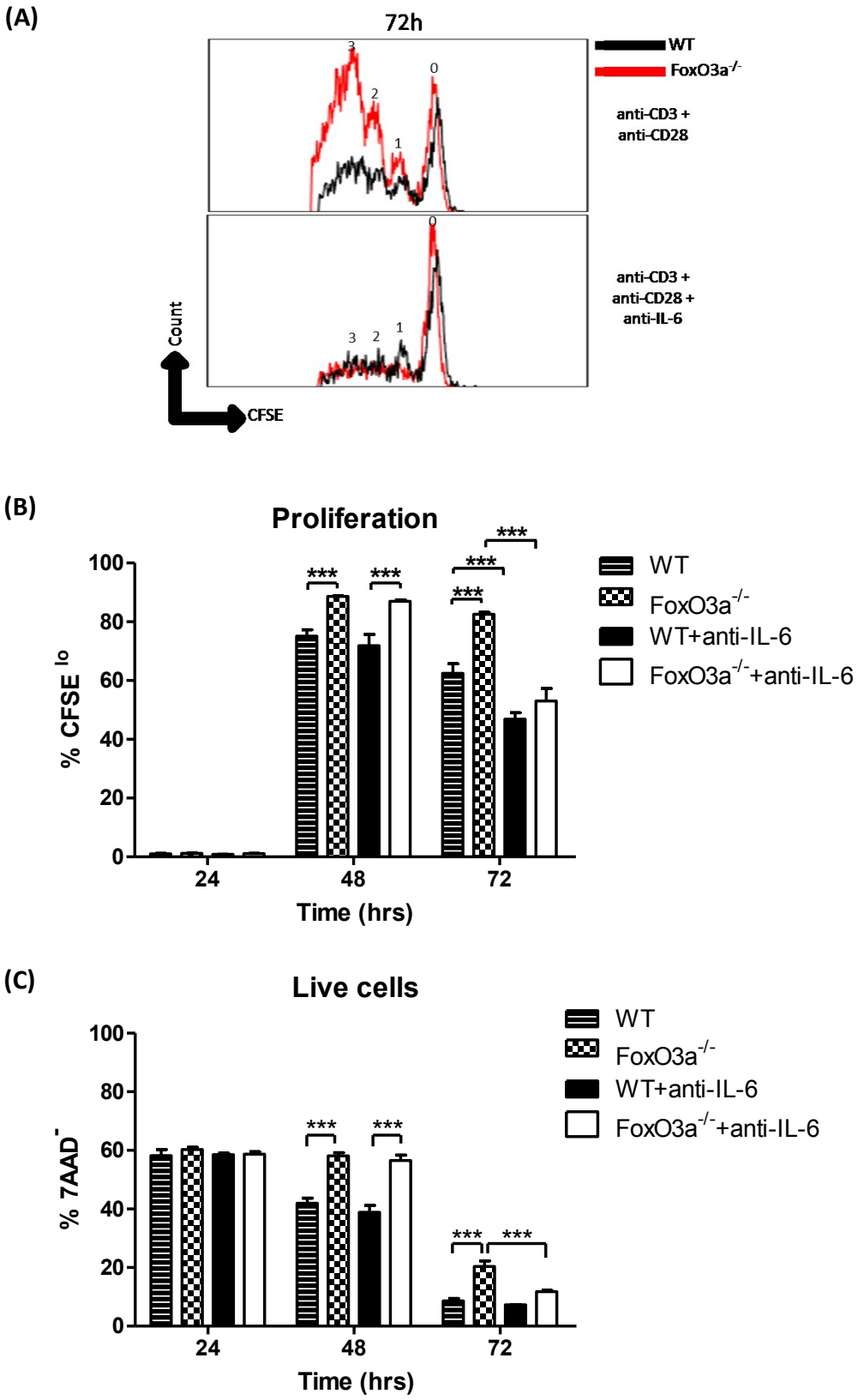
(A)
72h
WT
FoxO3a-/-
anti-CD3 +
anti-CD28
anti-CD3 +
anti-CD28 +
anti-IL-6
Count
CFSE
(B)
Proliferation
% CFSE lo
Time (hrs)
WT
FoxO3a-/-
WT+anti-IL-6
FoxO3a-/-+anti-IL-6
(C)
Live cells
% 7AAD-
Time (hrs)
WT
FoxO3a-/-
WT+anti-IL-6
FoxO3a-/-+anti-IL-6

Figure 19 – IL-6 signaling promotes the enhanced survival of activated FoxO3a-deficient $CD8^+$ T cells.

CFSE-labeled WT and FoxO3a-deficient $CD8^+$ T cells were stimulated with anti-CD3 and anti-CD28 antibodies as described before with and without neutralizing anti-IL-6 antibody (1 μg/ml). At various time points post-stimulation, cells were washed with PBS, stained with 7-AAD and acquired on the flow cytometer to evaluate their CFSE dilution with and without anti-IL-6 antibody. All live ($7AAD^-$) cells were gated on CFSE histograms.

(A) Representative CFSE histograms of activated WT and FoxO3a-deficient $CD8^+$ T cells treated with or without anti-IL-6 antibody at 72 h post-stimulation are shown.

(B) A graph showing the percentages of CFSE dilution of activated WT and FoxO3a-deficient $CD8^+$ T cells treated with and without anti-IL-6 antibody is displayed. Data are presented as mean ± SEM and are representative of two independent experiments (n=2). Statistical significance was calculated by two-way ANOVA. ***$p<0.001$

(C) A graph showing the percentages of live ($7AAD^-$) cells of activated WT and FoxO3a-deficient $CD8^+$ T cells treated with and without anti-IL-6 antibody is displayed. Data are presented as mean ± SEM and are representative of two independent experiments (n=2). Statistical significance was calculated by two-way ANOVA. ***$p<0.001$

Also, the NFκB pathway is one of the major inducers of cytokine signaling (Gerondakis and Siebenlist, 2010). I wanted to determine if enhanced NFκB activation was the mechanism underlying the enhanced cytokine expression in activated FoxO3a-deficient $CD8^+$ T cells observed at 24 h post-stimulation.

NFκB phosphorylation (ratio of phosphorylated NFκB to total NFκB) was evaluated by western blotting and compared between activated WT and FoxO3a-deficient $CD8^+$ T cells at various time points post-stimulation (Figure 20A). The levels of phosphorylated NFκB peaked at 24 h post-stimulation and gradually tapered off to basal levels at 48 and 72 h post-stimulation. However, there were no differences in NFκB phosphorylation between activated WT and FoxO3a-deficient $CD8^+$ T cells at various time points post-stimulation (Figure 20B). These results indicate that FoxO3a regulates cytokine expression in $CD8^+$ T cells in an NFκB-independent manner.

3.2.13. Antigen-specific proliferation of $CD8^+$ T cells is modulated by FoxO3a signaling

Until this point, all results were obtained using a polyclonal stimulation (anti-CD3 and anti-CD28 antibody) model of T cell activation. I wanted to determine if a similar response could be obtained using an antigen-specific stimulation model since it is a more relevant model of T cell activation *in vivo*. In this model (Figure 21A), I purified DCs from spleens of WT mice and infected them with a recombinant strain of Ovalbumin-expressing *Salmonella typhimurium*, ST-YopE-Ova (Tzelepis et al., 2012) at various multiplicities of infection (MOI).

(A)

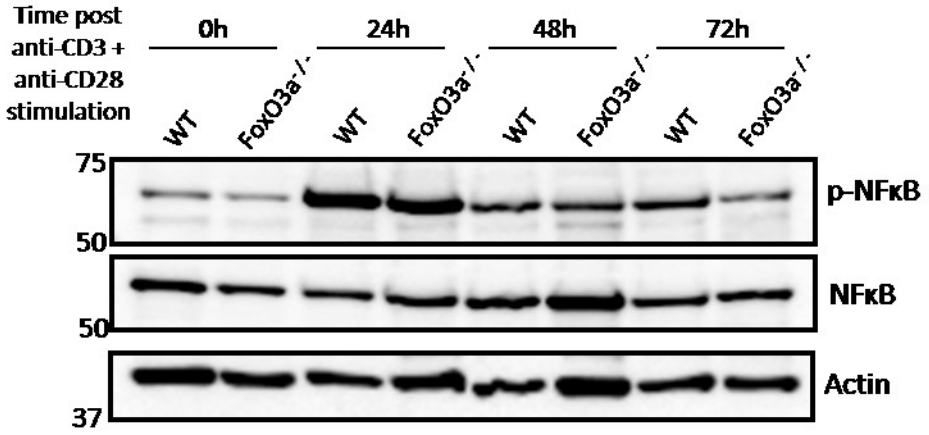
Time post anti-CD3 + anti-CD28 stimulation
0h
24h
48h
72h
WT
FoxO3a-/-
WT
FoxO3a-/-
WT
FoxO3a-/-
WT
FoxO3a-/-
75
50
50
37
p-NFκB
NFκB
Actin

(B)

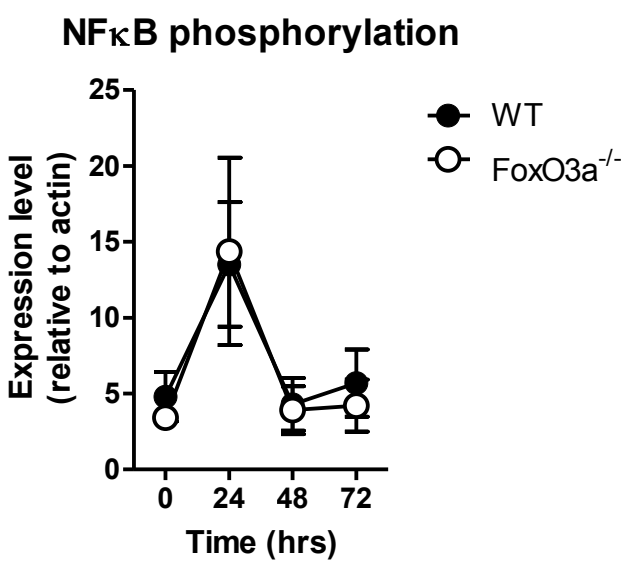
NFκB phosphorylation
Expression level (relative to actin)
25
20
15
10
5
0
0
24
48
72
Time (hrs)
WT
FoxO3a-/-

Figure 20 – FoxO3a signaling does not impact NFκB activation in activated $CD8^+$ T cells.

WT and FoxO3a-deficient $CD8^+$ T cells (10^6) were stimulated in 24 well plates with anti-CD3 and anti-CD28 antibodies as described before. At various time points post-stimulation, cell lysates were collected and NFκB activation was assessed by western blotting. NFkB phosphorylation (activation) was evaluated by comparing the band intensities of phosphorylated NFκB to total NFκB.

(A) Representative western blot images of the expression of phosphorylated and total NFκB in activated WT and FoxO3a-deficient $CD8^+$ T cells at various time points post-stimulation are shown along with β-actin which was used as a loading control.

(B) A graph showing the relative NFκB phosphorylation levels in WT and FoxO3a-deficient $CD8^+$ T cells at various time points post-stimulation is displayed. Data are presented as mean ± SEM pooled from three independent experiments (n=3).

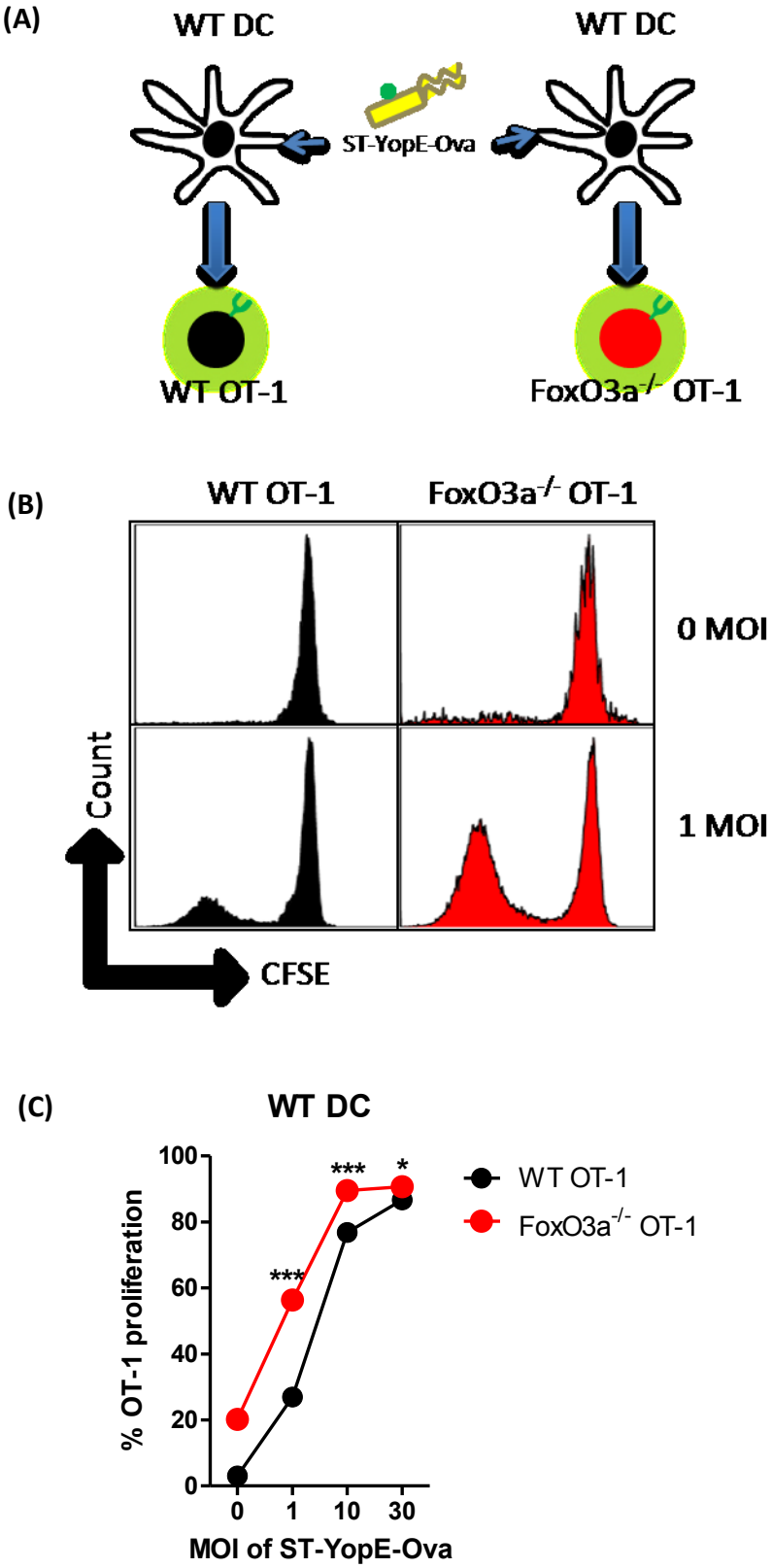
(A)
WT DC
WT DC
ST-YopE-Ova
WT OT-1
FoxO3a-/- OT-1
(B)
WT OT-1
FoxO3a-/- OT-1
0 MOI
1 MOI
Count
CFSE
(C)
WT DC
% OT-1 proliferation
100
80
60
40
20
0
***
***
*
0
1
10
30
MOI of ST-YopE-Ova
WT OT-1
FoxO3a-/- OT-1

Figure 21 – FoxO3a signaling modulates antigen-specific proliferation of $CD8^+$ T cells.

Dendritic cells (DCs) were isolated from the spleens of WT mice and were infected ($5x10^4$ DCs) with various multiplicities of infection (MOI) of ST-YopE-Ova and incubated for 2 h at 37°C. After washing to remove extracellular bacteria, CFSE-labeled WT OT-1 and FoxO3a-deficient OT-1 T cells were added ($5x10^4$ OT-1 T cells) on top of the infected DCs in R8 medium containing gentamycin to kill the remaining extracellular bacteria. OT-1 T cell proliferation was assessed by CFSE dilution after 72 h. Uninfected DCs were used as a negative control.

(A) A figure representing the *in vitro* model for antigen-specific proliferation used for this assay.

(B) Representative CFSE histograms of WT and FoxO3a-deficient OT-1 T cells at 72 h post-stimulation are shown.

(C) A graph comparing WT and FoxO3a-deficient OT-1 T cell proliferation across various MOIs of ST-YopE-Ova is displayed. Data are presented as mean ± SEM and are representative of three independent experiments (n=3). Statistical significance was calculated by two-way ANOVA. *$p<0.05$, ***$p<0.001$

The bacteria will be phagocytosed by the DC and the expressed Ova protein will be processed for antigen presentation through MHC-I. The peptide, SIINFEKL ($Ova_{257-264}$) is recognized by $CD8^+$ T cells of OT-1 TCR transgenic mice. CFSE-labeled OT-1 T cells were added on top of the infected DCs and so the peptide-MHC-I complex will be presented to the OT-1 TCR for antigenic stimulation. The magnitude of proliferation was compared at various MOIs, which effectively indicate various concentrations of antigen (Figure 21B). At all the indicated MOIs, FoxO3a-deficient OT-1 T cells displayed significantly enhanced proliferation compared to WT OT-1 T cells although the differences were greater at a lower MOI (Figure 21C). These results are in agreement with my previous data indicating a lower threshold of activation in FoxO3a-deficient $CD8^+$ T cells upon stimulation with anti-CD3 and anti-CD28 antibodies.

3.3. Role of FoxO3a in DC activation

3.3.1. FoxO3a signaling does not influence the expression of activation markers on DCs of naïve mice

Since an increase in the numbers of DCs was observed in the spleens of FoxO3a-deficient mice (Figure 1), I evaluated the expression of activation markers in DCs to determine whether the DCs in FoxO3a-deficient mice displayed any signs of activation. The expression levels of various activation markers, including MHC-II, CD80 and CD86, were evaluated in naïve WT and FoxO3a-deficient DCs (Figure 22A).

(A)

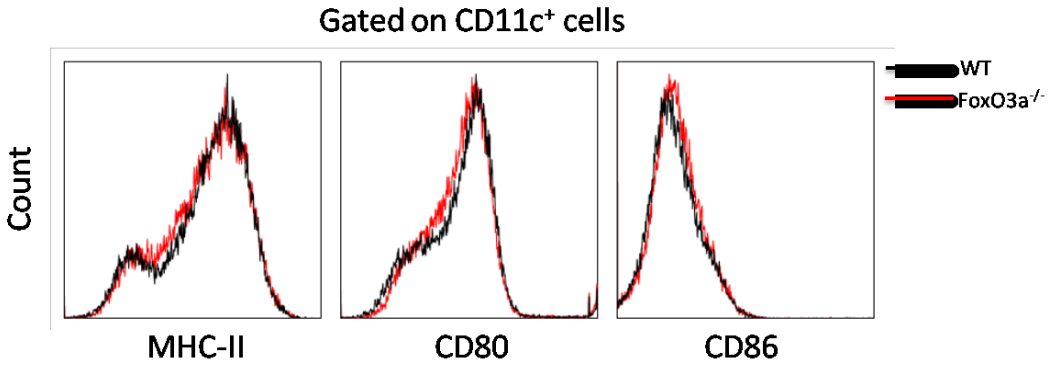
Gated on CD11c+ cells
Count
WT
FoxO3a-/-
MHC-II
CD80
CD86

(B)

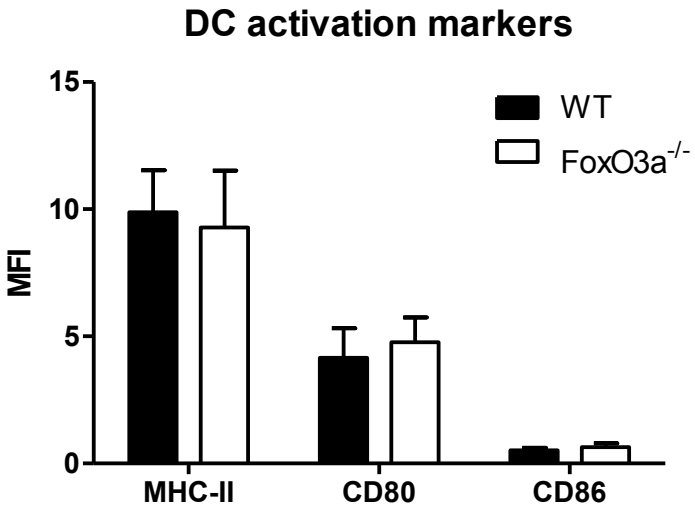
DC activation markers
MFI
15
10
5
0
WT
FoxO3a-/-
MHC-II
CD80
CD86

Figure 22 – FoxO3a signaling does not influence the expression of activation markers on DCs in naïve mice.

Single cell suspensions were prepared from whole spleens of WT and FoxO3a-deficient mice as described before. 10^6 cells were stained with the appropriate surface receptor antibodies against various activation markers (MHC-II, CD80 and CD86). After doublet-exclusion, DCs were gated on $CD11c^+$ cells and the expression of MHC-II, CD80 and CD86 was evaluated.

(A) Representative histograms showing the expressions of MHC-II, CD80 and CD86 on WT and FoxO3a-deficient DCs of naïve mice are displayed.

(B) A graph showing the mean fluorescence intensities of MHC-II, CD80 and CD86 on WT and FoxO3a-deficient DCs of naïve mice is displayed. Data are represented as mean ± SEM pooled from two independent experiments (n=2).

There were no differences in the expression levels of these activation markers between naïve WT and FoxO3a-deficient DCs (Figure 22B). These results indicate that although there are more DCs in FoxO3a-deficient mice, they do not display any overt signs of activation.

3.3.2. FoxO3a signaling modulates DC activation

As there was no difference in the activation status of naïve WT and FoxO3a-deficient DCs under homeostatic conditions, I wanted to determine whether FoxO3a signaling impacts DC activation upon PAMP stimulation. To this end, DCs were stimulated by LPS, which is a dominant PAMP present on the surface of gram negative bacteria. DCs were purified from the spleens of WT and FoxO3a-deficient mice and stimulated with LPS for various time points. FoxO3a-deficient DCs displayed significantly enhanced MTT reduction at 48 and 72 h post-stimulation compared to WT DCs (Figure 23). There was no difference in MTT reduction between activated WT and FoxO3a-deficient DCs at 24 h post-stimulation. There was also a subtle, but statistically significant, increase in MTT reduction in unstimulated FoxO3a-deficient DCs compared to WT DCs at 48 and 72 h post-culture (Figure 23).

3.3.3. FoxO3a signaling modulates cytokine expression by activated DCs

Expression of cytokines following PAMP engagement is a key function of DCs as the cytokines promote immune responses and enhance T cell priming following antigen presentation. Activated DCs secrete classical pro-inflammatory cytokines such as IL-1 and TNF-α that enhance endothelial cell adhesion molecule expression in order to facilitate extravasation of immune cells to the site of inflammation (Dinarello, 2000) and IL-6 that promotes survival of primed T cells (Rochman et al., 2005).

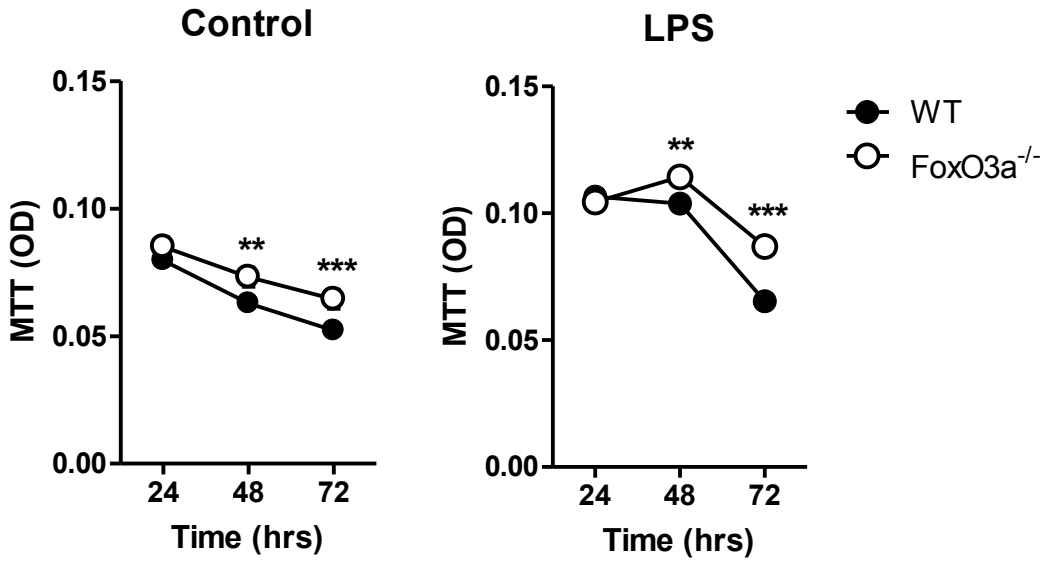
Control
LPS
0.15
0.10
0.05
0.00
MTT (OD)
**
***
24
48
72
Time (hrs)
WT
FoxO3a-/-

Figure 23 – FoxO3a signaling modulates DC activation.

DCs were isolated from the spleens of WT and FoxO3a-deficient mice and were stimulated (10^5 cells) with 100 ng/ml LPS in 96 well flat-bottom plates. RPMI was used as an unstimulated control. At the indicated time points post-stimulation, MTT assay was performed and the absorbance (OD) values were compared between WT and FoxO3a-deficient DCs.

Graphs comparing the OD values of WT and FoxO3a-deficient DCs are shown. Data are presented as mean ± SD and are representative of two independent experiments (n=2). Statistical significance was calculated by two-way ANOVA. **p<0.01, ***p<0.001

They also secrete IL-12 which directs T_H1 differentiation and promotes a CTL response (Joffre et al., 2009). In addition, activated DCs also secrete anti-inflammatory cytokines such as IL-10 and TGF-β that downregulate immune responses, promote tissue repair and wound healing (Opal and DePalo, 2000). Cell culture supernatants were collected from LPS-stimulated WT and FoxO3a-deficient DCs and cytokine expression was measured by sandwich-ELISA. Activated FoxO3a-deficient DCs expressed significantly increased levels of all cytokines indicated (IL-1α, IL-1β, TNF-α, IL-6, IL-12 and IL-10) compared to WT DCs at 24 h post-stimulation (Figure 24).

3.3.4. FoxO3a signaling in DCs modulates their antigen presentation to $CD8^+$ T cells

DCs are primarily responsible for priming naïve antigen-specific $CD8^+$ T cells *in vivo* (Jung et al., 2002). I wanted to determine how FoxO3a signaling in DCs influences antigen presentation to $CD8^+$ T cells. In order to achieve this objective, I used a strategy similar to the one used for measuring antigen-specific proliferation of $CD8^+$ T cells described before. But here, I purified DCs from the spleens of WT and FoxO3a-deficient mice and infected them with various MOIs of ST-YopE-Ova. CFSE-labeled WT OT-1 T cells were then added on top of the infected WT and FoxO3a-deficient DCs (Figure 25A). Antigen presentation by WT and FoxO3a-deficient DCs were compared at various MOIs by evaluating the proliferation, as assessed by CFSE dilution, of WT OT-1 T cells (Figure 25B). There was significantly enhanced proliferation of WT OT-1 T cells upon antigen presentation by FoxO3a-deficient DCs compared to WT DCs (Figure 25C).

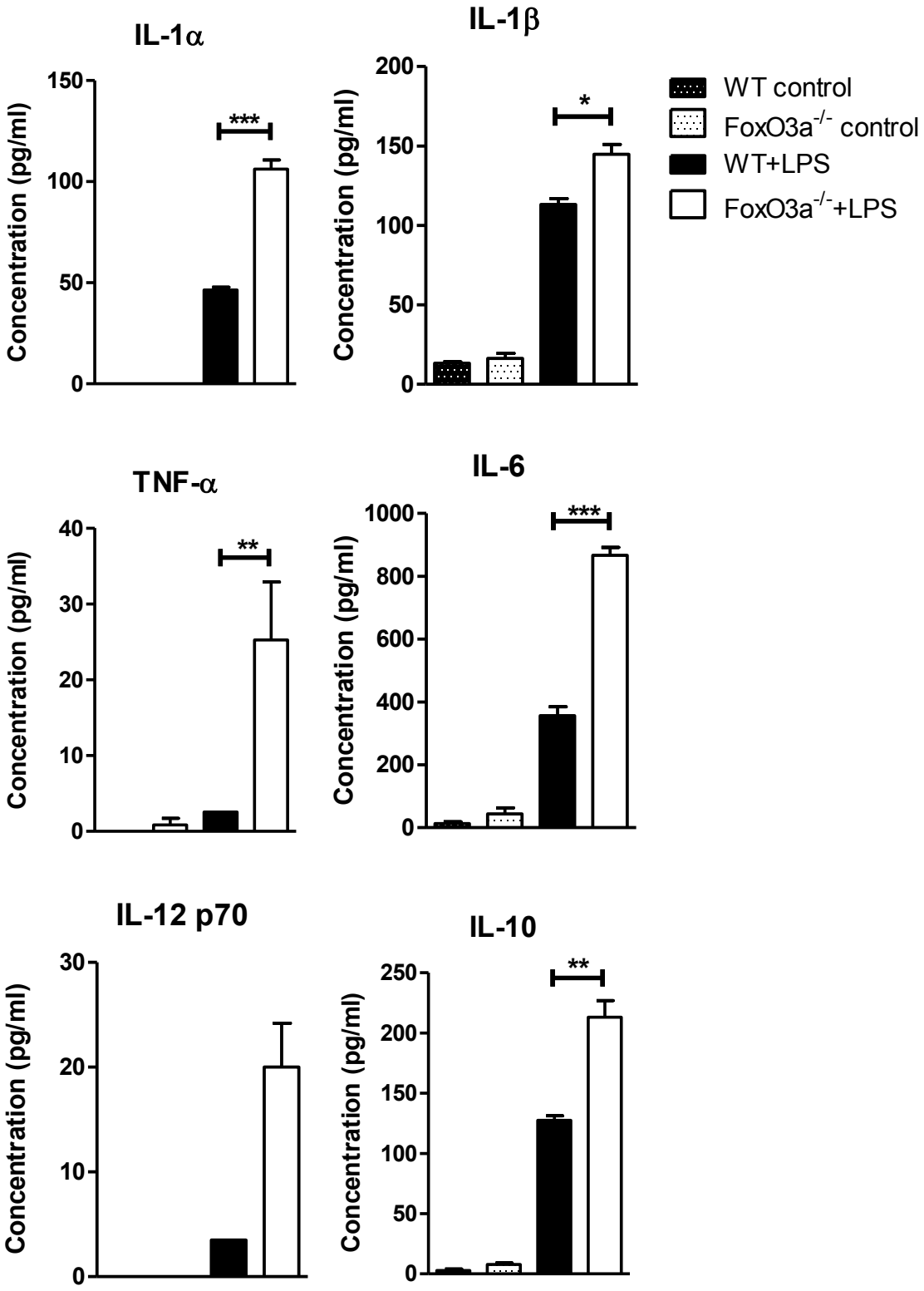
IL-1α
IL-1β
TNF-α
IL-6
IL-12 p70
IL-10
Concentration (pg/ml)
WT control
FoxO3a-/- control
WT+LPS
FoxO3a-/-+LPS
***
*
**
***
**

Figure 24 – Cytokine expression in activated DCs is limited by FoxO3a signaling.

DCs were isolated from spleens of WT and FoxO3a-deficient mice and stimulated with LPS as described before. Cell culture supernatants were collected at 24 h post-stimulation and cytokine expression was assayed by sandwich-ELISA.

Graphs comparing the expression of the indicated cytokine between WT and FoxO3a-deficient DCs are displayed. Data are presented as mean ± SEM and are representative of two independent experiments (n=2). Statistical significance was calculated by student's t test. *p<0.05, **p<0.01, ***p<0.001

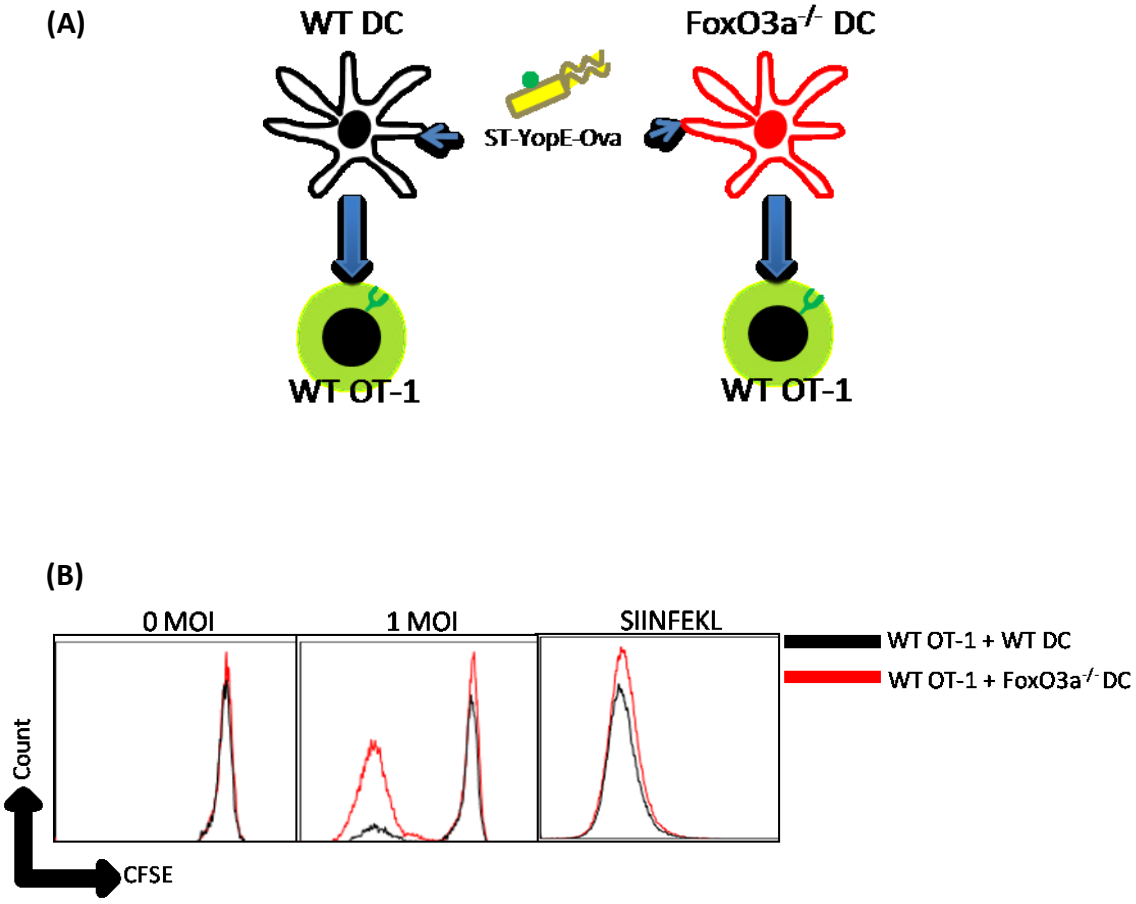
(A)
WT DC
FoxO3a-/- DC
ST-YopE-Ova
WT OT-1
WT OT-1
(B)
0 MOI
1 MOI
SIINFEKL
WT OT-1 + WT DC
WT OT-1 + FoxO3a-/- DC
Count
CFSE
(C)
WT OT-1
% WT OT-1 proliferation
100
80
60
40
20
0
***
***
WT DC
FoxO3a-/- DC
0
1
10
30
MOI of ST-YopE-Ova

Figure 25 – FoxO3a signaling in DCs modulates their antigen presentation to $CD8^+$ T cells.

DCs were isolated from the spleens of WT and FoxO3a-deficient mice and were infected ($5x10^4$ DCs) with various multiplicities of infection (MOI) of ST-YopE-Ova. After 2 h incubation at 37°C, the wells were washed to remove extracellular bacteria and CFSE-labeled WT OT-1 T cells were added ($5x10^4$ OT-1 T cells) on top of the infected DCs in R8 medium containing gentamycin to kill the remaining extracellular bacteria. OT-1 T cell proliferation was assessed after 72 h by CFSE dilution. Uninfected DCs were used as a negative control and $Ova_{(257-264)}$ peptide (SIINFEKL) was used a positive control for antigen presentation.

(A) A figure representing the *in vitro* antigen presentation model used for this assay.

(B) Representative CFSE histograms of WT OT-1 T cells stimulated by either infected WT or FoxO3a-deficient DCs at 72 h post-stimulation are shown along with the SIINFEKL peptide positive control.

(C) A graph comparing the WT OT-1 proliferation between stimulation by either WT or FoxO3a-deficient DCs is displayed. Data are presented as mean ± SEM and are representative of two independent experiments (n=2). Statistical significance was calculated by two-way ANOVA. ***$p<0.001$

Furthermore, the differences diminished as the MOI was increased. In the absence of infection, there was no proliferation of OT-1 T cells. When Ova peptide (SIINFEKL) was directly added to WT and FoxO3a-deficient DCs, there was no difference in proliferation of WT OT-1 T cells (Figure 25B). These results indicate that FoxO3a signaling in DCs modulates their antigen presentation to $CD8^+$ T cells in the context of infection at low doses.

4. DISCUSSION

4.1. Prelude

FoxO3a is a transcription factor that is involved in the regulation of a variety of vital cellular processes ranging from cell proliferation and cell metabolism to stress resistance and cell death (see section 1.3). All these processes are expected to have an impact during the various phases of a $CD8^+$ T cell response to infection. Therefore, deciphering the role of FoxO3a in $CD8^+$ T cell activation and differentiation could provide vital clues about the signaling mechanisms that operate during the expansion and contraction of the $CD8^+$ T cell response. Activation of $CD8^+$ T cells is mediated by dendritic cells (DCs) which induce rapid antigen-presentation (Joffre *et al*., 2009). I, therefore, determined the role of FoxO3a in $CD8^+$ T cell and DC activation by evaluating the various cell signaling mechanisms in these cells.

A complete and efficient T cell activation requires three signals; 1) T cell receptor-derived signal 2) co-stimulatory signal and 3) cytokine-derived signal (Curtsinger *et al*., 2003). The *in vitro* T cell stimulation model I have used in this study utilizes anti-CD3 and anti-CD28 antibodies to provide signals 1 and 2 to the T cell respectively. CD3 stimulation mimics TCR stimulation and results in the phosphorylation of ITAMs associated with the cytoplasmic domains of the ζ dimer of the CD3 complex. CD28 co-stimulation potentiates the effects of TCR stimulation and increases cytokine expression (esp. IL-2) thereby providing signal 3 to the T cell (Smith-Garvin *et al*., 2009). Following these events, various downstream signaling pathways are engaged as described before (see section 1.3.3.1) leading to activation of the

T cell. This model of T cell stimulation does not require high amounts of antigen and antigen-presenting cells and is better compared to using mitogenic stimulants (Riddell and Greenberg, 1990). Also, during the early phases of a T cell response *in vivo*, activated T cells cannot be tracked efficiently due to their low numbers and so this *in vitro* stimulation model aids in addressing some of the questions pertaining to the signaling events occurring during the very early phases (days 1-3) of a T cell response to infection.

My results indicated an intrinsic role of FoxO3a in limiting the proliferation of $CD8^+$ T cells through a $p27^{kip}$ independent mechanism and also in promoting the cell-death of primed $CD8^+$ T cells through a Bim-independent and Caspase-independent mechanism. My results also revealed that there is a role for FoxO3a in modulating cytokine expression globally as both activated $CD8^+$ T cells and activated DCs displayed enhanced cytokine expression in the absence of FoxO3a signaling. Modulation of cytokine expression by FoxO3a signaling in $CD8^+$ T cells seemed independent of NFκB activation. In addition, FoxO3a signaling in DCs also attenuated antigen presentation to $CD8^+$ T cells likely as a consequence of modulated cytokine expression.

4.2. FoxO3a and maintenance of immune cell homeostasis

FoxO3a deficient mice have been shown to display both lymphoproliferation (Lin *et al.*, 2004) and myeloproliferation (Yalcin *et al.*, 2010). My results also showed that both lymphoid as well as myeloid cell numbers were increased in the spleens of FoxO3a-deficient mice, although there was no impact on B cell numbers (Figure 1D). Furthermore, the impact on myeloid cell populations (neutrophils, monocytes and macrophages) was stronger

compared to lymphoid cell populations ($CD4^+$ and $CD8^+$ T cells). It is possible that FoxO3a signaling impacts both the myeloid and lymphoid cell populations independently, or the impact on myeloid populations in turn impacts the lymphoid populations indirectly. Currently, it is not clear which of these possibilities is true.

My results indicated that the numbers of B cells were unaffected by FoxO3a signaling. The study by Yalcin *et al.* reported a significant increase in the number of splenic B cells in their FoxO3a-deficient mice whereas another study that used a similar knock-out model (generated on a FVB background) showed no differences in splenic B cell numbers (Hinman *et al.*, 2009) between WT and FoxO3a-deficient mice. Interestingly, Lin *et al.* also reported similar numbers of splenic B cells although the average numbers were slightly higher in the FoxO3a-deficient mice. There seems to be some disparity between studies on whether or not FoxO3a regulates the homeostasis of B cells.

While naïve FoxO3a-deficient mice had more $CD8^+$ T cells and DCs in the spleens, there was no evidence of activation of these cells as revealed by phenotypic analysis of various activation markers by flow cytometry (Figure 2A-B). $CD8^+$ T cells of naïve FoxO3a-deficient mice did not undergo cell cycling as revealed by Ki67 staining (Figure 7A). Interestingly, when $CD8^+$ T cells and DCs from FoxO3a-deficient mice were cultured *in vitro* without any stimulation, they displayed very subtle, but significant, increases in MTT signals (Figure3B). This suggests that FoxO3a-deficiency might promote a higher basal metabolism in cells, which could be a consequence of increased basal mTOR activity in FoxO3a-deficient cells (Yalcin *et al.*, 2010). This is especially relevant at the early time point (24 h) where the

increases in MTT signals were observed when there were no differences in cell survival between unstimulated WT and FoxO3a-deficient $CD8^+$ T cells. Another possibility could be that in the absence of any stimulation, FoxO3a-deficient cells underwent reduced cell death. Indeed, there was enhanced survival of unstimulated FoxO3a-deficient $CD8^+$ T cells at 48 and 72 h post-culture (Figure 12B) but further characterization is required to determine the role of FoxO3a in promoting $CD8^+$ T cell and DC homeostasis.

4.3. Role of FoxO3a in $CD8^+$ T cell proliferation

At 24 h after polyclonal stimulation of $CD8^+$ T cells, FoxO3a did not appear to impact cell death or cell proliferation (Figures 6B and 12B). However, FoxO3a-deficient cells displayed enhanced blasting (Figure 5A-B) and higher levels of cell cycle protein, Ki67 (Figure 7A-B). There was a modest, but statistically insignificant, increase in the MTT signal (Figure 3A) and cell numbers (Figure 11) of FoxO3a-deficient $CD8^+$ T cells which suggests there may be a subtle impact of FoxO3a on cell proliferation at the early stages of activation. Interestingly, there was no difference in cell death between WT and FoxO3a-deficient cells at 24 h post-stimulation, suggesting that the impact of FoxO3a on cell proliferation at the early stages of activation is not related to its impact on cell death.

At later time periods (48 and 72 h) post-stimulation, FoxO3a-deficient $CD8^+$ T cells displayed increased proliferation as evaluated by MTT assays (Figure 3A), cell imaging (Figure 4A) and CFSE dilution (Figure 6A-B). Furthermore, all the FoxO3a-deficient $CD8^+$ T cells had undergone cell cycling, whereas there were still significant numbers of WT $CD8^+$ T cells that had not committed to cycling (Figure 6C). At the late stages of activation, there was also

significantly reduced cell death in the FoxO3a-deficient $CD8^+$ T cells. So, the increased proliferation that was observed later could be a direct consequence of decreased cell death of primed cells. These results indicate that FoxO3a could impact the cell cycle progression of activated $CD8^+$ T cells, either directly or indirectly by reducing the death of cells that had undergone more rounds of division.

In a murine model of acute LCMV infection, there were no differences in cell cycling, as revealed by Ki67 expression, in virus-specific WT and FoxO3a-deficient $CD8^+$ T cells at the peak of the response even though there was enhanced accumulation of virus-specific FoxO3a-deficient $CD8^+$ T cells (Sullivan *et al.*, 2012a). Similar results were obtained by our group in a murine model of *Listeria monocytogenes* infection (Tzelepis *et al*., 2013), where the Ki67 expression was similar, but there was increased accumulation of primed cells during late homeostatic stages. To gain a better understanding of the impact of FoxO3a signaling, I set up the *in vitro* experimental model so that the signaling mechanisms could be evaluated in a controlled setting without the impact of other environmental signals. My *in vitro* results contradict the studies mentioned above as I show increased Ki67 expression in activated FoxO3a-deficient $CD8^+$ T cells (Figure 7A-B). The fact that this was observed with anti-CD3 stimulation in the absence of any antigen-presenting cells indicates that the impact of FoxO3a on cell cycling is T cell intrinsic. In the *in vivo* models, it is not possible to evaluate Ki67 staining on primed cells because the numbers of such cells are too low to detect during the early phases of the response. Hence, the responses can only be measured during and after the peak phase (day 5-7 onwards), and it is quite likely that other compensatory mechanisms in WT cells promote Ki67 expression. What I have shown in my

in vitro model is that during the early activation phase (24 h), FoxO3a impacts cell cycling of primed $CD8^+$ T cells, and this appears to occur when there is no difference in cell death between WT and FoxO3a-deficient $CD8^+$ T cells.

FoxO3a has been shown to promote the transcription of the cell cycle arrest protein $p27^{kip}$ in T cells (Marie *et al.*, 2002). Having observed an impact of FoxO3a in the cycling of $CD8^+$ T cells *in vitro*, I evaluated the expression of $p27^{kip}$ by western blotting. As the cells differentiated *in vitro* and initiated cell cycling, the expression of $p27^{kip}$ decreased, which was followed by a gradual increase in the expression of $p27^{kip}$ at later stages. These results make sense since the expression of the cell cycle arrest protein must decline for cell cycle progression to occur. However, I did not notice any difference in the expression of $p27^{kip}$ between WT and FoxO3a-deficient $CD8^+$ T cells (Figure 8A-B). The lack of modulation in $p27^{kip}$ expression in the absence of FoxO3a signaling was further supported by the result where I did not observe any proliferation in unstimulated FoxO3a-deficient $CD8^+$ T cells (Figure 6A) although the possibility of low levels of proliferation (in lieu of subtle, but significant, increases in MTT signals at 24 h post-culture), cannot be ruled out. There have also been reports of Fox01 regulating $p27^{kip}$ expression (Marie *et al.*, 2002), although it was shown in CTLL-2 T cell lines. It is possible that this could be a compensatory mechanism occurring in the activated FoxO3a-deficient $CD8^+$ T cells. Another possibility could be that the western blotting is not sensitive enough to detect small changes in protein expression, as entire cell extracts are run on gels which includes live as well as dead cells. A better assay would be to evaluate the levels of this protein by intracellular staining, which could allow us to discriminate between the various cell populations.

Taken together, my results appear to reveal a role for FoxO3a in regulating $CD8^+$ T cell proliferation through $p27^{kip}$-independent mechanisms. Indeed, FoxO3a has been reported to suppress proliferation of mouse embryonic fibroblasts (MEFs) through downregulation of cyclin D1 and cyclin D2 and that this mechanism was $p27^{kip}$-independent (Schmidt *et al.*, 2002). This could be another potential mechanism by which FoxO3a regulates $CD8^+$ T cell proliferation. FoxO3a has also been shown to be involved during the G_2-M phase of the cell cycling by upregulating the expression of a DNA-repair protein, Gadd45 although this was shown in Rat-1 cell lines (Tran *et al.*, 2002). Reduced Gadd45 levels in FoxO3a-deficient $CD8^+$ T cells might indicate reduced time spent in the G_2 phase and consequently an enhanced rate of cell cycling.

One of the first studies examining the role of FoxO3a in the immune system reported hyperproliferation of FoxO3a-deficient $CD4^+$ T cells upon polyclonal stimulation *in vitro* (Lin *et al.*, 2004) although the time point at which the proliferation was evaluated was not indicated. The time point becomes an important factor as cells die at the late stages post-activation (due to nutrient deprivation and crowding) and the enhanced proliferation could be a direct consequence of the reduced cell death as explained before. Ironically, another study showed similar magnitudes of proliferation among WT and FoxO3a-deficient $CD4^+$ T cells at 72 h post-stimulation with anti-CD3 and anti-CD28 antibodies (Dejean *et al.*, 2009) although in this study, the FoxO3a-deficient mice (termed $FoxO3^{Kca}$ in the study) were generated in a different manner. $FoxO3^{Kca}$ mice were generated from C57BL/6 mice lacking *Foxo3* which were then backcrossed to the C57BL/6J strain, whereas the FoxO3a-deficient mice used by Lin *et al*. (termed $FoxO3a^{trap}$ in the study) were generated on a 129

background. To summarize, there seems to be a discrepancy between studies using differently generated knock-out models about the role of FoxO3a in modulating T cell proliferation. Both these studies (Lin *et al.* and Dejean *et al.*) utilize $CD4^+$ T cells and so these results must be carefully interpreted knowing the inherent differences between the activation and survival of $CD4^+$ and $CD8^+$ T cells (Ferreira *et al.*, 2000).

4.4. FoxO3a and the threshold of $CD8^+$ T cell activation

Upon TCR ligation with pMHC complex, co-receptor associated Lck is able to phosphorylate the ITAMs in the cytoplasmic domains of the CD3 ζ dimer. These phosphorylations provide a docking site for ζ-associated protein of 70kD (ZAP-70), which is in turn phosphorylated and activates a number of signaling mediators, of which the most important are Linker for Activation of T cells (LAT) and SH-2 domain containing-leukocyte phosphoprotein of 76 kD (SLP-76). LAT and SLP-76 in turn activate phospholipase C (PLC) and Growth factor Receptor Bound protein 2 (GRB2). PLC converts phosphatidyl inositol-2-phosphate (PIP2) to inositol-3-phosphate (IP3) and diacylglycerol (DAG). GRB2 activates the Ras-Erk pathway which in turn leads to the assembly of the AP-1 complex. IP3 leads to an increase in intracellular calcium levels which activates the NFAT pathway and DAG activates protein kinase C (PKC) which activates the NFκB pathway. NFAT, NFκB and AP-1 act synergistically to regulate the transcription of various genes involved in T cell activation (Smith-Garvin *et al*., 2009).

Upon CD28 co-stimulation, the PI3K-Akt pathway is engaged. First, the p85 regulatory subunit of PI3K is recruited to the cytoplasmic domain of CD28. This p85 subunit then recruits the p110 catalytic subunit of PI3K which converts PIP2 to phosphatidyl inositol

triphosphate (PIP3). PIP3 serves as a docking site for PDK1 which phosphorylates and activates Akt. Akt enhances the nuclear translocation of NFAT and NFκB, thereby potentiating the effects of TCR stimulation (Smith-Garvin *et al*., 2009).

For complete T cell activation, both these signals (TCR stimulation and co-stimulation) are required to be engaged. Since FoxO3a modulated the proliferation of $CD8^+$ T cells, I wanted to explore the possibility that FoxO3a regulated the threshold of T cell activation. Indeed, my results indicated that FoxO3a modulated the threshold of TCR stimulation as FoxO3a-deficient $CD8^+$ T cells displayed enhanced proliferation even with a low amount (0.2 μg/ml) of anti-CD3 antibody along with constant amount of co-stimulation (1 μg/ml anti-CD28) (Figure 9A-B). This is especially important as WT $CD8^+$ T cells exhibited little to no proliferation under similar conditions. This suggests that FoxO3a could be involved in the regulation of some of the kinases during proximal TCR signaling which remains to be tested. Interestingly, FoxO3a was reported to regulate the expression of diacylglycerol kinase α (DGKα) which in turn converts DAG to phosphatidic acid and thereby downregulates Ras-dependent pathways leading to anergy in primary murine T cells (Martinez-Moreno *et al*., 2012). Lower levels of DGKα in FoxO3a-deficient $CD8^+$ T cells could have led to the observed enhanced proliferation to low dose stimulation. Also, FoxO3a-deficient $CD8^+$ T cells exhibited increased MTT reduction when provided with TCR stimulus alone in the absence of co-stimulation (Figure 10). Taken together, these results suggest that FoxO3a impacts $CD8^+$ T cell proliferation mainly through TCR signaling and regulates the threshold of TCR stimulation.

4.5. FoxO3a and modulation of $CD8^+$ T cell death

While there was no difference in cell death between the WT and FoxO3a-deficient $CD8^+$ T cells at 24 h post-stimulation, FoxO3a-deficient $CD8^+$ T cells underwent significantly reduced cell death at the later stages (48 and 72 h) (Figure 12A-B). The impact of FoxO3a on cell death occurred at the later stages of cell division (divisions 2 and 3) with no influence during the first division (Figure 13 A-B). These results suggest that cell death occurring during the early stages (24 h) of activation is FoxO3a-independent. This also indicates that FoxO3a might play a role in regulating cell death during stress conditions as high oxidative stress conditions prevail as a result of increased metabolism and reactive oxygen species (ROS) accumulation in actively dividing cells (Havens *et al.*, 2006). Oxidative stress leads to the activation and nuclear localization of FoxO3a and consequent upregulation of antioxidant defenses (Kops *et al.*, 2002). But in cases where the stress increases beyond a certain threshold, FoxO3a activates the cell death program instead (Greer and Brunet, 2005).

Bim is a BH3-domain only member of the Bcl-2 family that mediates the intrinsic apoptotic death pathway (O'Connor *et al.*, 1998) and FoxO3a has been shown to regulate the levels of Bim in T cells (Marie *et al.*, 2002). There are three isoforms of Bim generated by alternative splicing; Bim_{EL}, Bim_L and Bim_S (O'Connor *et al.*, 1998) and the predominant isoform expressed in T cells has been reported to be Bim_{EL} (Hildeman *et al.*, 2002). Hence, I have evaluated the expression of Bim_{EL} (henceforth referred to as Bim) in WT and FoxO3a-deficient $CD8^+$ T cells. As evaluated by western blotting, the expression of Bim is relatively

higher even at 24 h post-stimulation when the expression of $p27^{kip}$ is very low in activated $CD8^+$ T cells. Marie *et al.* suggested that "the onset of apoptosis may require prolonged cell cycle arrest in the G_1 phase to be irreversibly established" (Marie *et al.*, 2002). They also reported that induction of Bim expression occurred much later than $p27^{kip}$ upregulation upon IL-2 withdrawal in CTLL-2 T cell lines. My results indicated no differences in the levels of Bim between activated WT and FoxO3a-deficient $CD8^+$ T cells *in vitro* even though experiments with an inhibitor of apoptosis (z-VAD) indicated FoxO3a impacts the apoptotic death of activated $CD8^+$ T cells (Figure 14). Also, the impact of FoxO3a seems to occur only at 72 h post-stimulation. This correlates with the increased mitochondrial activity (mitochondrial membrane potential) that was observed in activated FoxO3a-deficient $CD8^+$ T cells at the same time period (72 h) (Figure 17 A-B). Taking these results together, they indicate that FoxO3a regulates the intrinsic apoptotic pathway but the lack of differences in either Bim or cleaved (active) caspase 3 argues against this hypothesis. An issue to consider here would be the differences in expression levels of these pro-apoptotic markers between live and dead cells and that western blotting is done with entire cell extracts which limits the ability to differentiate between subtle changes in protein levels in live cells. A more comprehensive analysis using intracellular flow cytometry will aid in distinguishing the expression levels of any protein between live and dead cells. The levels of Bim might be lower in actively dividing FoxO3a-deficient $CD8^+$ T cells but further experiments have to be conducted in order to prove that hypothesis. A number of *in vivo* studies demonstrate lower levels of Bim in FoxO3a-deficient T cells but none of them indicate the specific isoform measured.

One of the first studies on FoxO3a signaling in human primary T cells reported enhanced survival of $CD4^+$ central memory T cells (T_{CM}) compared to effector memory T cells (T_{EM}). This was attributed to increased FoxO3a phosphorylation and a concomitant reduction in the levels of Bim in $CD4^+$ T_{CM} cells (Riou *et al.,* 2007). This correlates with my *in vitro* data where I observed increased survival of activated FoxO3a-deficient murine $CD8^+$ T cells although the expression levels (by western blotting) of Bim were similar between activated WT and FoxO3a-deficient $CD8^+$ T cells. The differences in results between this study and mine could be attributed to the possibility of varying mechanisms of Bim regulation in $CD4^+$ T cells compared to $CD8^+$ T cells.

Another study in a murine model of acute LCMV infection reported enhanced accumulation of virus-specific $CD8^+$ T cells at the peak of the response but attributed that to reduced apoptosis and not an enhanced rate of proliferation (Sullivan *et al.,* 2012a). Their data correlates with my *in vitro* results where FoxO3a-deficient $CD8^+$ T cells displayed reduced apoptotic cell death. They also report lower levels of Bim in FoxO3a-deficient virus-specific $CD8^+$ T cells at day 6 post-infection whereas I did not find any differences in Bim expression levels between activated WT and FoxO3a-deficient $CD8^+$ T cells in my *in vitro* stimulation model.

Sullivan *et al*. also reported an increased accumulation of virus-specific FoxO3-deficient $CD8^+$ T cells in a murine model of chronic LCMV infection (Sullivan *et al.,* 2012b) although the mice they used in this study were deficient for FoxO3 only in the T cell compartment (termed FoxO3L mice). They also did not observe differences in Ki67 expression but showed

lower Annexin-V$^+$ virus-specific CD8$^+$ T cells in the spleens of FoxO3L mice during the early phase of the chronic infection (day 8 post-infection) and attributed the increased accumulation to reduced apoptosis and not increased proliferation. The mechanistic aspect behind the reduced apoptosis in the virus-specific FoxO3L CD8$^+$ T cells was missing from this study although they state in their discussion that mRNA levels of Bim were lower in the FoxO3L CD8$^+$ T cells. My results indicate that the reduced apoptosis in activated FoxO3a-deficient CD8$^+$ T cells *in vitro* is neither Bim-dependent nor Caspase-dependent.

Tzelepis *et al.* reported reduced apoptosis in antigen-specific CD8$^+$ T cells in FoxO3a-deficient mice during various phases of the CD8$^+$ T cell response during an acute bacterial (*Listeria monocytogenes*) infection (Tzelepis *et al.*, 2013). They also showed lower levels of pro-apoptotic factors, Bim and Puma in the FoxO3a-deficient CD8$^+$ T cells during various phases of the response, including the post-contraction phase (day 15 post-infection), which was further supported by data indicating lower Annexin-V expression and lower TUNEL expression in FoxO3a-deficient antigen-specific CD8$^+$ T cells. The data indicating lower TUNEL expression is especially important as DNA fragmentation is downstream of caspase activation and is generally considered one of the endpoints of apoptosis. Having noted differences in Bim expression and apoptosis, surprisingly, WT and FoxO3a-deficient CD8$^+$ T cells underwent similar magnitudes of contraction from day 7 onwards. Similarly, Dejean *et al*. noted similar contraction of CD4$^+$ and CD8$^+$ T cell responses in WT and FoxO3a-deficient mice during LCMV infection, further demonstrating that there is significant confusion regarding the impact of FoxO3a in CD8$^+$ T cell differentiation and death.

Taken together, my results indicate FoxO3a promotes apoptotic death of activated $CD8^+$ T cells and that this effect is neither Bim-dependent nor caspase-dependent *in vitro*. Indeed, a recent study indicates FoxO3-mediated Bim transcription is dispensable for thymocyte apoptosis upon cytokine withdrawal (Herold *et al.*, 2013). The studies by Riou *et al.* and Tzelepis *et al.* use flow cytometry to sort the different cell populations before evaluating the expression levels of the various pro-apoptotic markers by western blotting. Also, the study by Sullivan *et al.* used intracellular flow cytometry to assess Bim expression levels in antigen-specific $CD8^+$ T cells. All these studies might have ignored dead cells in their analysis as opposed to mine. Further experimentation using comprehensive intracellular flow cytometric analysis will help in gaining a mechanistic insight into how FoxO3a impacts apoptotic death in $CD8^+$ T cells. I have not performed western blotting of cell extracts beyond 72 h, and it is possible that there may be differences beyond that point. What I can say from my study is that during the very early periods (days 1-3) of a response, during which primed T cells cannot be tracked *in vivo*, the levels of Bim and Caspase 3 are similar in WT and FoxO3a-deficient mice.

4.6. Role of FoxO3a in cytokine regulation

My results indicate that cytokine expression is enhanced in both activated $CD8^+$ T cells and activated DCs in the absence of FoxO3a signaling, suggesting a global role of FoxO3a in regulating cytokine expression in activated immune cells. FoxO3a-deficient $CD8^+$ T cells produced increased levels of IFN-γ, TNF-α and IL-6 and FoxO3a-deficient DCs produced increased levels of IL-1α, IL-1β, IL-6, TNF-α, IL-12 and IL-10. Lin *et al.* observed enhanced

expression of IL-2 and IFN-γ in $CD4^+$ T cells upon polyclonal stimulation *in vitro* (Lin *et al.*, 2004). They also observed enhanced 'basal' NFκB activity in the FoxO3a-deficient $CD4^+$ T cells; however, the mRNA levels of NFκB were similar between WT and FoxO3a-deficient $CD4^+$ cells indicating regulation at the post-transcriptional level. In contrast to this, I did not observe any differences in the protein expression levels, as measured by western blotting, of phosphorylated and total NFκB between WT and FoxO3a-deficient $CD8^+$ T cells. The phosphorylation of NFκB peaked at 24 h post-stimulation and tapered off to basal levels at 48 and 72 h post-stimulation (Figure 20 A-B). These results are in agreement with the scientific literature, as NFκB is known as a pro-survival factor (Oeckinghaus and Ghosh, 2009). At the early stages (24 h) of activation, the high levels of phosphorylated (activated) NFκB allow the cells to survive and progress through the cell cycle, followed by a gradual decline at the later stages (48 and 72 h) when there is also a considerable amount of cell death.

Lin *et al.* also reported downregulation of certain NFκB inhibitor proteins. They show reduced mRNA and protein levels of IκBβ and IκBε in FoxO3a-deficient $CD4^+$ T cells although they did not find any promoter binding sites for FoxO3a on the IκBβ and IκBε sequences. Lin *et al.* also report similar mRNA and protein levels of IκBα in the FoxO3a-deficient $CD4^+$ T cells whereas another study in human epithelial HT-29 cells indicates FoxO3a regulates the expression levels of IκBα (Snoeks *et al.*, 2008). These results indicate that FoxO3a signaling might regulate NFκB activation by reciprocal regulation of the inhibitory IκB proteins through interaction with other transcription factors (Lin *et al*. also report lower mRNA levels of Foxj1). Knowing the impact of FoxO3 on the transcriptional regulation of other Fox

proteins (Karadedou *et al.*, 2012; Zhou *et al.*, 2012), the possibilities of transactivation dependent IκB regulation are manifold. Another factor contributing to the differences between the study by Lin *et al.* and mine could be cell type specific NFκB regulation by FoxO3a as my results were from $CD8^+$ T cells whereas Lin *et al.* reported the differences in $CD4^+$ T cells. Also, Lin *et al*. reported a modest upregulation in activation markers, CD44 and CD25, in the FoxO3a-deficient $CD4^+$ T cells which correlated with higher spontaneous NFκB activity. In contrast, my results indicated no differences in the activation status of naïve FoxO3a-deficient $CD8^+$ T cells compared to WT $CD8^+$ T cells (Figure 2) which correlates with similar levels of basal NFκB activities as evaluated by its phosphorylation status (Figure 20A). Lin *et al*. also observed enhanced NFκB activity using luciferase reporter assays. The assay does not provide information on the post-translational modification (PTM) that controls its activity. Indeed, another important PTM that controls the transcriptional activity of NFκB is acetylation (Ghizzoni *et al*., 2011; Yang *et al*., 2012). Differences in the levels of acetylated NFκB between WT and FoxO3a-deficient cells have to be evaluated before confirming an NFκB-independent mechanism of cytokine regulation by FoxO3a signaling.

IL-6 is known as a T cell survival factor as it prevents the downregulation of Bcl-2 (Rochman *et al*., 2005). The enhanced IL-6 expression by FoxO3a-deficient $CD8^+$ T cells affected their survival in an autocrine manner. Upon neutralization of IL-6, the proliferation and survival of FoxO3a-deficient $CD8^+$ T cells were drastically reduced whereas the survival of WT $CD8^+$ T cells was unaffected (Figure 19C). Dejean *et al*. report the increased IL-6 secretion by $FoxO3^{Kca}$ DCs contributed to enhanced $CD8^+$ T cell survival upon activation whereas my data

indicate a DC-independent modulation of $CD8^+$ T cell survival mediated by increased IL-6 signaling in the absence of FoxO3a signaling.

During an acute LCMV infection, splenic DCs from $FoxO3^{Kca}$ mice were reported to display enhanced expression of IL-6 and TNF-α but not IL-10 and IL-12 (Dejean *et al.*, 2009). This suggests a role of FoxO3a in regulating specific cytokines; whereas my results indicate FoxO3a regulates the expression of various cytokines including IL-1α, IL-1β, IL-6, TNF-α, IL-10 and IL-12 in activated DCs (Figure 24). Thus, it appears that a global mechanism of cytokine expression is regulated by FoxO3a signaling. There are a few differences between these studies; 1) The $FoxO3^{Kca}$ mice were generated in a different manner (explained in section 4.3) and 2) the type of stimulation was different as their results were obtained from LCMV-infected DCs cultured *ex vivo* and mine were from LPS-stimulated DCs *in vitro*. Moreover, Dejean *et al.* do not provide a mechanistic insight into the inhibition of cytokine signaling by FoxO3a other than the observation that nuclear localization of FoxO3a in DCs correlated with inhibition of cytokine secretion.

Taken together, my results indicate an NFκB-independent mechanism of cytokine regulation by FoxO3a signaling in $CD8^+$ T cells. This leads to various possibilities by which FoxO3a could regulate cytokine signaling. Lnk, a negative regulator of cytokine signaling, was reported to be deregulated in FoxO3a-deficient mice as a result of increased ROS levels (Yalcin *et al.*, 2010). Mitogen-activated protein kinases (MAPK) have been implicated in the transcriptional regulation of cytokines (Costa-Pereira, 2014; Tiedje *et al.*, 2014). Increased c-Jun N-terminal kinase (JNK) signaling has been reported to result in enhanced inflammatory

cytokine expression in thymocytes during *Salmonella typhimurium* infection in mice (Deobagkar-Lele *et al.*, 2014). Further characterization is required to gain mechanistic insights into the modulation of cytokine signaling by FoxO3a.

4.7. FoxO3a and regulation of DC activation

My results indicate that FoxO3a does not modulate DC activation under steady state conditions as evaluated by the expression of activation markers CD80, CD86 and MHC-II on naïve DCs isolated from the spleens of WT and FoxO3a-deficient mice (Figure 22A-B). Dejean *et al.* reported increased activation of naïve DCs from spleens of $FoxO3^{Kca}$ mice and show increased expression of co-stimulatory molecules CD80 and CD86 but not MHC-II (Dejean *et al*., 2009). This indicates enhanced co-stimulatory capacity of naïve DCs in the absence of FoxO3a signaling. Since naïve DCs have a diminished capacity to present antigen to T cells (Cella *et al.*, 1997), the enhanced co-stimulatory molecule expression reported on naïve $FoxO3^{Kca}$ DCs (Dejean *et al*., 2009) may not have a significant biological impact (the differences were <2 fold). Also, the inherent differences in the way the FoxO3a-deficient mice were generated (explained in section 4.4) could have contributed to the differences observed in the activation status of DCs between the two studies.

4.8. Role of FoxO3a in DC mediated antigen presentation

I observed enhanced antigen presentation by FoxO3a-deficient DCs as evaluated by increased proliferation of WT OT-1 CD8+ T cells (Figure 25). These differences were noted only at lower infection doses. These results indicate that FoxO3a-deficient DCs might be more efficient at inducing $CD8^+$ T cell activation during the initial stages of an infection

when the pathogen burden is not too high and the antigen amounts are minimal. These results correlate with my data showing that FoxO3a deficient T cells display a lower threshold of activation in response to polyclonal stimulation (Figure 9). Also, my results indicated that FoxO3a-deficient DCs produced increased levels of cytokines upon activation, which could potentially lead to enhanced antigen presentation. When $Ova_{(257-264)}$ peptide (SIINFEKL) was added to the WT and FoxO3a-deficient DCs, there was no difference in antigen presentation. This further supports the model wherein the enhanced $CD8^+$ T cell proliferation is dependent on the increased levels of cytokines secreted by activated (infected) FoxO3a-deficient DCs. The increased IL-6 secreted by FoxO3a-deficient DCs has been reported to impact T cell survival (Dejean *et al.*, 2009). Consequently, the enhanced $CD8^+$ T cell survival following activation would favor enhanced cycling following antigen presentation. My results were from splenic DCs although similar results were reported by Dejean *et al.* where they used bone marrow derived dendritic cells (BMDC) and found enhanced antigen presentation by $FoxO3^{Kca}$ BMDC to both $CD4^+$ and $CD8^+$ T cells. On the other hand, Tzelepis *et al.* reported similar antigen presentation by WT and FoxO3a-deficient BMDCs to WT OT-1 $CD8^+$ T cells and this could be due to the inherent differences in the way the FoxO3a-deficient mice were generated (explained in section 4.3). Also, BMDCs are primarily $CD11b^+$ DCs whereas splenic DCs are a population of $CD11b^+$, $CD8\alpha^+$ and $B220^+$ DCs (Shortman and Liu, 2002). Knowing the inherent differences in the capacities of antigen presentation by the various DC subsets (Mildner and Jung, 2014), this is a factor to be considered when comparing the results of Tzelepis *et al.* and mine even though the same FoxO3a-deficient mice were used. In addition, the infection model used between

these two studies was different; I used a recombinant strain of Ovalbumin-expressing *Salmonella typhimurium* whereas Tzelepis *et al*. used a recombinant strain of Ovalbumin-expressing *Listeria monocytogenes*. Differences in specific pathogen virulence could have contributed to the contrasting results between the two studies.

Taken together, these results indicate FoxO3a signaling modulates antigen presentation in activated DCs. The importance of FoxO3a signaling in DCs has also been demonstrated in human and murine tumor models where FoxO3a signaling was reported to induce tolerogenic properties in tumor-associated DCs (TADCs). The impact of FoxO3a was reported to be mediated by increased expression of TGF-β and decreased expression of inflammatory cytokines. Silencing *FoxO3* in murine TADCs led to decreased expression of TGF-β and increased expression of pro-inflammatory cytokines which in turn led to enhanced CTL-mediated anti-tumor responses (Watkins *et al*., 2011). These studies further the model wherein FoxO3a acts as a negative regulator of DC mediated antigen presentation to T cells, likely through modulation of cytokine expression.

5. CONCLUSIONS

5.1. Concluding remarks

I initiated this study with the hypothesis that FoxO3a modulates the activation of innate and adaptive immune cells by regulating the transcription of cell death genes. Although, my data does indicate that FoxO3a impacts apoptotic cell death of $CD8^+$ T cells, the mechanism(s) by which this happens during the early stages of $CD8^+$ T cell activation remain(s) to be uncovered. Also, the impact of FoxO3a on cell death seems to occur at the later stages of cell division (divisions 2 and 3) and at the later stages of activation (days 2 and 3). In addition to modulation of cell death, FoxO3a also seems to impact cell cycling during the very early stages of activation independently of cell death. The mechanism also appears to be $p27^{kip}$-independent.

There seems to be a disparity between various studies as to the role of FoxO3a in modulating the $CD8^+$ T cell response to infection. Some report a T cell-intrinsic role of FoxO3a in modulating their survival, and not proliferation, whereas others report an extrinsic role where FoxO3a signaling in DCs modulates $CD8^+$ T cell survival upon antigen presentation. Another compounding problem is the use of FoxO3a-deficient mouse models that were generated on different backgrounds in the various studies discussed. I show, in this study, that FoxO3a acts in a $CD8^+$ T cell-intrinsic manner to regulate its proliferation and survival, at least during the early stages (days 1-3) of a response.

I also show that FoxO3a signaling modulates the expression of IL-6 in activated $CD8^+$ T cells and that IL-6 acts in an autocrine manner to modulate $CD8^+$ T cell survival. Another

noteworthy finding in this study is the role of FoxO3a in regulating global cytokine production. Activated $CD8^+$ T cells expressed increased levels of IFN-γ, TNF-α and IL-6 in the absence of FoxO3a signaling. FoxO3a signaling also modulated the expression of various cytokines (IL-1α, IL-1β, IL-6, TNF-α, IL-12 and IL-10) in activated DCs. This modulation of cytokine expression seemed to occur independently of NFκB signaling as I observed no differences in the extent of phosphorylation of NFκB between WT and FoxO3a-deficient $CD8^+$ T cells. FoxO3a signaling in dendritic cells also modulated their antigen presentation to $CD8^+$ T cells, most likely as a consequence of the modulated cytokine expression.

Taken together, my results indicate FoxO3a as a negative regulator of $CD8^+$ T cell and dendritic cell mediated immune responses during an infection (as depicted in Figure 26). Deciphering the mechanisms involved could lead to targeting FoxO3a signaling components in $CD8^+$ T cells and/or dendritic cells for novel therapeutic strategies in vaccine development.

5.2. Future directions

My results displaying increased MTT reduction by both unstimulated FoxO3a-deficient $CD8^+$ T cells and DCs suggest high basal levels of metabolism in the FoxO3a-deficient cells. This could be due to two factors; 1) increased mTOR activity or 2) decreased protein turnover leading to prolonged activity of proteins involved in regulating metabolism among others. Evaluating these factors will also aid in providing mechanistic insights into the role of FoxO3a in regulating immune cell homeostasis.

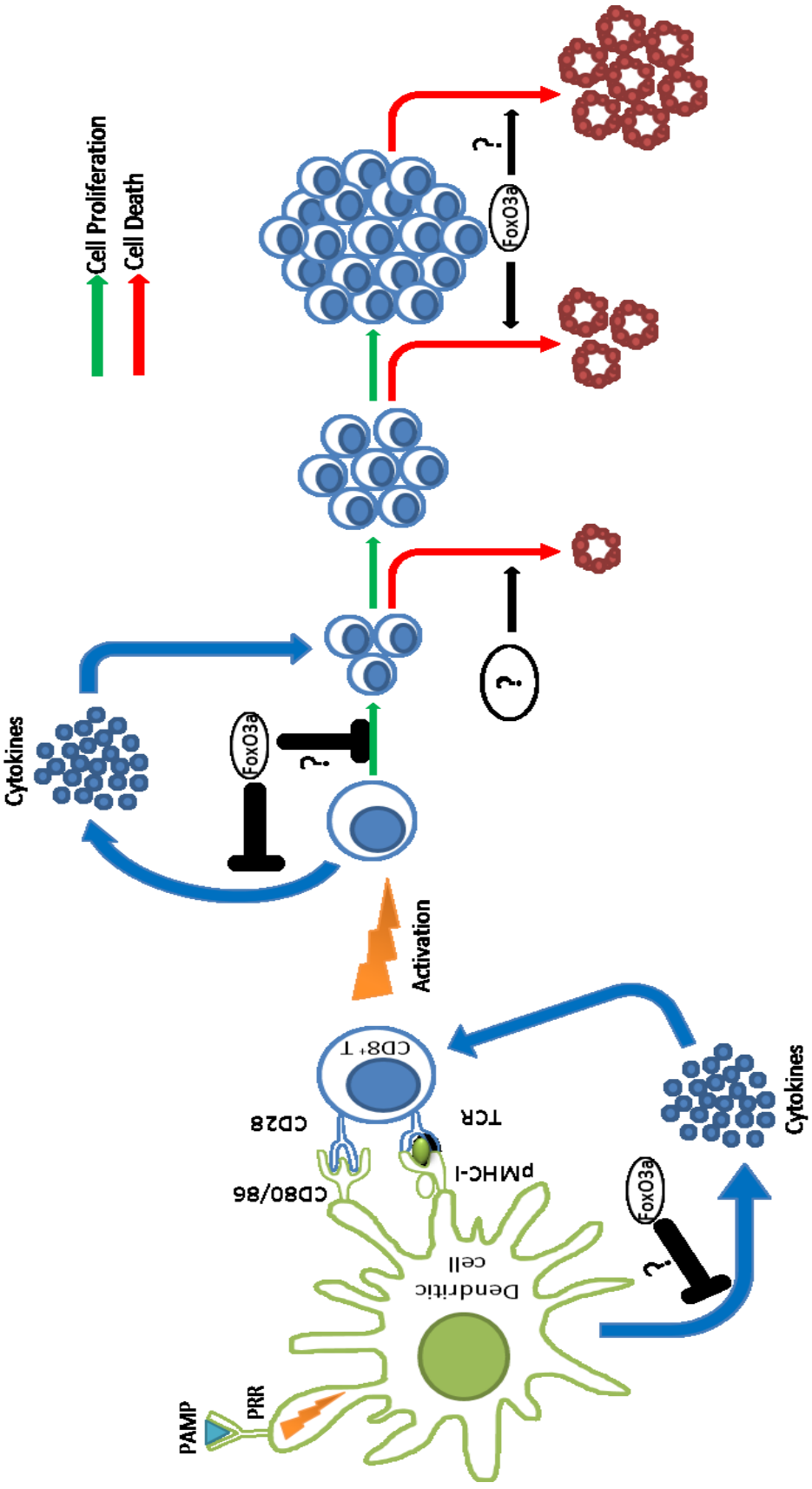
Cell Proliferation
Cell Death
FoxO3a
?
Cytokines
Activation
CD8+T
TCR
CD28
pMHC-I
CD80/86
Dendritic cell
PAMP
PRR

Figure 26 – A model depicting the negative regulation of dendritic cell and $CD8^+$ T cell activation by FoxO3a.

The blue arrows indicate action performed by the cell, the green arrows indicate cell proliferation and the red arrows indicate cell death. The question marks indicate the gaps in scientific literature and consequently, future directions for this study.

Modulation of $CD8^+$ T cell proliferation by FoxO3a during the early stages (days 1-3) of activation seems to be $p27^{kip}$-independent. Seeing as how the levels of Ki67, a cell cycle protein, was upregulated in the absence of FoxO3a, evaluating the expression of other cell cycle progression proteins like cyclins D1 and D2 and DNA-repair protein, Gadd45 would help gain mechanistic insights into the modulation of $CD8^+$ T cell proliferation by FoxO3a. Another possibility, leading to the increased proliferation, could be increased levels of ROS as a direct consequence of increased metabolism and lack of antioxidant defenses in the FoxO3a-deficient $CD8^+$ T cells.

Cell death during the very early stage (day 1) of activation seems to be FoxO3a-independent whereas during the later stages (days 2 and 3) of activation and cell division (divisions 2 and 3) FoxO3a impacts cell death. This modulation of apoptotic cell death seems to be neither Bim-dependent not Caspase-dependent. As discussed in the previous chapter (section 4.5), a more comprehensive analysis using intracellular flow cytometry will be required to differentiate the levels of Bim between live and dead cells. Also, apoptotic cells, in the absence of phagocytosis, have been reported to progress to secondary necrosis (Krysko *et al*., 2008). Since my culture consists of purified $CD8^+$ T cells, the possibility of this phenomenon cannot be ruled out. Nevertheless, cell death is still reduced in the FoxO3a-deficient $CD8^+$ T cells. If this (secondary necrosis) is true, then the role of FoxO3a in modulating necrotic cell death will be a novel finding. Of course, further experimentation is required in order to prove this hypothesis. Evaluating the levels of the DAMP, high mobility group box 1 protein (HMGB-1) in the cell culture supernatants will aid in providing an insight into this mechanism.

My data indicated a role of FoxO3a in regulating global cytokine expression in both $CD8^+$ T cells and DCs. This modulation in cytokine signaling seemed to be NFκB-independent. Although, as discussed in the previous chapter (section 4.6), the levels of acetylated NFκB have to be evaluated before ruling out this hypothesis. Additionally, MAPK signaling (Tiedje *et al*., 2014) and JNK signaling (Deobagkar-Lele *et al*., 2014) have been implicated in the regulation of cytokine signaling. Hence, increased MAPK and/or JNK activation in the FoxO3a-deficient cells could explain the increased cytokine secretion.

REFERENCES

Acuto, O., and Michel, F. (2003). CD28-mediated co-stimulation: a quantitative support for TCR signalling. Nat Rev Immunol *3*, 939-951.

Akira, S., Uematsu, S., and Takeuchi, O. (2006). Pathogen recognition and innate immunity. Cell *124*, 783-801.

Anderson, M.J., Viars, C.S., Czekay, S., Cavenee, W.K., and Arden, K.C. (1998). Cloning and characterization of three human forkhead genes that comprise an FKHR-like gene subfamily. Genomics *47*, 187-199.

Arai, K.I., Lee, F., Miyajima, A., Miyatake, S., Arai, N., and Yokota, T. (1990). Cytokines: coordinators of immune and inflammatory responses. Annual review of biochemistry *59*, 783-836.

Banchereau, J., Bazan, F., Blanchard, D., Briere, F., Galizzi, J.P., van Kooten, C., Liu, Y.J., Rousset, F., and Saeland, S. (1994). The CD40 antigen and its ligand. Annu Rev Immunol *12*, 881-922.

Banchereau, J., Briere, F., Caux, C., Davoust, J., Lebecque, S., Liu, Y.J., Pulendran, B., and Palucka, K. (2000). Immunobiology of dendritic cells. Annu Rev Immunol *18*, 767-811.

Beutler, B. (2000). Tlr4: central component of the sole mammalian LPS sensor. Current opinion in immunology *12*, 20-26.

Beutler, B. (2004). Innate immunity: an overview. Molecular immunology *40*, 845-859.

Bevan, M.J. (2004). Helping the CD8(+) T-cell response. Nat Rev Immunol *4*, 595-602.

Boise, L.H., Minn, A.J., Noel, P.J., June, C.H., Accavitti, M.A., Lindsten, T., and Thompson, C.B. (1995). CD28 costimulation can promote T cell survival by enhancing the expression of Bcl-xL. Immunity *3*, 87-98.

Bonilla, F.A., and Oettgen, H.C. (2010). Adaptive immunity. J Allergy Clin Immunol *125*, S33-40.

Brunet, A., Bonni, A., Zigmond, M.J., Lin, M.Z., Juo, P., Hu, L.S., Anderson, M.J., Arden, K.C., Blenis, J., and Greenberg, M.E. (1999). Akt promotes cell survival by phosphorylating and inhibiting a Forkhead transcription factor. Cell *96*, 857-868.

Calnan, D.R., and Brunet, A. (2008). The FoxO code. Oncogene *27*, 2276-2288.

Carroll, M.C. (2004). The complement system in regulation of adaptive immunity. Nat Immunol *5*, 981-986.

Castrillon, D.H., Miao, L., Kollipara, R., Horner, J.W., and DePinho, R.A. (2003). Suppression of ovarian follicle activation in mice by the transcription factor Foxo3a. Science *301*, 215-218.

Cella, M., Sallusto, F., and Lanzavecchia, A. (1997). Origin, maturation and antigen presenting function of dendritic cells. Current opinion in immunology *9*, 10-16.

Cho, B.K., Wang, C., Sugawa, S., Eisen, H.N., and Chen, J. (1999). Functional differences between memory and naive CD8 T cells. Proceedings of the National Academy of Sciences *96*, 2976-2981.

Choi, J., Oh, S., Lee, D., Oh, H.J., Park, J.Y., Lee, S.B., and Lim, D.S. (2009). Mst1-FoxO signaling protects Naive T lymphocytes from cellular oxidative stress in mice. PLoS One *4*, e8011.

Costa-Pereira, A.P. (2014). Regulation of IL-6-type cytokine responses by MAPKs. Biochemical Society transactions *42*, 59-62.

Curtsinger, J.M., Lins, D.C., and Mescher, M.F. (2003). Signal 3 determines tolerance versus full activation of naive CD8 T cells: dissociating proliferation and development of effector function. J Exp Med *197*, 1141-1151.

Cyster, J.G. (1999). Chemokines and the homing of dendritic cells to the T cell areas of lymphoid organs. J Exp Med *189*, 447-450.

Dejean, A.S., Beisner, D.R., Ch'en, I.L., Kerdiles, Y.M., Babour, A., Arden, K.C., Castrillon, D.H., DePinho, R.A., and Hedrick, S.M. (2009). Transcription factor Foxo3 controls the magnitude of T cell immune responses by modulating the function of dendritic cells. Nat Immunol *10*, 504-513.

Dejean, A.S., Hedrick, S.M., and Kerdiles, Y.M. (2011). Highly specialized role of Forkhead box O transcription factors in the immune system. Antioxid Redox Signal *14*, 663-674.

den Haan, J.M.M., Lehar, S.M., and Bevan, M.J. (2000). Cd8+ but Not Cd8- Dendritic Cells Cross-Prime Cytotoxic T Cells in Vivo. Journal of Experimental Medicine *192*, 1685-1696.

Deobagkar-Lele, M., Victor, E.S., and Nandi, D. (2014). c-Jun NH2 -terminal kinase is a critical node in the death of CD4+ CD8+ thymocytes during Salmonella enterica serovar Typhimurium infection. Eur J Immunol *44*, 137-149.

Dinarello, C.A. (2000). Proinflammatory cytokines. Chest *118*, 503-508.

Donlon, T.A., Curb, J.D., He, Q., Grove, J.S., Masaki, K.H., Rodriguez, B., Elliott, A., Willcox, D.C., and Willcox, B.J. (2012). FOXO3 gene variants and human aging: coding variants may not be key players. J Gerontol A Biol Sci Med Sci *67*, 1132-1139.

Eijkelenboom, A., and Burgering, B.M. (2013). FOXOs: signalling integrators for homeostasis maintenance. Nat Rev Mol Cell Biol *14*, 83-97.

Ferreira, C., Barthlott, T., Garcia, S., Zamoyska, R., and Stockinger, B. (2000). Differential survival of naive CD4 and CD8 T cells. J Immunol *165*, 3689-3694.

Fujii, S., Liu, K., Smith, C., Bonito, A.J., and Steinman, R.M. (2004). The linkage of innate to adaptive immunity via maturing dendritic cells in vivo requires CD40 ligation in addition to antigen presentation and CD80/86 costimulation. J Exp Med *199*, 1607-1618.

Ganz, T., and Lehrer, R.I. (1998). Antimicrobial peptides of vertebrates. Current opinion in immunology *10*, 41-44.

Germain, R.N. (2002). T-cell development and the CD4-CD8 lineage decision. Nat Rev Immunol *2*, 309-322.

Gerondakis, S., and Siebenlist, U. (2010). Roles of the NF-kappaB pathway in lymphocyte development and function. Cold Spring Harb Perspect Biol *2*, a000182.

Ghizzoni, M., Haisma, H.J., Maarsingh, H., and Dekker, F.J. (2011). Histone acetyltransferases are crucial regulators in NF-kappaB mediated inflammation. Drug discovery today *16*, 504-511.

Greer, E.L., and Brunet, A. (2005). FOXO transcription factors at the interface between longevity and tumor suppression. Oncogene *24*, 7410-7425.

Guermonprez, P., Valladeau, J., Zitvogel, L., Thery, C., and Amigorena, S. (2002). Antigen presentation and T cell stimulation by dendritic cells. Annu Rev Immunol *20*, 621-667.

Hagenbuchner, J., Kuznetsov, A., Hermann, M., Hausott, B., Obexer, P., and Ausserlechner, M.J. (2012). FOXO3-induced reactive oxygen species are regulated by BCL2L11 (Bim) and SESN3. Journal of cell science *125*, 1191-1203.

Harty, J.T., and Badovinac, V.P. (2002). Influence of effector molecules on the CD8(+) T cell response to infection. Current opinion in immunology *14*, 360-365.

Harty, J.T., and Badovinac, V.P. (2008). Shaping and reshaping CD8+ T-cell memory. Nat Rev Immunol *8*, 107-119.

Havens, C.G., Ho, A., Yoshioka, N., and Dowdy, S.F. (2006). Regulation of late G1/S phase transition and APC Cdh1 by reactive oxygen species. Mol Cell Biol *26*, 4701-4711.

Hedrick, S.M., Ch'en, I.L., and Alves, B.N. (2010). Intertwined pathways of programmed cell death in immunity. Immunol Rev *236*, 41-53.

Herold, M.J., Rohrbeck, L., Lang, M.J., Grumont, R., Gerondakis, S., Tai, L., Bouillet, P., Kaufmann, T., and Strasser, A. (2013). Foxo-mediated Bim transcription is dispensable for the apoptosis of hematopoietic cells that is mediated by this BH3-only protein. EMBO Rep *14*, 992-998.

Hespel, C., and Moser, M. (2012). Role of inflammatory dendritic cells in innate and adaptive immunity. Eur J Immunol *42*, 2535-2543.

Heusel, J.W., Wesselschmidt, R.L., Shresta, S., Russell, J.H., and Ley, T.J. (1994). Cytotoxic lymphocytes require granzyme B for the rapid induction of DNA fragmentation and apoptosis in allogeneic target cells. Cell *76*, 977-987.

Hildeman, D.A., Zhu, Y., Mitchell, T.C., Bouillet, P., Strasser, A., Kappler, J., and Marrack, P. (2002). Activated T cell death in vivo mediated by proapoptotic bcl-2 family member bim. Immunity *16*, 759-767.

Hinman, R.M., Nichols, W.A., Diaz, T.M., Gallardo, T.D., Castrillon, D.H., and Satterthwaite, A.B. (2009). Foxo3-/- mice demonstrate reduced numbers of pre-B and recirculating B cells but normal splenic B cell sub-population distribution. Int Immunol *21*, 831-842.

Hoshino, K., Takeuchi, O., Kawai, T., Sanjo, H., Ogawa, T., Takeda, Y., Takeda, K., and Akira, S. (1999). Cutting edge: Toll-like receptor 4 (TLR4)-deficient mice are hyporesponsive to lipopolysaccharide: evidence for TLR4 as the Lps gene product. J Immunol *162*, 3749–3752.

Huang, H., and Tindall, D.J. (2007). Dynamic FoxO transcription factors. J Cell Sci *120*, 2479-2487.

Huseby, E.S., White, J., Crawford, F., Vass, T., Becker, D., Pinilla, C., Marrack, P., and Kappler, J.W. (2005). How the T cell repertoire becomes peptide and MHC specific. Cell *122*, 247-260.

Huster, K.M., Koffler, M., Stemberger, C., Schiemann, M., Wagner, H., and Busch, D.H. (2006). Unidirectional development of CD8+ central memory T cells into protective Listeria-specific effector memory T cells. Eur J Immunol *36*, 1453-1464.

Janeway, C.A. (2001). How the immune system protects the host from infection. Microbes and Infection *3*, 1167-1171.

Joffre, O., Nolte, M.A., Sporri, R., and Reis e Sousa, C. (2009). Inflammatory signals in dendritic cell activation and the induction of adaptive immunity. Immunol Rev *227*, 234-247.

Jung, S., Unutmaz, D., Wong, P., Sano, G., De los Santos, K., Sparwasser, T., Wu, S., Vuthoori, S., Ko, K., Zavala, F.*, et al.* (2002). In vivo depletion of CD11c+ dendritic cells abrogates priming of CD8+ T cells by exogenous cell-associated antigens. Immunity *17*, 211-220.

Karadedou, C.T., Gomes, A.R., Chen, J., Petkovic, M., Ho, K.K., Zwolinska, A.K., Feltes, A., Wong, S.Y., Chan, K.Y., Cheung, Y.N.*, et al.* (2012). FOXO3a represses VEGF expression through FOXM1-dependent and -independent mechanisms in breast cancer. Oncogene *31*, 1845-1858.

Kawai, T., and Akira, S. (2006). TLR signaling. Cell Death Differ *13*, 816-825.

Kawai, T., and Akira, S. (2010). The role of pattern-recognition receptors in innate immunity: update on Toll-like receptors. Nat Immunol *11*, 373-384.

Kim, J.J., Nottingham, L.K., Sin, J.I., Tsai, A., Morrison, L., Oh, J., Dang, K., Hu, Y., Kazahaya, K., Bennett, M.*, et al.* (1998). CD8 positive T cells influence antigen-specific immune responses through the expression of chemokines. J Clin Invest *102*, 1112-1124.

Kolumam, G.A., Thomas, S., Thompson, L.J., Sprent, J., and Murali-Krishna, K. (2005). Type I interferons act directly on CD8 T cells to allow clonal expansion and memory formation in response to viral infection. J Exp Med *202*, 637-650.

Kops, G.J., Dansen, T.B., Polderman, P.E., Saarloos, I., Wirtz, K.W., Coffer, P.J., Huang, T.T., Bos, J.L., Medema, R.H., and Burgering, B.M. (2002). Forkhead transcription factor FOXO3a protects quiescent cells from oxidative stress. Nature *419*, 316-321.

Kroemer, G., Galluzzi, L., and Brenner, C. (2007). Mitochondrial membrane permeabilization in cell death. Physiol Rev *87*, 99-163.

Krysko, D.V., Berghe, T.V., Parthoens, E., D'Herde, K., and Vandenabeele, P. (2008). Chapter 16 Methods for Distinguishing Apoptotic from Necrotic Cells and Measuring Their Clearance. Methods in enzymology *442*, 307-341.

Lee, H.Y., Youn, S.W., Kim, J.Y., Park, K.W., Hwang, C.I., Park, W.Y., Oh, B.H., Park, Y.B., Walsh, K., Seo, J.S.*, et al.* (2008). FOXO3a turns the tumor necrosis factor receptor signaling towards apoptosis through reciprocal regulation of c-Jun N-terminal kinase and NF-kappaB. Arterioscler Thromb Vasc Biol *28*, 112-120.

Lin, L., Hron, J.D., and Peng, S.L. (2004). Regulation of NF-kappaB, Th activation, and autoinflammation by the forkhead transcription factor Foxo3a. Immunity *21*, 203-213.

Lowin, B., Hahne, M., Mattmann, C., and Tschopp, J. (1994). Cytolytic T-cell cytotoxicity is mediated through perforin and Fas lytic pathways. Nature *370*, 650-652.

Macian, F. (2005). NFAT proteins: key regulators of T-cell development and function. Nat Rev Immunol *5*, 472-484.

Marie, S., Pascale, F.D., Geert, J.K., Susanne, M.L., Paul, J.C., Boudewijn, M.B., and René, H.M. (2002). The forkhead transcription factor FoxO regulates transcription of p27Kip1 and Bim in response to IL-2. J Immunol *168*, 5024-5031.

Martinez-Moreno, M., Garcia-Lievana, J., Soutar, D., Torres-Ayuso, P., Andrada, E., Zhong, X.P., Koretzky, G.A., Merida, I., and Avila-Flores, A. (2012). FoxO-dependent regulation of diacylglycerol kinase alpha gene expression. Mol Cell Biol *32*, 4168-4180.

Masopust, D., and Ahmed, R. (2004). Reflections on CD8 T-Cell Activation and Memory. Immunologic Research *29*, 151-160.

Medzhitov, R. (2001). Toll-like receptors and innate immunity. Nat Rev Immunol *1*, 135-145.

Medzhitov, R., and Janeway, C.A., Jr. (1997). Innate immunity: the virtues of a nonclonal system of recognition. Cell *91*, 295-298.

Mildner, A., and Jung, S. (2014). Development and Function of Dendritic Cell Subsets. Immunity *40*, 642-656.

Min, C., Yunlong, H., Yong, Z., and Jialin, Z. (2008). Transcription factor FOXO3a mediates apoptosis in HIV-1-infected macrophages. Journal of immunology (Baltimore, Md : 1950) *180*, 898-906.

Mittrucker, H.W., Kursar, M., Kohler, A., Hurwitz, R., and Kaufmann, S.H. (2001). Role of CD28 for the generation and expansion of antigen-specific CD8(+) T lymphocytes during infection with Listeria monocytogenes. J Immunol *167*, 5620-5627.

Morelli, A.E., Zahorchak, A.F., Larregina, A.T., Colvin, B.L., Logar, A.J., Takayama, T., Falo, L.D., and Thomson, A.W. (2001). Cytokine production by mouse myeloid dendritic cells in relation to differentiation and terminal maturation induced by lipopolysaccharide or CD40 ligation. Blood *98*, 1512-1523.

Mosmann, T.R., Li, L., and Sad, S. (1997). Functions of CD8 T-cell subsets secreting different cytokine patterns. Semin Immunol *9*, 87-92.

Mosmann, T.R., and Sad, S. (1996). The expanding universe of T-cell subsets: Th1, Th2 and more. Immunol Today *17*, 138-146.

Nagai, Y., Akashi, S., Nagafuku, M., Ogata, M., Iwakura, Y., Akira, S., Kitamura, T., Kosugi, A., Kimoto, M., and Miyake, K. (2002). Essential role of MD-2 in LPS responsiveness and TLR4 distribution. Nat Immunol *3*, 667-672.

O'Connor, L., Strasser, A., O'Reilly, L.A., Hausmann, G., Adams, J.M., Cory, S., and Huang, D.C. (1998). Bim: a novel member of the Bcl-2 family that promotes apoptosis. EMBO J *17*, 384-395.

Oeckinghaus, A., and Ghosh, S. (2009). The NF-kappaB family of transcription factors and its regulation. Cold Spring Harb Perspect Biol *1*, a000034.

Ogg, S., Paradis, S., Gottlieb, S., Patterson, G.I., Lee, L., Tissenbaum, H.A., and Ruvkun, G. (1997). The Fork head transcription factor DAF-16 transduces insulin-like metabolic and longevity signals in C. elegans. Nature *389*, 994-999.

Opal, S.M., and DePalo, V.A. (2000). Anti-inflammatory cytokines. Chest *117*, 1162-1172.

Orabona, C., Grohmann, U., Belladonna, M.L., Fallarino, F., Vacca, C., Bianchi, R., Bozza, S., Volpi, C., Salomon, B.L., Fioretti, M.C.*, et al.* (2004). CD28 induces immunostimulatory signals in dendritic cells via CD80 and CD86. Nat Immunol *5*, 1134-1142.

Osborn, M.J., Rick, P.D., Lehmann, V., Rupprecht, E., and Singh, M. (1974). Structure and biogenesis of the cell envelope of gram-negative bacteria. Ann N Y Acad Sci *235*, 52-65.

Riddell, S.R., and Greenberg, P.D. (1990). The use of anti-CD3 and anti-CD28 monoclonal antibodies to clone and expand human antigen-specific T cells. Journal of immunological methods *128*, 189-201.

Riou, C., Yassine-Diab, B., Van grevenynghe, J., Somogyi, R., Greller, L.D., Gagnon, D., Gimmig, S., Wilkinson, P., Shi, Y., Cameron, M.J.*, et al.* (2007). Convergence of TCR and cytokine signaling leads to FOXO3a phosphorylation and drives the survival of CD4+ central memory T cells. J Exp Med *204*, 79-91.

Rochman, I., Paul, W.E., and Ben-Sasson, S.Z. (2005). IL-6 increases primed cell expansion and survival. J Immunol *174*, 4761-4767.

Rus, H., Cudrici, C., and Niculescu, F. (2005). The role of the complement system in innate immunity. Immunol Res *33*, 103-112.

Schmidt, M., Fernandez de Mattos, S., van der Horst, A., Klompmaker, R., Kops, G.J., Lam, E.W., Burgering, B.M., and Medema, R.H. (2002). Cell cycle inhibition by FoxO forkhead transcription factors involves downregulation of cyclin D. Mol Cell Biol *22*, 7842-7852.

Schwartz, R.H. (2003). T cell anergy. Annu Rev Immunol *21*, 305-334.

Shortman, K., and Liu, Y.J. (2002). Mouse and human dendritic cell subtypes. Nat Rev Immunol *2*, 151-161.

Skurk, C., Maatz, H., Kim, H.S., Yang, J., Abid, M.R., Aird, W.C., and Walsh, K. (2004). The Akt-regulated forkhead transcription factor FOXO3a controls endothelial cell viability through modulation of the caspase-8 inhibitor FLIP. J Biol Chem *279*, 1513-1525.

Smith-Garvin, J.E., Koretzky, G.A., and Jordan, M.S. (2009). T cell activation. Annu Rev Immunol *27*, 591-619.

Snoeks, L., Weber, C.R., Turner, J.R., Bhattacharyya, M., Wasland, K., and Savkovic, S.D. (2008). Tumor suppressor Foxo3a is involved in the regulation of lipopolysaccharide-induced interleukin-8 in intestinal HT-29 cells. Infect Immun *76*, 4677-4685.

Steinman, R.M., and Hemmi, H. (2006). Dendritic cells: translating innate to adaptive immunity. Current topics in microbiology and immunology *311*, 17-58.

Stemberger, C., Neuenhahn, M., Buchholz, V.R., and Busch, D.H. (2007). Origin of CD8+ effector and memory T cell subsets. Cellular & molecular immunology *4*, 399-405.

Sullivan, J.A., Kim, E.H., Plisch, E.H., Peng, S.L., and Suresh, M. (2012a). FOXO3 regulates CD8 T cell memory by T cell-intrinsic mechanisms. PLoS Pathog *8*, e1002533.

Sullivan, J.A., Kim, E.H., Plisch, E.H., and Suresh, M. (2012b). FOXO3 regulates the CD8 T cell response to a chronic viral infection. J Virol *86*, 9025-9034.

Swanson, J.A., and Hoppe, A.D. (2004). The coordination of signaling during Fc receptor-mediated phagocytosis. J Leukoc Biol *76*, 1093-1103.

Takeda, K., and Akira, S. (2005). Toll-like receptors in innate immunity. Int Immunol *17*, 1-14.

Teague, T.K., Marrack, P., Kappler, J.W., and Vella, A.T. (1997). IL-6 rescues resting mouse T cells from apoptosis. J Immunol *158*, 5791-5796.

Thery, C., and Amigorena, S. (2001). The cell biology of antigen presentation in dendritic cells. Current opinion in immunology *13*, 45-51.

Tiedje, C., Holtmann, H., and Gaestel, M. (2014). The role of mammalian MAPK signaling in regulation of cytokine mRNA stability and translation. Journal of interferon & cytokine research : the official journal of the International Society for Interferon and Cytokine Research *34*, 220-232.

Tran, H., Brunet, A., Grenier, J.M., Datta, S.R., Fornace, A.J., Jr., DiStefano, P.S., Chiang, L.W., and Greenberg, M.E. (2002). DNA repair pathway stimulated by the forkhead transcription factor FOXO3a through the Gadd45 protein. Science *296*, 530-534.

Trapani, J.A., and Smyth, M.J. (2002). Functional significance of the perforin/granzyme cell death pathway. Nat Rev Immunol *2*, 735-747.

Triantafilou, M., and Triantafilou, K. (2002). Lipopolysaccharide recognition: CD14, TLRs and the LPS-activation cluster. Trends Immunol *23*, 301-304.

Tseng, A.H., Shieh, S.S., and Wang, D.L. (2013). SIRT3 deacetylates FOXO3 to protect mitochondria against oxidative damage. Free Radic Biol Med *63*, 222-234.

Tzelepis, F., Alcon, V., Dudani, R., Gurnani, K., Zafer, A., Everson, E.S., Young, K.G., Russmann, H., Krishnan, L., and Sad, S. (2012). Modulation of antigenic location converts chronic into acute infection by forcing CD8+ T cell recognition. Cell Rep *2*, 1710-1721.

Tzelepis, F., Joseph, J., Haddad, E.K., Maclean, S., Dudani, R., Agenes, F., Peng, S.L., Sekaly, R.P., and Sad, S. (2013). Intrinsic role of FoxO3a in the development of CD8+ T cell memory. J Immunol *190*, 1066-1075.

van der Vos, K.E., Eliasson, P., Proikas-Cezanne, T., Vervoort, S.J., van Boxtel, R., Putker, M., van Zutphen, I.J., Mauthe, M., Zellmer, S., Pals, C.*, et al.* (2012). Modulation of glutamine metabolism by the PI(3)K-PKB-FOXO network regulates autophagy. Nat Cell Biol *14*, 829-837.

Veillette, A., Bookman, M.A., Horak, E.M., and Bolen, J.B. (1988). The CD4 and CD8 T cell surface antigens are associated with the internal membrane tyrosine-protein kinase p56lck. Cell *55*, 301-308.

Watkins, S.K., Zhu, Z., Riboldi, E., Shafer-Weaver, K.A., Stagliano, K.E., Sklavos, M.M., Ambs, S., Yagita, H., and Hurwitz, A.A. (2011). FOXO3 programs tumor-associated DCs to become tolerogenic in human and murine prostate cancer. J Clin Invest *121*, 1361-1372.

Wherry, E.J., and Ahmed, R. (2004). Memory CD8 T-cell differentiation during viral infection. J Virol *78*, 5535-5545.

Williams, M.A., and Bevan, M.J. (2007). Effector and memory CTL differentiation. Annu Rev Immunol *25*, 171-192.

Wong, P., and Pamer, E.G. (2003). CD8 T cell responses to infectious pathogens. Annu Rev Immunol *21*, 29-70.

Yalcin, S., Marinkovic, D., Mungamuri, S.K., Zhang, X., Tong, W., Sellers, R., and Ghaffari, S. (2010). ROS-mediated amplification of AKT/mTOR signalling pathway leads to myeloproliferative syndrome in Foxo3(-/-) mice. EMBO J *29*, 4118-4131.

Yanagihara, S., Komura, E., Nagafune, J., Watarai, H., and Yamaguchi, Y. (1998). EBI1/CCR7 is a new member of dendritic cell chemokine receptor that is up-regulated upon maturation. J Immunol *161*, 3096-3102.

Yang, H., Zhang, W., Pan, H., Feldser, H.G., Lainez, E., Miller, C., Leung, S., Zhong, Z., Zhao, H., Sweitzer, S.*, et al.* (2012). SIRT1 activators suppress inflammatory responses through promotion of p65 deacetylation and inhibition of NF-kappaB activity. PLoS One *7*, e46364.

Yoneyama, M., and Fujita, T. (2009). RNA recognition and signal transduction by RIG-I-like receptors. Immunol Rev *227*, 54-65.

You, H., Pellegrini, M., Tsuchihara, K., Yamamoto, K., Hacker, G., Erlacher, M., Villunger, A., and Mak, T.W. (2006). FOXO3a-dependent regulation of Puma in response to cytokine/growth factor withdrawal. J Exp Med *203*, 1657-1663.

Zhang, N., and Bevan, M.J. (2011). CD8(+) T cells: foot soldiers of the immune system. Immunity *35*, 161-168.

Zhao, J., Brault, J.J., Schild, A., Cao, P., Sandri, M., Schiaffino, S., Lecker, S.H., and Goldberg, A.L. (2007). FoxO3 coordinately activates protein degradation by the autophagic/lysosomal and proteasomal pathways in atrophying muscle cells. Cell Metab *6*, 472-483.

Zhou, J., Liao, W., Yang, J., Ma, K., Li, X., Wang, Y., Wang, D., Wang, L., Zhang, Y., Yin, Y.*, et al.* (2012). FOXO3 induces FOXO1-dependent autophagy by activating the AKT1 signaling pathway. Autophagy *8*, 1712-1723.

Zhu, J., and Paul, W.E. (2008). CD4 T cells: fates, functions, and faults. Blood *112*, 1557-1569.

CURRICULUM VITAE

NAVEEN HARIBABU

EDUCATION

Master of Science, Microbiology and Immunology **2012 – 2014**

Department of Biochemistry, Microbiology and Immunology,
Faculty of Medicine, University of Ottawa, Ottawa, Ontario

Thesis: FoxO3a modulates the activation of innate and acquired immune cells
Supervisor: Dr. Subash Sad

Bachelor of Technology, Biotechnology **2007 – 2011**

Department of Biotechnology, Sri Venkateswara College of Engineering, Pennalur, Sriperumbudur, Tamil Nadu, India

Thesis: Development of an edible vaccine against cervical cancer
Supervisor: Dr. Muthukumaran Sivanandham

AWARDS AND SCHOLARSHIPS

- **Admission Scholarship**, University of Ottawa **2012-2014**
- **Dean's Scholarship**, University of Ottawa **2014**
- **2nd place** – cash prize, BMI Seminar day, University of Ottawa **2014**
- **Academic merit scholarship,** University of Ottawa **2013**
- **3rd place** – cash prize, BMI Poster day, University of Ottawa **2013**
- **Full tuition scholarship**, Anna University **2008**

RESEARCH EXPERIENCE

Graduate student, M.Sc. thesis, Department of Biochemistry Microbiology and Immunology, University of Ottawa **2012 – 2014**

- Undertook research in the area of T cell Immunology.
- Examined T cell activation in order to modulate the kinetics of T cell expansion and contraction to contribute to novel strategies in vaccine development.

- Experienced in a variety of techniques in the fields of Molecular Biology, Microbiology and Immunology (listed under laboratory skills).

Undergraduate research, Honour's thesis, **2010 – 2011**
Department of Biotechnology, Anna University

- Worked towards developing an edible vaccine against cervical cancer.
- Grew plants in culture to collect explants in order to generate a callus culture and infect it with a bacterium (*Agrobacterium tumefaciens*) harboring a plasmid containing the gene of interest.
- Gained experience in bacterial culture, plasmid extraction, agarose gel electrophoresis, plant cell culture and general aseptic techniques and cell culture in the laboratory.

SKILLS

- Excellent organizational skills.
- Ability to work efficiently under pressure.
- Able to record, analyze and present data in a concise and structured manner.
- Perform statistical analysis on multiple sets of data collected from experiments.
- Ability to work independently, as a team member and a team leader.

LABORATORY SKILLS

- Flow Cytometry
- Western Blotting
- PCR, SDS-PAGE
- Microscopy
- Cell proliferation and cell death assays
- Biochemical assays
- Mouse handling, restraint and injection techniques
- Aseptic primary cell culture and working with infectious pathogens in a BSL-2 laboratory

VOLUNTEER WORK

Member-at-large, Biochemistry Microbiology and Immunology Graduate Student Association (BMIGSA), University of Ottawa **2013 – 2014**

- Voiced the opinions and suggestions from students to the members of the student council.
- Facilitated communication between the president, council members and students.

- Assisted in setting up social events to allow for students from various fields of study to get together and mingle.

CERTIFICATION

- Canadian Council on Animal Care's (CCAC's) Institutional Animal User Training Program **2012**
- Workplace Hazardous Materials Information System (WHMIS) training **2012**
- Biosafety Training **2013**
- Laboratory Safety **2013**
- Autoclave Safety **2013**

INTERESTS

- **Sports**: volleyball, table tennis, cricket
- **Technology**: computers, mobile phones
- **Finance**: budgeting, investments